

UNCLASSIFIED

AD NUMBER

AD860371

LIMITATION CHANGES

TO:

Approved for public release; distribution is unlimited.

FROM:

Distribution authorized to U.S. Gov't. agencies only; Administrative/Operational Use; OCT 1969. Other requests shall be referred to Space and Missile Systems Organization, Los Angeles, CA 90045.

AUTHORITY

SAMSO ltr 16 Aug 1973

THIS PAGE IS UNCLASSIFIED

AEDC-TR-69-146



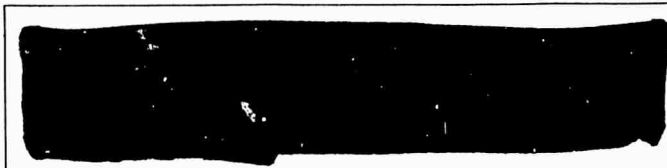
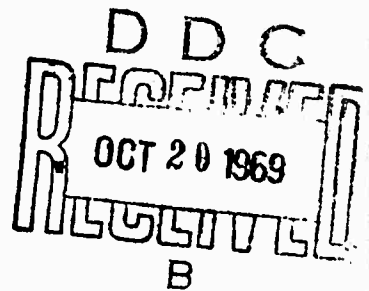
AD 860371

**EFFECTS AND CONTROL OF CONTAMINATION FROM
A SCALED MOL ATTITUDE CONTROL THRUSTER
IN A TANGENTIAL ORIENTATION**

**EACH TRANSMISSION OF THIS DOCUMENT OUTSIDE
THE AGENCIES OF THE US GOVERNMENT MUST HAVE
PRIOR APPROVAL OF THE OFFICE OF INFORMATION
(SMEA), SPACE & MISSILE SYSTEMS ORGANIZATION,
AF UNIT P.O., LOS ANGELES, CA 90045**

**David W. Hill, Jr. and Dale K. Smith
ARO, Inc.**

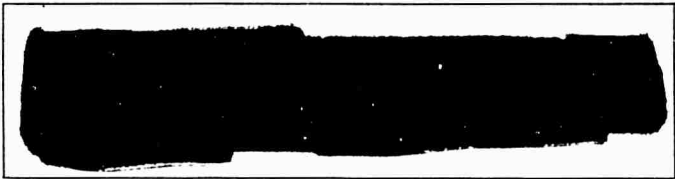

October 1969



**AEROSPACE ENVIRONMENTAL FACILITY
ARNOLD ENGINEERING DEVELOPMENT CENTER
AIR FORCE SYSTEMS COMMAND
ARNOLD AIR FORCE STATION, TENNESSEE**

EFFECTS AND CONTROL OF CONTAMINATION FROM
A SCALED MOL ATTITUDE CONTROL THRUSTER
IN A TANGENTIAL ORIENTATION

David W. Hill, Jr. and Dale K. Smith
ARO, Inc.



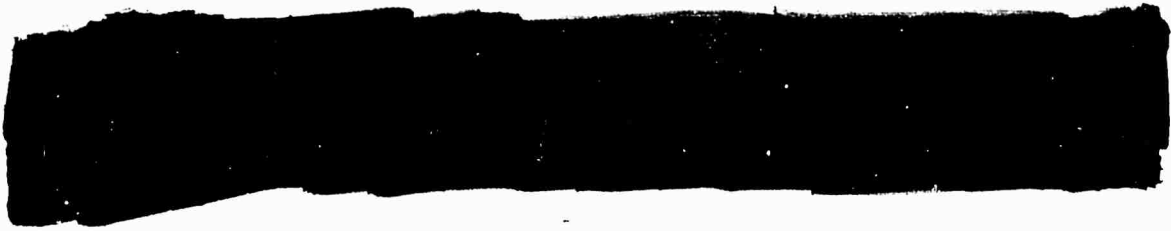
EACH TRANSMISSION OF THIS DOCUMENT OUTSIDE
THE AGENCIES OF THE US GOVERNMENT MUST HAVE
PRIOR APPROVAL OF THE OFFICE OF INFORMATION
(SMEA), SPACE & MISSILE SYSTEMS ORGANIZATION,
AF UNIT P.O., LOS ANGELES, CA 90045

FOREWORD

The work reported herein was performed at the request of Space and Missile Systems Organization (SAMSO), Air Force Systems Command (AFSC), under Program Element 35121F, Program Area 632A.

The rocket engine and simulated vehicle skin were designed and fabricated by Marquardt Corporation and McDonnell Douglas Corporation, Missiles and Space Systems Division (MSSD), respectively.


The test results were obtained by ARO, Inc. (a subsidiary of Sverdrup & Parcel and Associates, Inc.), contract operator of the Arnold Engineering Development Center (AEDC), AFSC, Arnold Air Force Station, Tennessee, under Contract F40600-69-C-0001. The tests were conducted from May through December 21, 1968, under ARO Project No. SB0721, and the manuscript was submitted for publication on June 9, 1969.



This technical report has been reviewed and is approved.

Robert T. Otto
Major, USAF
AF Representative, AEE
Directorate

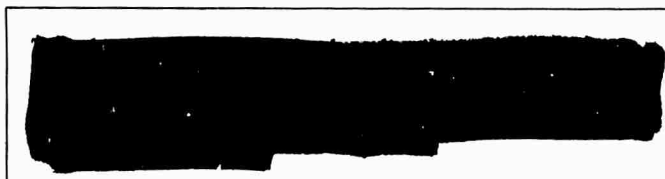
Roy R. Croy, Jr.
Colonel, USAF
Director of Test



EACH TRANSMISSION OF THIS DOCUMENT OUTSIDE
THE AGENCIES OF THE US GOVERNMENT MUST HAVE
PRIOR APPROVAL OF THE OFFICE OF INFORMATION
(SMEA), SPACE & MISSILE SYSTEMS ORGANIZATION,
AF UNIT P.O., LOS ANGELES, CA 90045

ABSTRACT

A test was conducted to determine the effects of contamination produced by a 1-lb-scale Manned Orbital Laboratory thruster. The test required pulsing the 1-lb attitude control thruster in its tangential position and determining the effects of contaminants from the thruster impinging on optical and thermal control surface test specimens located on a flat plate exposed to the thruster exhaust plume. The thruster was pulsed with durations of 20, 50, 100, and 1000 msec with 1000 msec off time at altitudes above 400,000 ft. Significant contamination was produced for the pulse-mode operation. Methods for control of contamination from the thruster and on the plate were investigated. In situ reflectance, emittance, and transmittance measurements were made on the optical and thermal control surface test specimens under vacuum conditions and at atmospheric pressure. Pretest and posttest laboratory measurements were made at nitrogen atmosphere. Contamination deposited on the plate was focused along and near the axis of the thruster, and the amount of contamination produced by the thruster decreased as the thruster pulse duration increased. Contamination controls evaluated during the test were: heated shroud, heated thruster, heated propellant lines, fuel additives, fences, various oxidizer-to-fuel ratios, and changing thruster orientation relative to the plate. The heated shroud at 300°F and changed thruster orientation were most effective in reducing contamination on the plate. However, none of the control methods eliminated the contaminants produced by the thruster.



EACH TRANSMISSION OF THIS DOCUMENT OUTSIDE
THE AGENCIES OF THE US GOVERNMENT MUST HAVE
PRIOR APPROVAL OF THE OFFICE OF INFORMATION
(SMEA), SPACE & MISSILE SYSTEMS ORGANIZATION,
AF UNIT P.O., LOS ANGELES, CA 90045.

CONTENTS

	<u>Page</u>
ABSTRACT	iii
NOMENCLATURE	vi
I. INTRODUCTION	1
II. TEST FACILITY	1
III. TEST ARTICLES	1
IV. TEST INSTRUMENTATION	5
V. PROCEDURE	6
VI. DISCUSSION AND RESULTS	8
VII. CONCLUSIONS	14
REFERENCES	16

APPENDIXES

I. ILLUSTRATIONS

Figure

1. Manned Orbital Laboratory with Thrusters	19
2. Aerospace Research Chamber (ARC) (8V)	20
3. 1-lb-Thrust Engine and Components	22
4. Propellant System	23
5. Detail Dimensions of Panel 1	24
6. Detail Dimensions of Panels 1 and 2	25
7. Test Specimen and Holder	26
8. Test Installation of Thruster and Specimens	27
9. Nozzle Shroud Configuration	28
10. Scanner Mechanism with Instrumentation	29
11. Test Installation of In Situ Instrumentation	30
12. Test Data System	31
13. Combustion Chamber Pressure versus Engine Firing Time	32
14. Predicted ARC 8V Chamber Performance	33
15. ARC 8V Chamber Pressure versus Engine Firing Time	34
16. Chemical Corrosion on Specimen, Location S ₅ , Type A, after Test 7	35
17. Test 7—Reflectance Measurements on Specimen, Location S ₁ , Type C	36
18. Test 7—Reflectance Measurements on Specimen, Location S ₂ , Type C	37
19. Test 7—Reflectance Measurements on Specimen, Location S ₅ , Type A	38
20. Test 7—Reflectance Measurements on Specimen, Location S ₆ , Type A	39
21. Test 7—Reflectance Measurements on Specimen, Location S ₉ , Type E	40
22. Test 7—Reflectance Measurements on Specimen, Location S ₁₄ , Type E	41
23. Test 8—Contamination on Specimen, Location S ₁ , Type C, after Test	42
24. Test 8—Contamination on Specimen, Location S ₆ , Type A, after Test	43
25. Test 8—Reflectance Measurements on Specimen, Location S ₁ , Type C	44
26. Test 8—Reflectance Measurements on Specimen, Location S ₂ , Type C	45

Figure	Page
27. Test 8—Reflectance Measurements on Specimen, Location S_6 , Type A	46
28. Test 8—Reflectance Measurements on Specimen, Location S_{10} , Type K	47
29. Test 8—Reflectance Measurements on Specimen, Location S_{19} , Type B	48
30. Test 8—Reflectance Measurements on Specimen, Location S_{25} , Type M	49
31. Test 9—Reflectance Measurements on Specimen, Location S_5 , Type A	50
32. Test 9—Reflectance Measurements on Specimen, Location S_6 , Type A	51
33. Test 9—Reflectance Measurements on Specimen, Location S_{10} , Type K	52
34. Test 10B—Reflectance Measurements on Specimen, Location S_5 , Type A	53
35. Test 10B—Reflectance Measurements on Specimen, Location S_6 , Type A	54
36. Test 10B—Reflectance Measurements on Specimen, Location S_{10} , Type K	55
37. Impingement Patterns on Panel 1 for 0- and 10-deg Thruster Angle	56
38. Test 11—Reflectance Measurements on Specimen, Location S_{10} , Type K	57
39. Test 11—Reflectance Measurements on Specimen, Location S_1 , Type C	58
40. Test 11—Reflectance Measurements on Specimen, Location S_2 , Type C	59
41. Test 11—Reflectance Measurements on Specimen, Location S_5 , Type A	60
42. Test 11—Reflectance Measurements on Specimen, Location S_6 , Type A	61
43. Test 12—Reflectance Measurements on Specimen, Location S_5 , Type K	62
44. Test 16—Reflectance Measurements on Specimen, Location S_1 , Type A	63
45. Test 16—Reflectance Measurements on Specimen, Location S_2 , Type A	64
46. Test 16—Reflectance Measurements on Specimen, Location S_5 , Type A	65
47. Test 16—Reflectance Measurements on Specimen, Location S_6 , Type A	66
48. Test 16—Reflectance Measurements on Specimen, Location S_9 , Type A	67
49. Test 16—Reflectance Measurements on Specimen, Location S_{10} , Type A	68
50. Test 16—Transmittance Measurements on Specimen, Location S_{23} , Type W	69
51. Test 16—Reflectance Measurements on Specimen, Location S_{27} , Type T_2	70
52. Test 16—Reflectance Measurements on Specimen, Location H_1 , Cube, Type T_1	71
II. TEST LOG	72
III. TABLES OF OPTICAL MEASUREMENTS	91

NOMENCLATURE

h	Distance from center of nozzle exit plane to the plate
J	Solar spectral irradiance as defined by Johnson
P_c	Combustion chamber pressure, psia
P_F	Fuel inlet pressure, psia
P_{ox}	Oxidizer inlet pressure, psia

R	Spectral reflectance
\bar{R}	Average visible reflectance
S	Calibration factor
T	Spectral transmittance
\bar{T}	Average visible transmittance
T_{em}	Temperature of emissometer
T_o	Initial prefire spectrum
T_s	Temperature of specimen
t_s	Relative solar transmittance
V_{em}	Voltage of emissometer
x	Distance from thruster exit plane
y	Transverse distance from thruster axis
z	Distance from detector to surface of panel
α	Angle between thruster axis and surface of plate, deg
a_s	Solar absorptance
ϵ	Emittance
θ	Angle of instrument rotation
μ	Wavelength, microns
ν	Wave number, cm^{-1}

SECTION I INTRODUCTION

The exhaust plumes from attitude control rocket engines fired at orbital attitudes expand to the extent that the exhaust products strike spacecraft surfaces and externally mounted components located within a large envelope extending downstream from the nozzle exit plane. The impingement of the gas results in local surface heating, surface pressures, and possible contamination of spacecraft surfaces. These effects may cause malfunctions of apparatus mounted on or inside the spacecraft. It is, therefore, important to identify and understand the conditions that cause these effects so that they may be properly considered in the design and operation of the spacecraft. There have been several analytical predictions of exhaust plume behavior and some limited experimental tests at high altitude (Refs. 1 through 5). These tests have been limited to short durations with transient altitudes from 400,000 to 200,000 ft.

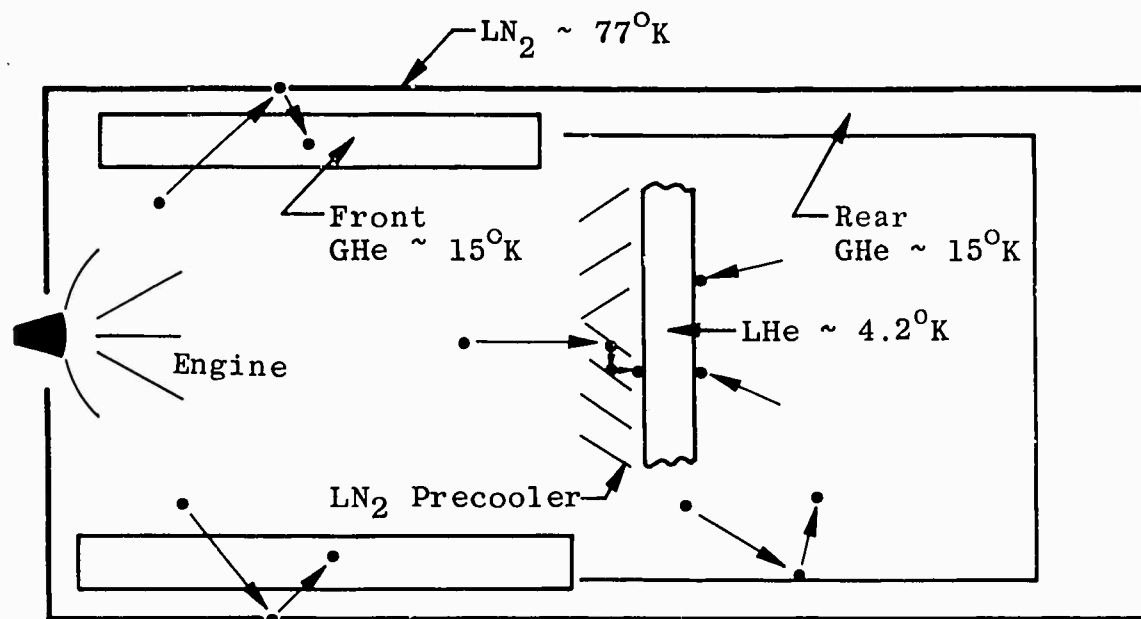
A series of tests was conducted at AEDC in a 10-ft-diam chamber to determine plume symmetry (Ref. 6); heat flux, and surface pressures (Ref. 7); and effects of contamination from a 1-lb thruster plume impinging on flat plates at an altitude over 400,000 ft. The 1-lb thruster is scaled to simulate both the 100-lb (longitudinal orientation) translational thruster, and the 22-lb (tangential and radial orientation) attitude control thrusters of the Manned Orbital Laboratory (MOL) as shown in Fig. 1, Appendix I. The flat plate simulates the MOL surface. The purpose of this test was to determine if contamination is produced by the 1-lb scaled attitude control thruster in its tangential orientation, to identify any contaminate produced, and to determine the performance degradation, if any, of optical and thermal control surfaces that have been exposed to contamination. The test required that the 1-lb scaled thruster be fired in pulses with pulse durations from 20 to 1000 (msec) while maintaining a minimum simulated altitude of 400,000 ft.

SECTION II TEST FACILITY

The test was conducted in the Aerospace Research Chamber (ARC) (8V) of the Aerospace Environmental Facility. The stainless steel chamber (Fig. 2) is 20 ft long and 10 ft in diameter. The cryopumping surfaces were designed (Ref. 8) for removing gas products from rocket engines and low density nozzles of high enthalpy. The 620 ft² of liquid-nitrogen (LN₂)-cooled surfaces, 800 ft² of gaseous-helium (GHe)-cooled surfaces, and 50 ft² of liquid-helium (LHe)-cooled surfaces were arranged to remove 16 kw from the exhaust gas products in an optimum manner.

The sketch below and Fig. 2 show the arrangement of the cryosurfaces to pump the high enthalpy exhaust gas products. The gas leaving the engine passes through the radially arranged, forward GHe surfaces and impinges on the annular LN₂ cryosurface where 8 kw is removed. The cooled gas is then either cryopumped by the LN₂ surface or reflected onto the GHe cryosurface where it is condensed. There is a total GHe refrigeration capacity of 8 kw—7 kw for the front GHe cryopump and the remaining 1 kw for the rear section. Since hydrogen (H₂) has a high vapor pressure (10⁻⁴ torr) on

15°K GHe surfaces, LHe (4.2°K) was used to remove the H₂ in the plume. The H₂ and nitrogen (N₂) exhaust gases moving axially down the chamber impinge on the LN₂ precooler, where energy is removed, and then are cryopumped on the LHe cryosurfaces.



The front GHe cryosurfaces consist of fifty-two 8- by 1-ft panels positioned in a radial array about the axis of the chamber. The rear GHe cryosurface is 8 ft long and 6 ft in diameter. The supply of the gas to the front or rear GHe cryosurfaces could be distributed by externally operated valves.

The LHe was made in the Aerospace Environmental Facility. A 30-liter/hr He liquefier was used in conjunction with a 4-kw GHe refrigerator as a precooler for the gas. A 1000-liter dewar located on top of the chamber housed a Joule-Thompson valve for the final stages of liquefaction and stored the LHe.

SECTION III TEST ARTICLES

3.1 1-LB-THRUST SCALED THRUSTER

The 1-lb-thrust MOL scaled thruster used in the test was supplied by Marquardt Corporation. The bipropellant, monomethylhydrazine and nitrogen-tetroxide (MMH-N₂O₄) thruster (Fig. 3) was designed for both steady and pulsing operation. The performance of the engine was investigated by Marquardt Corporation personnel who found that the lower thrust level with pulsing performance resulted in lower combustion efficiency. During the firing, the propellant valves and injectors were held at 60°F with cooling water.

The thruster design parameters and performance are shown below.

Thrust	1.0 lb
Fuel	MMH (Monomethylhydrazine)
Oxidizer	N_2O_4
Chamber Pressure	90 psi
Mixture Ratio	1.65 ± 1.5
Nozzle Expansion Ratio	40:1
Nozzle Geometry	Contoured
Chamber Temperature	4000°F
Throat Diameter	0.090 in.
Nozzle Exit Diameter	0.569 in.
Combustion Efficiency	0.830

Shown in Fig. 3 is the assembled 1-lb thruster. It consists of a water-cooled, single-doublet injector head, two fast response solenoid valves, and two 5-micron (μ) nominal filters upstream of each valve. The nozzle and combustion chamber are an integral part, machined from molybdenum.

Figure 4 shows the 1-lb thruster propellant system. The system consists mainly of three parts: the engine N_2 purge, high-point bleeds, and propellant supply system. Each propellant tank has a capacity of 2 liters. The propellants were pressurized with dry N_2 . The propellant lines were 0.180-in.-ID stainless steel tubing.

3.2 TEST PANELS

There were two test panels (Figs. 5 and 6) used during the test. Panel 1 is 22.5 in. wide by 34 in. long, and panel 2 is 16 in. wide by 34 in. long. Panel 2 is mounted at the bottom of panel 1, as shown in Fig. 6, on a pivot point so it could be remotely controlled and rotated flush with the panel 1 for in situ measurements. Figure 6, side view, illustrates the position of panel 2 during thruster firings. Panel 1 was mounted in a vertical plane parallel to the chamber centerline, offset 1.14 in. from the thruster centerline at the exit.

There are twenty-eight 1-in.-diam holes and six 1.5-in.-diam holes drilled through panel 1 for the purpose of inserting specimens (Fig. 6). There were also ten 1-in.-diam holes drilled through panel 2 for the same purpose.

3.3 SPECIMENS

Eleven types of specimens were used during the test to simulate the thermal control coatings and optical surfaces on the outside of the MOL vehicle. They are the following:

Type	Description	Use on MOL Vehicle
A	Zinc Oxide and Potassium Silicate ($\text{ZNO} + \text{K}_2 \text{SiO}_3$)	Radiator Coating
B	Aluminum Silicone Paint (ALS_i)	Laboratory Module Coating
C	Schjeldahl Mylar® Tape (Adhesive Back Surface)	Forward Unpressurized Compartment Coating
D	Polished Aluminum	Thermal Control
G	Fused Quartz (High Efficiency Anti-reflective Coating)	View Port Window
H	Germanium Glass/Fluoride Coating	Horizon Sensor Window
J	Zinc Oxide and Potassium Silicate (with Alpo Coating)	Radiator Coating
K	Black Spinal (Potassium Silicate)	Laboratory Module Coating
T ₁	Silicon Paint ($\text{K}_2 \text{SiO}_3$)	Thermal Control
T ₂	Silicon Oxide (SiO_2)	Thermal Control
M	High Quality Mirror (Optical Grade)	Startracker
W	Quartz (Optical Grade)	Window

The above thermal control and optical specimens were each applied or attached to a 15/16-in.-diam disk which was mounted on a specimen holder (Fig. 7). The holder was threaded so it could be inserted into holes of the test panels (Fig. 8). The holders contained a heater tape with a thermocouple for maintaining the specimens at 60°F while in the vacuum.

3.4 THRUSTER SHROUD

Figure 9 illustrates the shroud used during the tests in an attempt to reduce the contamination on the test panels by capturing and decomposing the contaminants dripping from the nozzle exit. The shroud was provided with two electrodes for electrical heating. The lower part of Fig. 9 shows a stainless steel wire mesh cloth inserted between the thruster and shroud in an attempt to absorb the contaminants ejected from the thruster and captured by the shroud if the previous method failed.

SECTION IV TEST INSTRUMENTATION

4.1 THRUSTER INSTRUMENTATION

The thruster was instrumented with three Taber® 500-psia pressure transducers. Two were used on the inlet side of the injector head for monitoring oxidizer and fuel pressures. One transducer was located on the engine combustion chamber. The response time of the transducers is less than 1 sec.

4.2 CHAMBER INSTRUMENTATION

There were four Bayard-Alpert-type ionization pressure gages located at various positions in the chamber. One gage was located behind the thruster for measuring the pressure during firings. The remaining gages were positioned near the LHe cryopump in order to evaluate its performance. One Alphatron® and one Baratron® were installed behind the thruster for monitoring pressures above 10^{-3} torr.

4.3 SCANNER MECHANISM

A scanner mechanism was installed in the test chamber (Figs. 10 and 11) to mount and position instrumentation for in situ measurements. The scanner mechanism provided the instruments four degrees of movement; three linear—x, y, and z; and one angular— θ . Each movement was driven by a gear train and motor which could be controlled from outside the chamber. A light source was placed behind and adjacent to each specimen transmitting a light beam through an appropriately located small hole in the panel. A photocell was mounted on each of the in situ measuring instruments. When the instrument was properly positioned relative to the desired specimen, the light beam impinged on the photocell and gave positive indication that the test instrument on the scanner mechanism was correctly located for the measurement.

4.4 IN SITU MEASUREMENTS

A Block Engineering, Inc. Model P-4 interferometer spectrometer and a locally fabricated emissometer (Ref. 9) were mounted on the scanner mechanism for making in situ measurements. The P-4 spectrometer was equipped with a locally designed and fabricated integrating sphere attachment (Ref. 9). The P-4 instrument is a quartz-polarization interferometer spectrometer which measures spectra in the range of 4,000 to 27,000 cm^{-1} .

(2.5 to 0.37 μ). The P-4 was used to measure in situ absolute spectral reflectance, $R(\nu)$, for the thermal control surface and mirror specimens, and relative spectra, $T(\nu)$, of the light transmitted through the window specimens from a tungsten lamp. The emissometer was used for making in situ total emittance, ϵ , measurements on selected thermal control surface specimens during the test. The raw data were reduced for analysis and presentation as described in Section 5.2.

4.5 LABORATORY MEASUREMENTS

The spectral reflectance of the specimens before and after each test were measured with a Beckman DK-2A spectrophotometer in the 0.25- to 2.5- μ wavelength region. The instrument had been modified (Ref. 10) to measure absolute, directional-hemispherical spectral reflectance. For the present tests, the instrument was installed and operated in an airtight box which was purged with dry N_2 . All postfire measurements were taken before the samples were exposed to air.

4.6 DATA SYSTEM

Figure 12 shows a schematic of the test data system which was used during the test. The specimen temperatures, P-4 spectrometer signals, emissometer, and engine flow rate data went into signal conditioning equipment, a commutator, analog-to-digital converter, digital tape, and then to the computer and/or data printout. In addition, for rapid analysis, the engine pressures and flow rates were recorded directly on an oscillograph.

SECTION V PROCEDURE

5.1 TEST PROCEDURE

Before and after each test, DK-2A reflectance measurements were made on selected test specimens in the laboratory. White gloves were used in handling the specimens. After completing installation of specimens in the test panels, the proper scanner mechanism movement at each specimen location was checked by remote operation using position indicators (x, y, z, and θ) located outside the chamber.

After the thruster position was set, the chamber was purged with N_2 and then evacuated, first by means of a 140-cfm mechanical pump, and then by a 6-in. diffusion pump. These pumps evacuated the chamber to 10^{-4} torr pressure. At this time, the LN_2 and GHe liners were cooled down. With the cryosystems at the desired temperatures, the chamber pressure stabilized at approximately 10^{-7} torr. In situ reflectance, transmittance, and emittance measurements were then taken on selected specimens. Panel 2 was positioned so that its surface was flush with panel 1, allowing measurements to be made on the specimens. After completing the measurements, the scanner mechanism was moved to the parking position for firing (Fig. 10). The propellant tanks and lines were then pressurized, panel 2 was positioned at 45 deg relative to panel 1, and the LHe cryopump was cooled down to 4.2°K. After a selected number of firings, in situ measurements were repeated on the specimens. After completion of the firings, the chamber was pressurized to atmosphere with dry N_2 where, in some cases, sea-level in situ measurements were repeated on the specimens.

In order to prevent exposure of the specimens to air, following the test, personnel entered the dry N₂ atmosphere chamber with special breathing apparatus and placed the specimens in special containers for transmittal to the laboratory.

5.2 DATA REDUCTION

Laboratory measurements of absolute spectral reflectance and transmittance resulted in continuous curves drawn by an x-y plotter as the measurement was made at each wavelength.

In situ measurements for spectral reflectance and transmittance also resulted in plots by an x-y plotter, but the curves were not continuous and were not drawn as the measurement was made. Data reduction for the in situ spectrometer was done by a computer which produced a series of discrete values from which the curves were plotted. These discrete values were stored in computer memory before plotting and hence were available for further computation.

The absolute spectral reflectance data, $R(\nu)$, for the mirror and thermal control surface specimens were reduced by computer to obtain the average visible reflectance, \bar{R} , which is defined by

$$\bar{R} = \frac{\int_{12,500}^{27,000} R(\nu) d\nu}{\int_{12,500}^{27,000} d\nu}$$

The absolute spectral reflectance curves are included in the figures of Appendix I, and the corresponding computed values for the average visible reflectance, \bar{R} , are included in the data tabulated in Appendix III.

The absolute spectral reflectance data, $\bar{R}(\nu)$, were also used to compute values for the solar absorptance, α_s , in accord with

$$\alpha_s = \frac{\int_{4,000}^{27,000} [1 - \bar{R}(\nu)] J(\nu) d\nu}{\int_{4,000}^{27,000} J(\nu) d\nu}$$

where $J(\nu)$ is the generally accepted Johnson solar spectral irradiance. The values of α_s calculated for the mirror and thermal control surface samples are included in the data tabulated in Appendix III.

Spectral curves of the transmittance lamp, modified by the transmittance of the window specimen and attenuation in the spectrometer, which were obtained during testing, were used with initial, pretest spectra to compute the relative spectral transmittance, $T/T_0(\nu)$, which is plotted in the figures of Appendix I. These values were used, in turn, to compute values of average visible relative transmittance, \bar{T} , defined by

$$\bar{T} = \frac{\int_{12,500}^{27,000} [T/T_o(\nu)] d\nu}{\int_{12,500}^{27,000} d\nu}$$

The computed values of \bar{T} are tabulated in Appendix III with the other reduced data.

The relative spectral transmittance was also used to compute the relative solar transmittance, t_s , which is defined by

$$t_s = \frac{\int_{4,000}^{27,000} [T/T_o(\nu)] J(\nu) d\nu}{\int_{4,000}^{27,000} J(\nu) d\nu}$$

where, again, $J(\nu)$ is the Johnson solar spectral irradiance. The values of t_s are also tabulated in Appendix III.

In situ measurements of emittance for the thermal control surface specimens resulted in a value, ϵ , calculated from the emissometer voltage, V_{em} , the specimen temperature, T_s , and the emissometer temperature, T_{em} , in accord with

$$\epsilon = \frac{V_{em}}{(T_s^4 - T_{em}^4)S}$$

where S is a calibration factor. Values of ϵ are also tabulated in Appendix III.

In addition to the preceding values which were calculated directly from measured data, the ratio a_s/ϵ was computed for the thermal control surface specimens; and values of the ratio are included with the other data tabulated in Appendix III.

SECTION VI DISCUSSION AND RESULTS

The effects of rocket exhaust plume impingement on surface coatings in the contamination tests conducted can be categorized into the following (Ref. 11):

- a. Erosion or ablation of the coatings as a result of aerodynamic heating.
- b. Chemical corrosion of the coatings as a result of unburned propellants reacting with the coatings.
- c. Condensation or deposition on the coatings.

In the present tests (tangential orientation), the aerodynamic heating effect is insignificant because of the short duration of firing (1000 msec or less) as compared to 1000-msec off time. For this duty cycle, the maximum observed temperature on the panel was

150°F. Most surface coatings are designed to withstand temperatures greater than 150°F. The heating effect is more evident in steady-state thruster operation (greater than 1000 msec) where the maximum observed temperature on the panel is 650°F (Ref. 7). Chemical corrosion occurs when the unburned propellants deposited on the surface coatings react with the coatings and create permanent damage. Since the rocket exhaust plume composition is approximately 30-percent water vapor by weight (Ref. 11), condensation is more likely to occur on the low temperature coatings. This condensation would be temporary contamination since it would evaporate with higher operational surface temperatures.

Since the contamination tests of the longitudinal, radial, and tangential orientation were not conducted in sequence, the test numbers reported for this phase (tangential orientation) will not be consecutive. There was a total of 11 tests with the thruster angle fixed at 10 deg and 1.14 in. from the surface of panel 1 (see Fig. 10) and one test with the thruster angle at 0 deg and 1.14 in. from the surface of panel 1. Within each test, the objective, results, test hardware, measurements, and number of firings varied, as indicated in Appendixes II and III.

The thruster was fired with pulse durations of 20, 50, 100, and 1000 msec with 1000-msec off time between pulses. Figure 13 shows a plot of combustion chamber pressure as a function of pulse firing time. From the figure it can be seen that the combustion chamber pressure for 1000 msec approaches 90 psia, the design steady-state pressure.

Figure 14 shows the ARC 8V predicted chamber performance as a function of engine thrust level. From the figure it can be seen the 1-lb thruster can be fired indefinitely (more than 100 sec) maintaining 8×10^{-5} torr ARC 8V chamber pressure. For thruster pulsing, the ARC 8V chamber pressure would be lower than for steady-state firing as shown in Fig. 15. As can be seen from the figure, the altitude decreases from 600,000 to 400,000 ft for pulses from 20 to 1000 msec, respectively.

The full-scale 22- and 100-lb thrusters use multiple hole injectors for providing optimum combustion. The injector holes have to introduce and meter the flow to the combustion chamber and atomize and mix the propellants by impingement in such a manner that a correctly proportioned, homogenous fuel-oxidizer mixture will result, one that can be readily vaporized and burned. Only the nozzle of the 1-lb thruster and mass flow rate were scaled from the full-scale thrusters. The valves were the same as for the 22- and 100-lb engines. Because of the relatively small mass flow rate of the 1-lb scaled thruster, a single doublet injector design resulted (Fig. 3). In such a simple design, misalignment of either the oxidizer or fuel injector hole can result in incomplete combustion, especially in the pulse-mode operation. The accumulated unburned propellants in the combustion chamber would be blown out of the nozzle.

Another possibility for the formation of the unburned propellants in the combustion chamber is from the "dribble volume" located between the valve seat and the exit of the injector holes. When the valves are closed, the propellants within this volume flow into the combustion chamber; when the thruster is again fired, the residue is blown out of the combustion chamber into the nozzle. Therefore, more contamination would be expected in the pulse-mode than in the steady-state operation. In addition, since this engine

had an abnormally large dribble volume to combustion chamber size, the likelihood of contamination formation is large.

Several attempts were made to minimize the contamination ejected from the thruster or deposited from the plume on the coatings:

1. A method was employed to decompose or collect the contamination on the exit of the thruster.
2. The oxidizer-to-fuel ratio was varied.
3. The oxidizer fuel temperature was varied.
4. Additives were made to the fuel.
5. The panel was heated.
6. The ambient pressure or altitude was varied.
7. Shields or fences were used on the panel.
8. The orientation of the thruster was varied relative to the test panel.

Because of the large amounts of contamination ejected from the thruster and the generally random distribution of contamination on the test panel, visual observations rather than optical measurements were used to evaluate the effectiveness of methods for controlling the contamination.

6.1 TEST 7

During Test 7, large amounts of reddish-brown liquid contamination collected at the thruster exit momentarily and then were blown by the rocket exhaust onto the panel and coatings. The appearance of this contamination occurred continuously after the first 10 or 15 pulses (20- and 50-msec durations). In addition, a deposition of white frost occurred on the panel and specimens from the impinging plume.

The photograph in Fig. 16 shows the contamination typically on specimen, location S₅, type A, after exposure to the plume. The corrosion effect of the contaminant is noticeable. In this test a large quantity (approximately half a cup after 3000 pulses) of contamination impinged on the surface of the panel. There was a heavy white frost (water) deposit that covered specimens located at S₅ and S₉ and was observed in all tests. This deposit had the shape of a parabola (Ref. 6). Reddish-brown contamination deposits were visible on specimen locations S₁, S₂, S₃, S₄, S₆, S₈, S₁₂, S₁₇, and S₂₄. This was caused from a gravity flow effect; the contamination that had impinged on the panel in the vicinity of the thruster exit had flowed under the influence of gravity down the panel, thus contaminating every specimen in its path. All other specimens showed very little, if any, contamination after being exposed to the plume. This was as expected since these other specimens were in the more rarefied regions of the plume. Most of the specimens became contaminated when the chamber was repressurized to atmosphere. This was caused by the

contamination on the cryosurfaces migrating through the chamber and to the test panels when the cryosurfaces became warm. The white frost (water) evaporated completely from the panel when the chamber was brought to atmosphere.

Figures 17 through 22 show the reflectance measurements on the specimens before installation and after removal from the test panel. Figure 17 shows the decrease in reflectance for the entire measured wavelength spectrum as would be expected for the chemically corroded specimen shown in Fig. 16.

6.2 TEST 8

In test 8, a shroud was installed around the engine (Fig. II-1, Appendix II) as shown in Fig. 9 to eliminate the effect and subsequent flow that was experienced in test 7. The shroud reduced this effect, but contamination was still observed on specimens located at S_1 , S_2 , S_3 , S_5 , S_6 , S_9 , and S_{10} . The heavy, white frost deposit still existed on the panel and corroded specimens located at S_5 and S_9 . Contamination still occurred on most of the specimens when the chamber was brought to atmosphere and was typical in all tests.

Figures 23 through 30 show photographs of contaminated specimens and plots of reflectance measurements made before installation and after removal of the specimens from the test panel. Figures 25 and 27 show the decrease in reflectance after being exposed to the plume, and the measurements are consistent with Figs. 23 and 24. Figures 29 and 30 illustrate the insignificant change in reflectance measurements on the specimens outside the plume when exposed to a change in environmental conditions.

6.3 TEST 9

In test 9, a 1.5-in.-high fence (Fig. II-1) was installed on the panel in specimen locations S_1 , S_2 , S_3 , and S_4 to determine its effect on the contamination deposited downstream of the fence, i.e., on specimens located at S_5 and S_9 . The shroud was not used during this test. During the test there was a buildup of contamination in front of and on the fence. Contamination was noticed at S_5 and S_9 . As the pulse duration was increased to 1000 msec, the contamination evaporated from the fence.

The contamination which accumulated on the fence drained into a flask where it was captured for laboratory analysis. The chemical laboratory analysis of the reddish-brown contamination indicated the contamination was MMH (30.5 percent), H_2O (31.7 percent) and $-NO_3$ (37.8 percent).

Figures 31 through 33 illustrate the decrease in reflectance on specimens located at S_5 , S_6 , and S_{10} as indicated by measurements before installation and after removal from the test panel.

6.4 TESTS 10A AND 10B

In tests 10A and B, a heated thruster shroud and collector flask (Fig. II-1) were used to reduce the contamination on the panel and collect the contamination that was generated,

respectively. The effect was the same as in test 8. The heavy white deposit or parabola around S_5 and S_7 began to evaporate when the pulse duration approached 1000 insec.

Figures 34 through 36 illustrate the decrease in reflectance on specimens located at S_5 , S_6 , and S_{10} after being exposed to the plume and environment.

6.5 TEST 11

In test 11 a stainless steel mesh (Fig. 9) was used between the shroud and nozzle for absorbing the liquid contamination accumulating on the thruster skirt exit to further decrease the contamination deposited on the panel. The absorptance of the mesh decreased after the first firing, and the contamination began to spill onto the test panel near the exit plane of the thruster. There was a noticeable amount of contamination impacting on the thruster mount beneath the thruster when the thruster was pulsed. This was caused by a reversal of flow on the test panel at the stagnation region (Refs. 2, 6, and 7). Figure 37 illustrates the contamination (parabolic frost layer) on the panel for thruster angles of 10 and 0 deg (test 25). The parabolic contamination pattern moves upstream toward the thruster exit as the angle is decreased from 10 to 0 deg.

Figures 38 through 42 show reflectance measurements on some of the specimens during the test. Figures 38 and 41 show the change in reflectance as the environment of the specimens changes. Figure 38 illustrates the increase in reflectance on specimen at location S_{10} , type K, when the chamber is brought to atmosphere (curve 4). This again is caused by contamination from the cryosurfaces condensing on the test panel. Figure 41 shows the decrease in reflectance on specimen at location S_5 , type A after being exposed to the plume (curve 3). The reflectance increases at the lower wave numbers when the measurements were made in the laboratory (curve 5).

6.6 TEST 12

In test 12 the nozzle was heated to 200°F, the propellants were heated to 100°F, and the oxidizer-to-fuel ratio was varied between 1.2 and 2.0. The contamination from the thruster exhibited no significant decrease as a result of heating the propellant lines and nozzle. Varying the oxidizer-to-fuel ratio from the design value of 1.6 caused an increase in contamination relative to the other tests.

Figure 43 shows the increase in reflectance on specimen at location S_5 , type K, before being exposed to the plume (curve 2) as a result of contamination during chamber evacuation. Curve 3 illustrates the increase in reflectance or contamination on the specimen after being exposed to the plume.

6.7 TEST 16

In test 16 the shroud temperature was varied from 200 to 700°F to determine the minimum temperature required to eliminate the contamination accumulated on the thruster exit. In addition, the test panels were heated (radiation from flood lamps) to determine if

the contamination would evaporate from the panels. The minimum shroud temperature to eliminate accumulation at the thruster exit was found to be 300°F, and there was no noticeable effect by heating the panel to 100°F.

Figures 44 through 52 illustrate changes in reflectance and transmittance of the specimens as measured at various times in the environmental cycle. Figure 50 illustrates an insignificant effect from the plume contamination on the transmittance of the window.

6.8 TEST 24

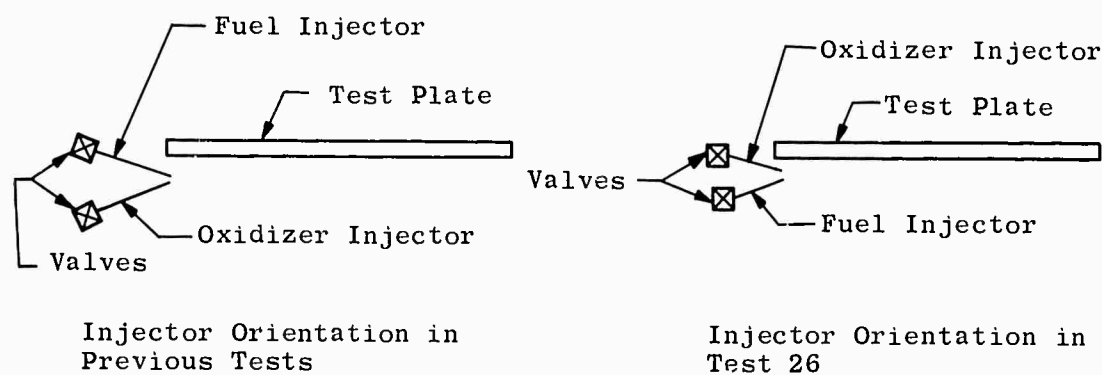
The production of contamination from the thruster at low altitudes (150,000 to 250,000 ft) was greater than at the higher altitudes (400,000 to 600,000 ft). The plume collapses significantly at this lower altitude, thus dispersing the contamination further downstream and along the axis of the thruster. The gravity flow effect of the contamination on the panel was still apparent. There were no optical measurements made during this test.

6.9 TEST 25

There was no noticeable change in contamination produced by the thruster as a result of heating the propellant lines, heating the nozzle, and adding 10 percent by weight of water and alcohol to the fuel. The white deposit again surrounded specimens at locations S₅ and S₉, and the gravity flow effect of the contamination on the panels was significant. No optical measurements were made during this test.

6.10 TEST 26

The thruster was rotated 180 deg; the propellant lines were heated; and 10-, 15-, and 20 percent water was added to the fuel. The reduction of contamination on the panel from the thruster as result of being rotated relative to the panel was significant.



The reddish-brown contamination on the panel before thruster rotation was thought to be a result of injector orientation relative to the panel. The above sketch shows the orientation of the injectors before and after being rotated 180 deg relative to the test panel.

The parabolic-shaped white frost deposit appeared on the panel. There were no optical measurements made in this test.

6.11 SUMMARY

Most of the specimens near and along the centerline of the thruster became significantly contaminated when exposed to the plume; therefore, the radiative properties changed significantly. The radiative properties of specimens located on panel 2 showed insignificant changes when exposed to the plume. The following is a list of various specimens with the maximum change in reflectance and the wavelength for which the maximum change occurred.

<u>Specimen Type</u>	<u>Percent Change In Reflectance</u>	<u>Wavelength, μ</u>
A	60 - Decrease	0.4
B	6 - Decrease	0.40
C	55 - Decrease	0.35
D	10 - Decrease	0.35
E	4 - Decrease	0.70
K	43 - Increase	0.55
M	10 - Decrease	0.5
T ₁	4 - Decrease	0.45
T ₂	27 - Decrease	0.75

Specimen types A, C, K, and T₂ show the largest change in reflectance per wavelength after being exposed to the plume. These larger changes in reflectance occur on the specimens in the ultraviolet and visible region. The reflectance will change significantly in this shorter wavelength region because of the interference effect of the small particles with the shorter wavelength.

The heated shroud and thruster rotation proved to be the most effective control in reducing the contamination on the test panel. However these controls do not eliminate the contamination in the thruster plume.

Since the tests indicated that the contamination originated in the injector and combustion chamber of the 1-lb thruster, future test work should be conducted on various injectors to minimize the contamination. One possibility is to adapt the scaled nozzle to the full-scale injector and combustion chamber. The excess combustion gas not required for thruster operation could then be vented from the combustion chamber to outside the vacuum chamber.

SECTION VII CONCLUSIONS

The results from the test for the control and effect of contamination ejected from a 1-lb scaled attitude control thruster in its tangential orientation are summarized by the following observations, conclusions, and recommendations:

1. The test indicated that a high degree of contamination resulted from the specific injector and combustion chamber configuration.
2. The amount of contaminants produced by the thruster decreased as the thruster pulse firing time increased (i.e., from 20 to 1000 msec).
3. The chemical analysis of the reddish-brown contamination collected during the tests indicated the contamination by weight was MMH (30-5 percent), H_2O (31.7 percent), and $-NO_3$ (37.8 percent).
4. Most of the contamination on the panel occurred along and near the thruster axis. Outside this region the contamination was not noticeable.
5. There was a parabolic-shaped deposit that formed on the panel during all the tests conducted. This deposit approached the thruster exit plane when the thruster angle was decreased from 10 to 0 deg.
6. There was a large amount of contamination deposited behind the thruster as a result of reversal of flow on the panel at the stagnation region.
7. Specimen types A, C, K, and T_2 showed as much as a 27- to 60-percent change, respectively, in reflectance in the ultraviolet and visible region after being exposed to the plume. Other specimens exposed to the plume showed 10 percent or less change in reflectance.
8. The thruster exhaust contaminants that impinged on the panel had a corrosive effect on some of the specimens.
9. The reflectance and transmittance measurements illustrate that the measurement environment (i.e., measurements in vacuum or atmosphere) affected the magnitudes or trends of the measurements made. The in situ measurements at the simulated altitudes are believed to be more representative of the true contamination on the panel than are the laboratory measurements.
10. The accumulation of contaminants at the thruster exit followed by ejection to the panels was eliminated by a shroud heated to a minimum of 300°F.
11. Of the contamination controls used during this test (i.e., heated shroud, heated thruster, heated propellant lines, fuel additives, fences, varying oxidizer-to-fuel ratio, and thruster rotation), the heated shroud and thruster rotation proved to be most effective in reducing the contamination on the panel. However, none of the control methods eliminated the deposition of contaminants produced by the thruster.
12. Further tests should be conducted to determine the variation in contamination production with varied injector and combustion chamber configurations.

REFERENCES

1. Llinas, J., Sheeran, J., and Hendershot, K.C. "A Short Duration Experimental Technique for Investigating Solid Propellant Rocket Plume Impingement Effects At High Altitudes." Cornell Aeronautical Laboratory, Buffalo, New York, ICRPG/AIAA 3rd Solid Propulsion Conference, No. 68-517, June 4-6, 1968.
2. Bauer, R.C. and Schlumpf, R.L. "Experimental Investigation of Free Jet Impingement on a Flat Plate." AEDC-TN-60-223 (AD253229), March 1961.
3. Barebo, R.L. and Ansley, R.C. "Effects of Rocket Exhaust Jet Impingement on a Movable Flat Plate at Pressure Altitudes Above 200,000 Feet." AEDC-TDR-63-214, January 1964.
4. Llinas, J. "Electron Beam Measurements of Temperature and Density in the Base Region of a Clustered Rocket Model." Cornell Aeronautical Laboratory, Buffalo, New York, AIAA 2nd Flight Test Simulation and Support Conference, No. 68-236, March 25-27, 1968.
5. Burch, B.A. "Effect of Contamination on Spacecraft Surfaces Exposed to Rocket Exhausts." AEDC-TR-68-23 (AD831624L), April 1968.
6. Hill, D.W., Jr. "Investigation at High Altitudes of Rocket Exhaust Plume Symmetry and Interaction with a Plate with a Scaled MOL Thruster." AEDC-TR-69-75, April 1969.
7. Hill, D.W., Jr. and Smith, D.K. "Flat Plate Heat Flux and Pressure Measurement in an MOL Scaled Thruster Plume at 400,000-Ft Altitude." AEDC-TR-69-84, May 1969.
8. Heald, J.H., Jr., Dawbarn, R., and Arnold, F. "Test Chamber Concept Development for Very High Altitude Rocket Plume and Space Vehicle Systems Testing." AEDC-TR-68-205 (AD841628), October 1968.
9. Frazine, D.F. and Cox, G.S. "Instrumentation for Evaluating Effects of Plume Contamination on Optical Properties of MOL Spacecraft Surfaces." AEDC-TR-69-188, to be published.
10. Cox, George S. "Absolute Reflectance Measurements with a Ratio Recording Spectroreflectometer." AEDC-TR-69-123, to be published.
11. Borson, E.N. and Landsbaum, E.M. "A Review of Available Rocket Contamination Results." Aerospace Report No. TR-0200 (4250-20)-2.

APPENDIXES

- I. ILLUSTRATIONS**
- II. TEST LOG**
- III. TABLES OF OPTICAL MEASUREMENTS**

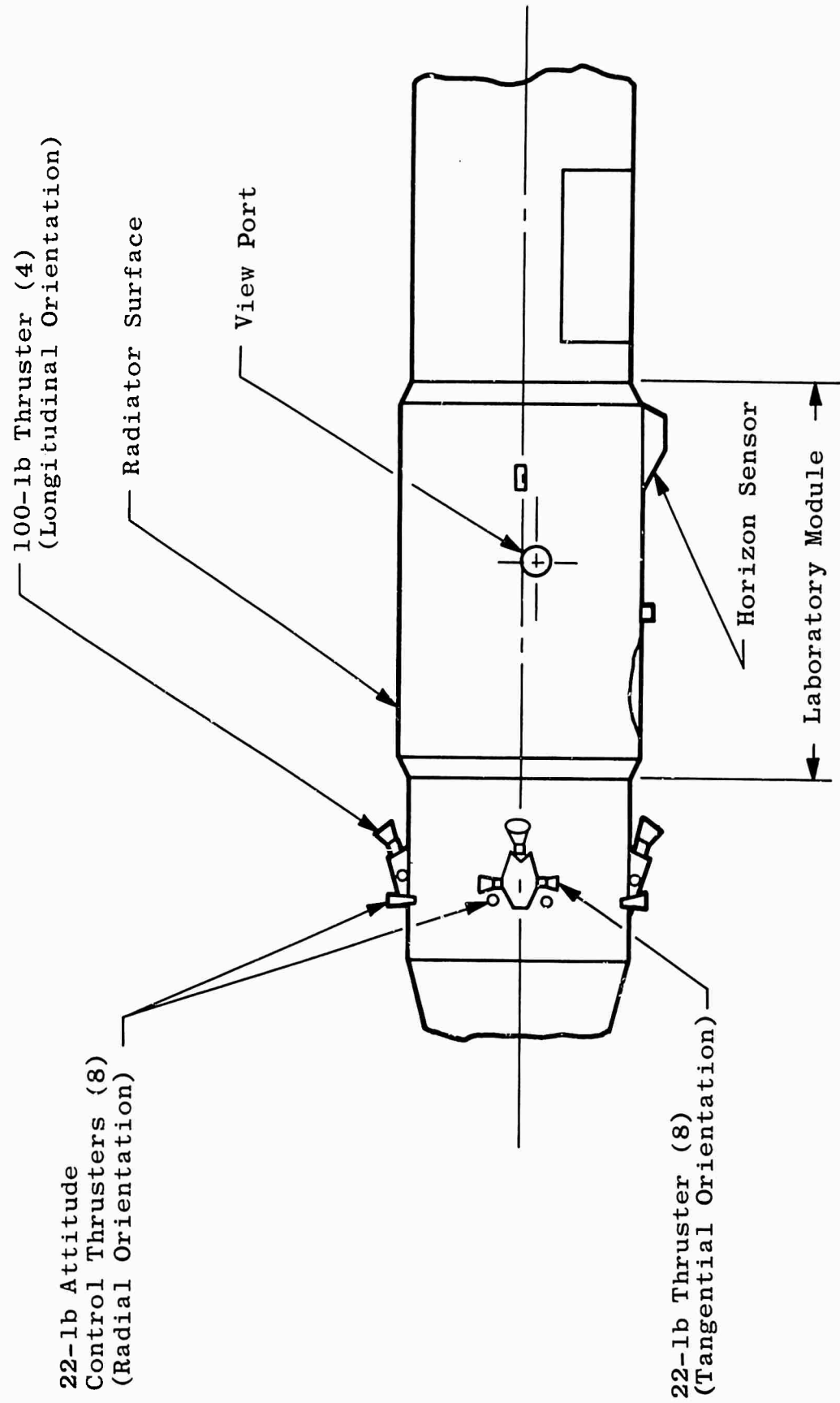


Fig. 1 Manned Orbital Laboratory with Thrusters

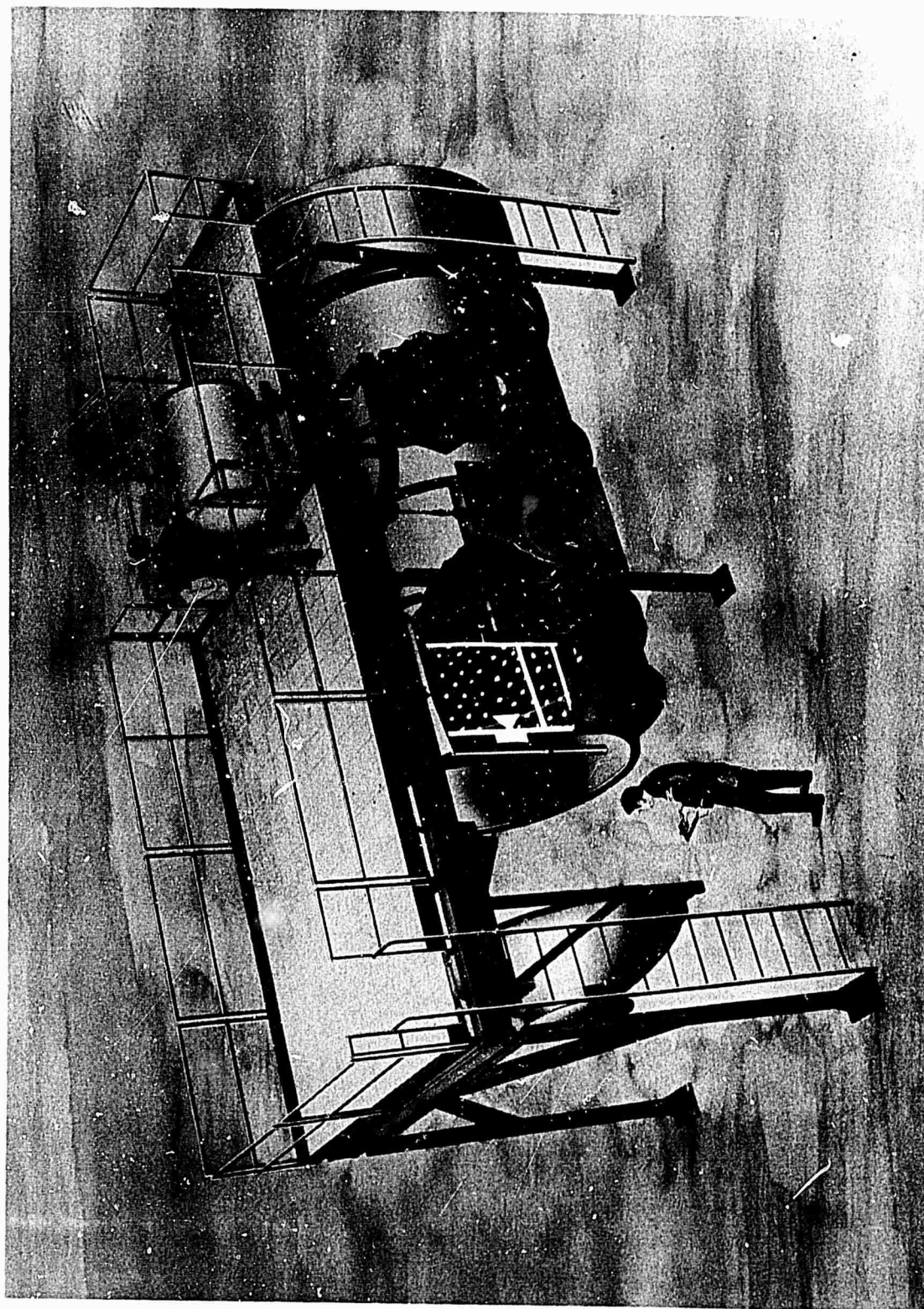


Fig. 2 Aerospace Research Chamber (ARC)(8V)

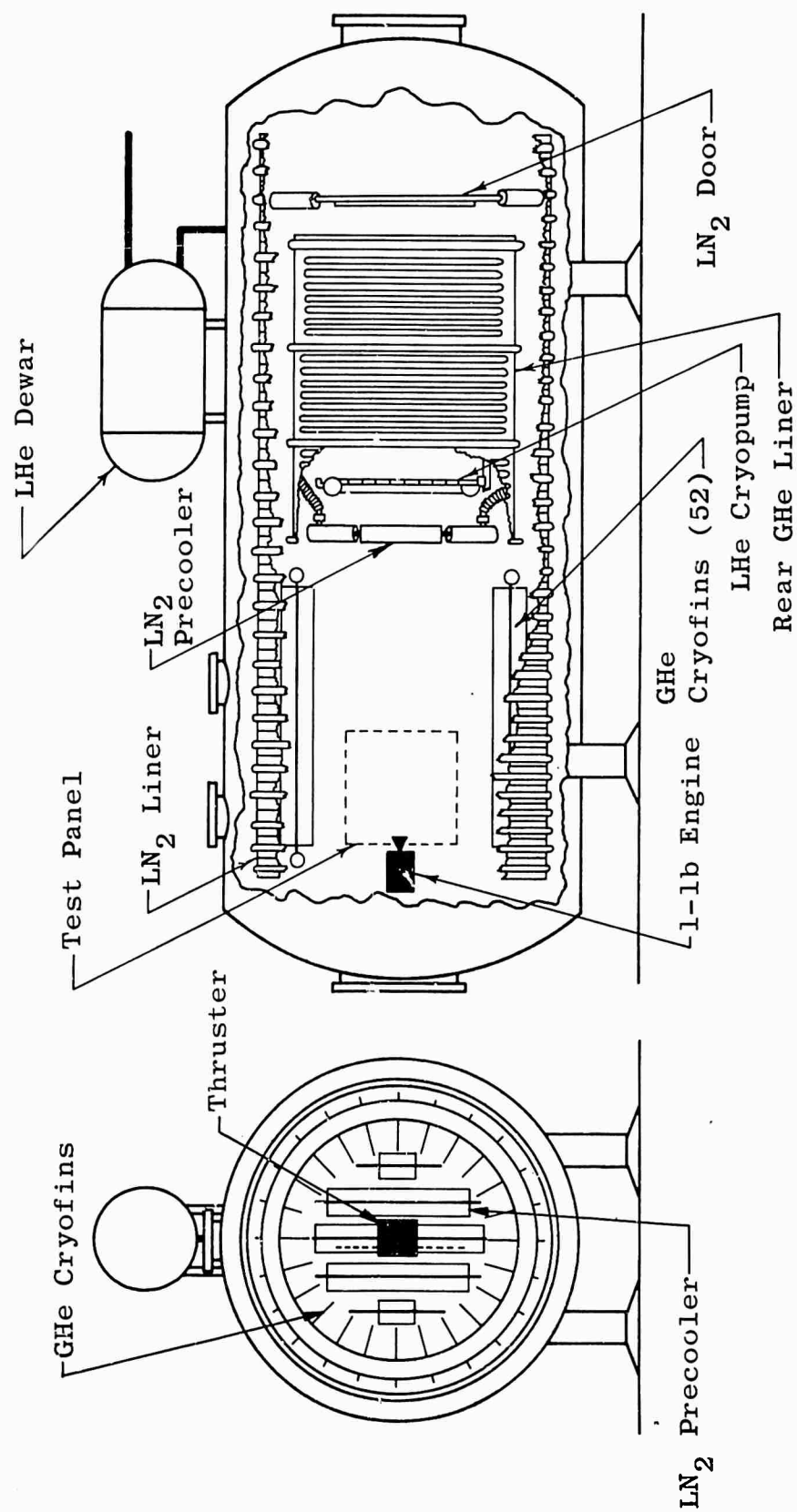
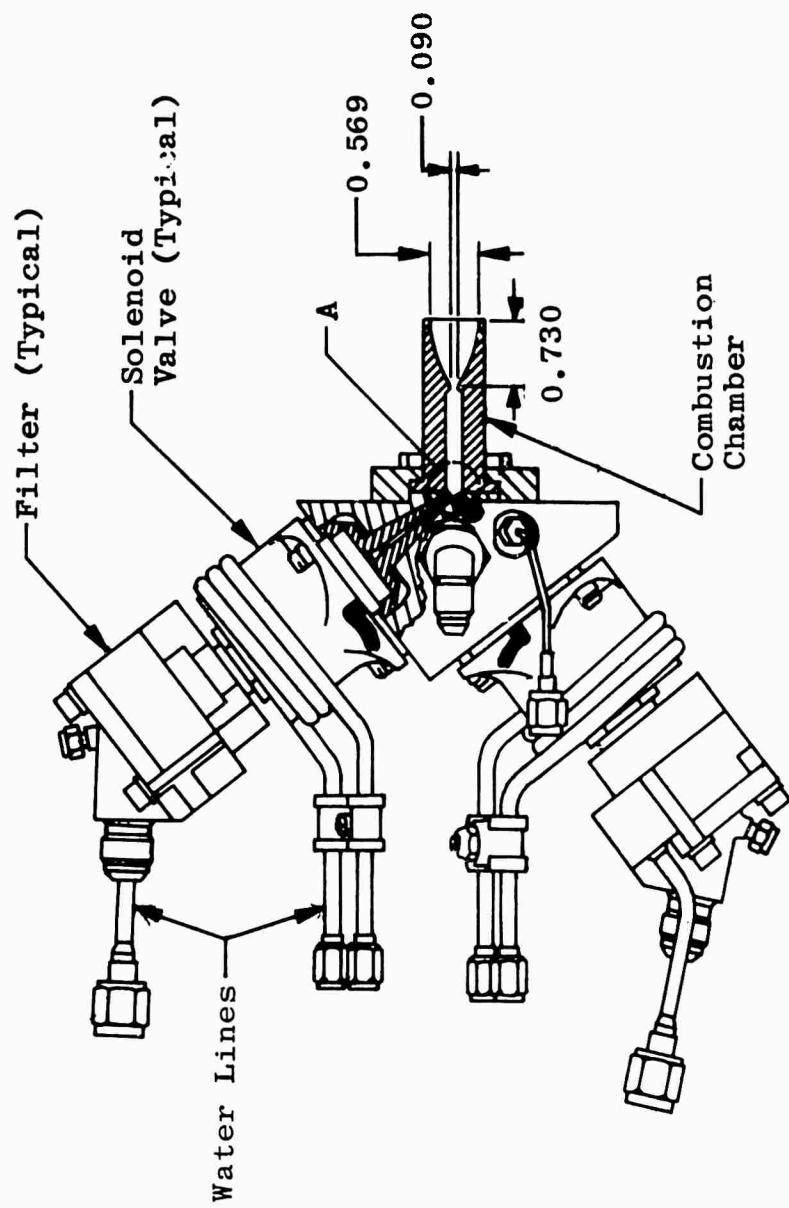


Fig. 2 Concluded



Detail A
Injectors

Fig. 3 1-lb-Thrust Engine and Components

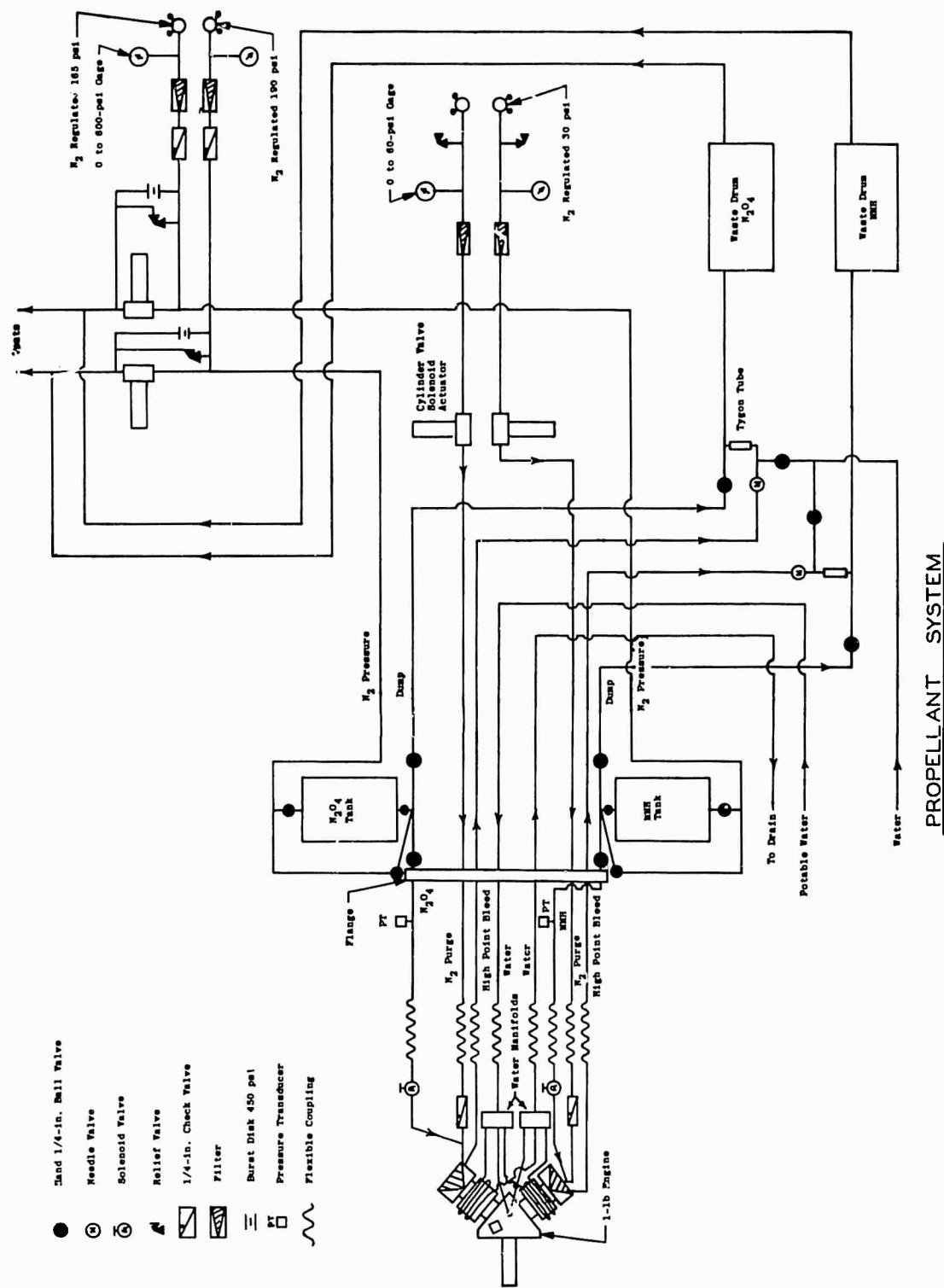


Fig. 4 Propellant System

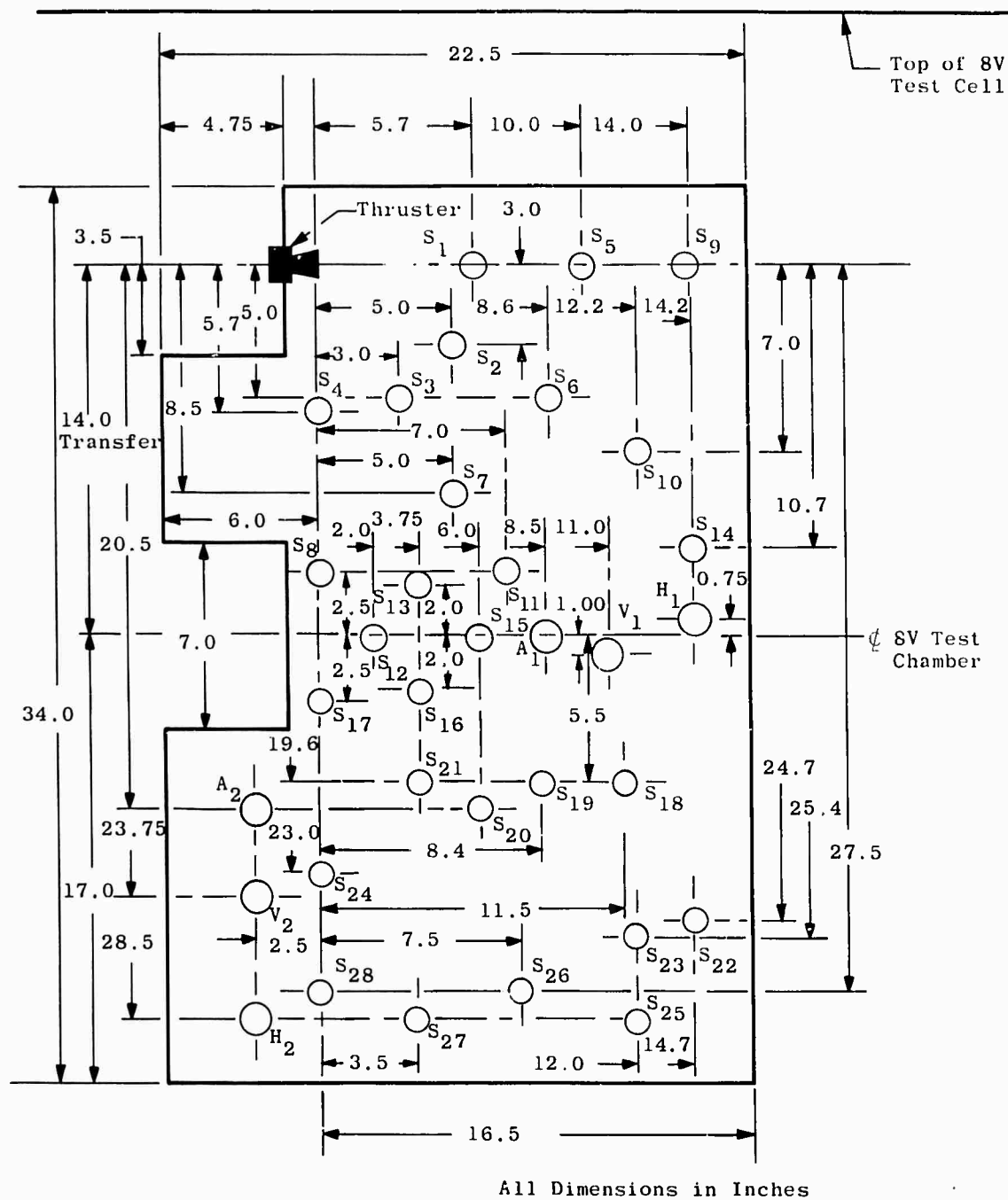


Fig. 5 Detail Dimensions of Panel 1

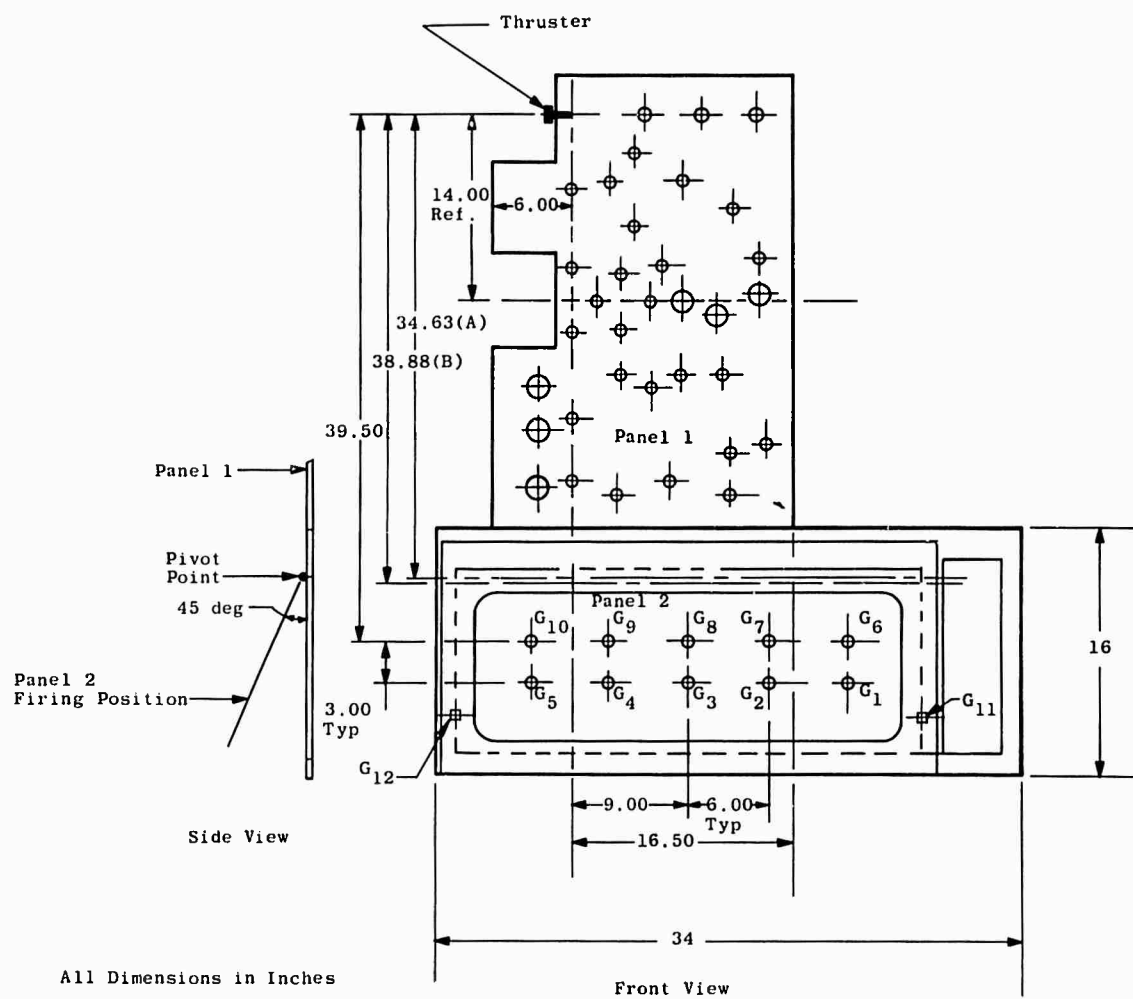


Fig. 6 Detail Dimensions of Panels 1 and 2

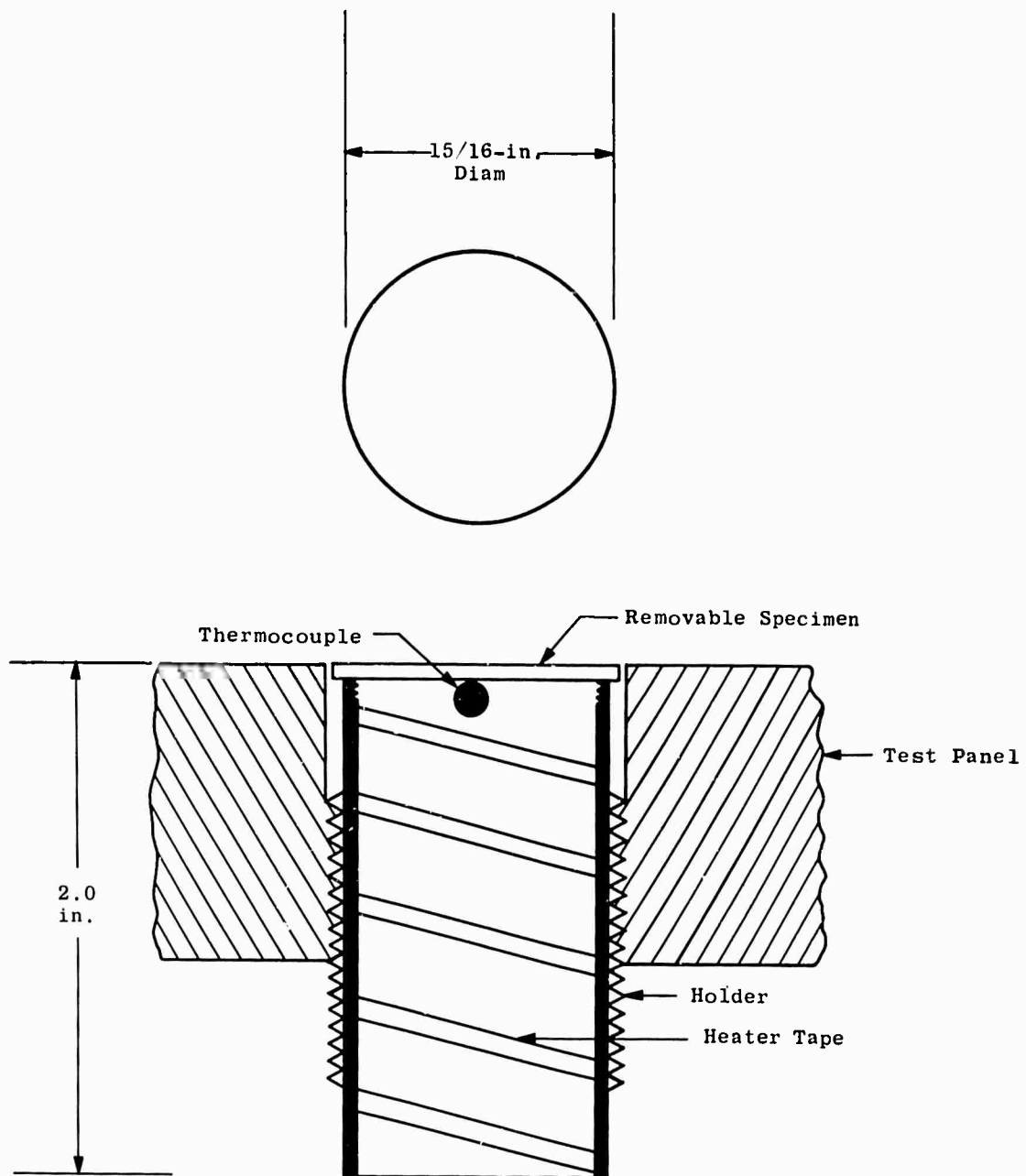


Fig. 7 Test Specimen and Holder

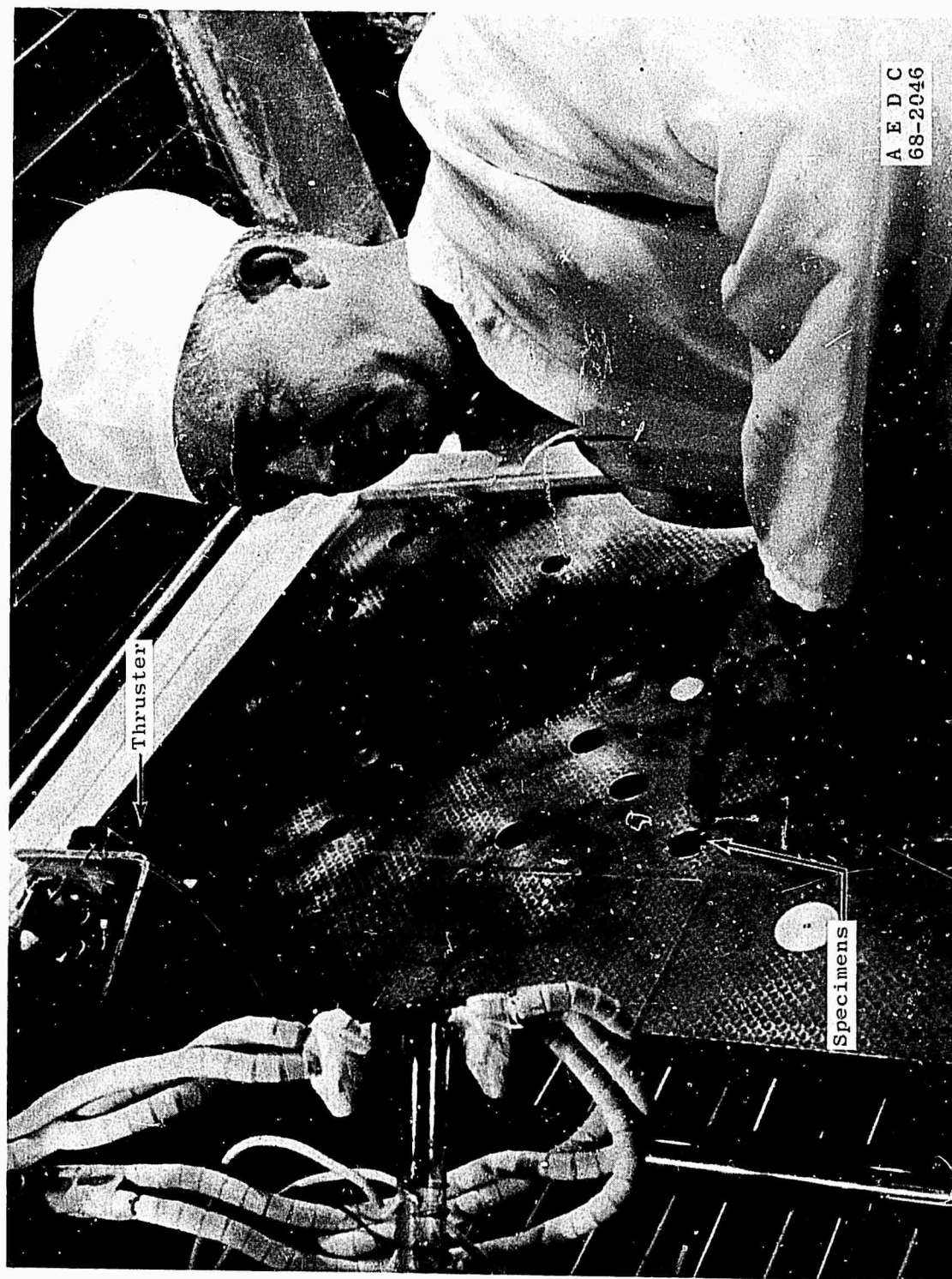
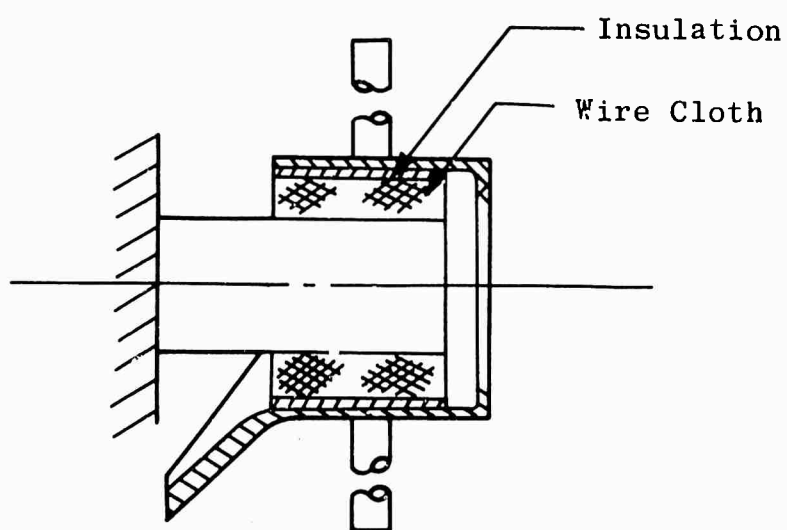
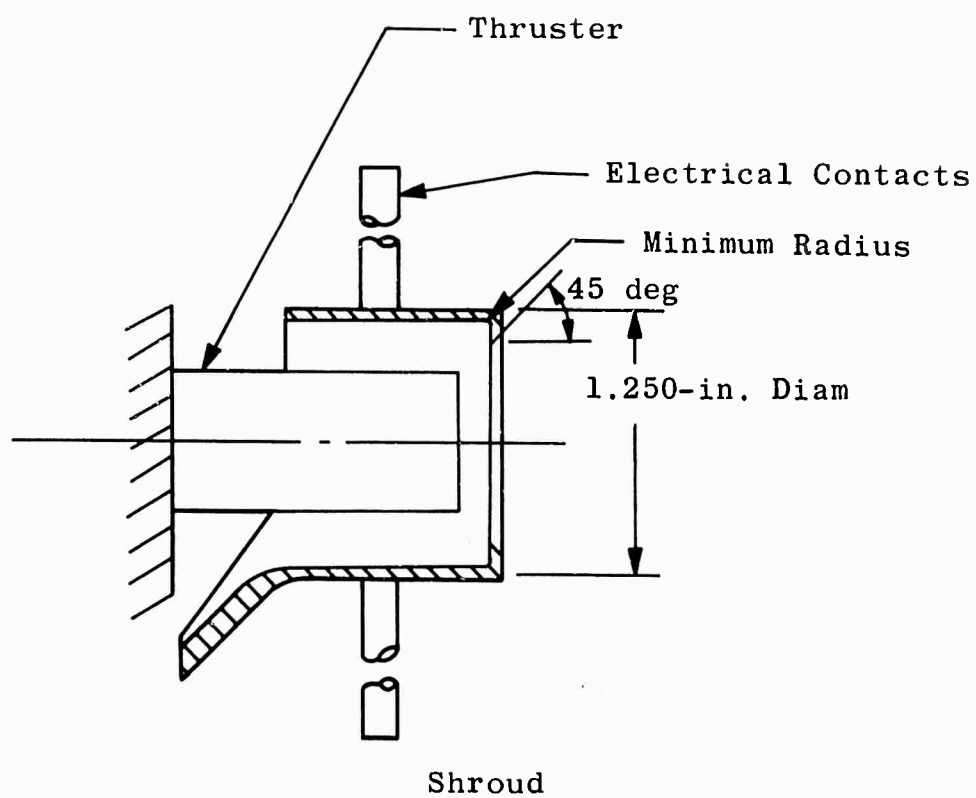


Fig. 8 Test Installation of Thruster and Specimens



Shroud with Wire Cloth

Fig. 9 Nozzle Shroud Configuration

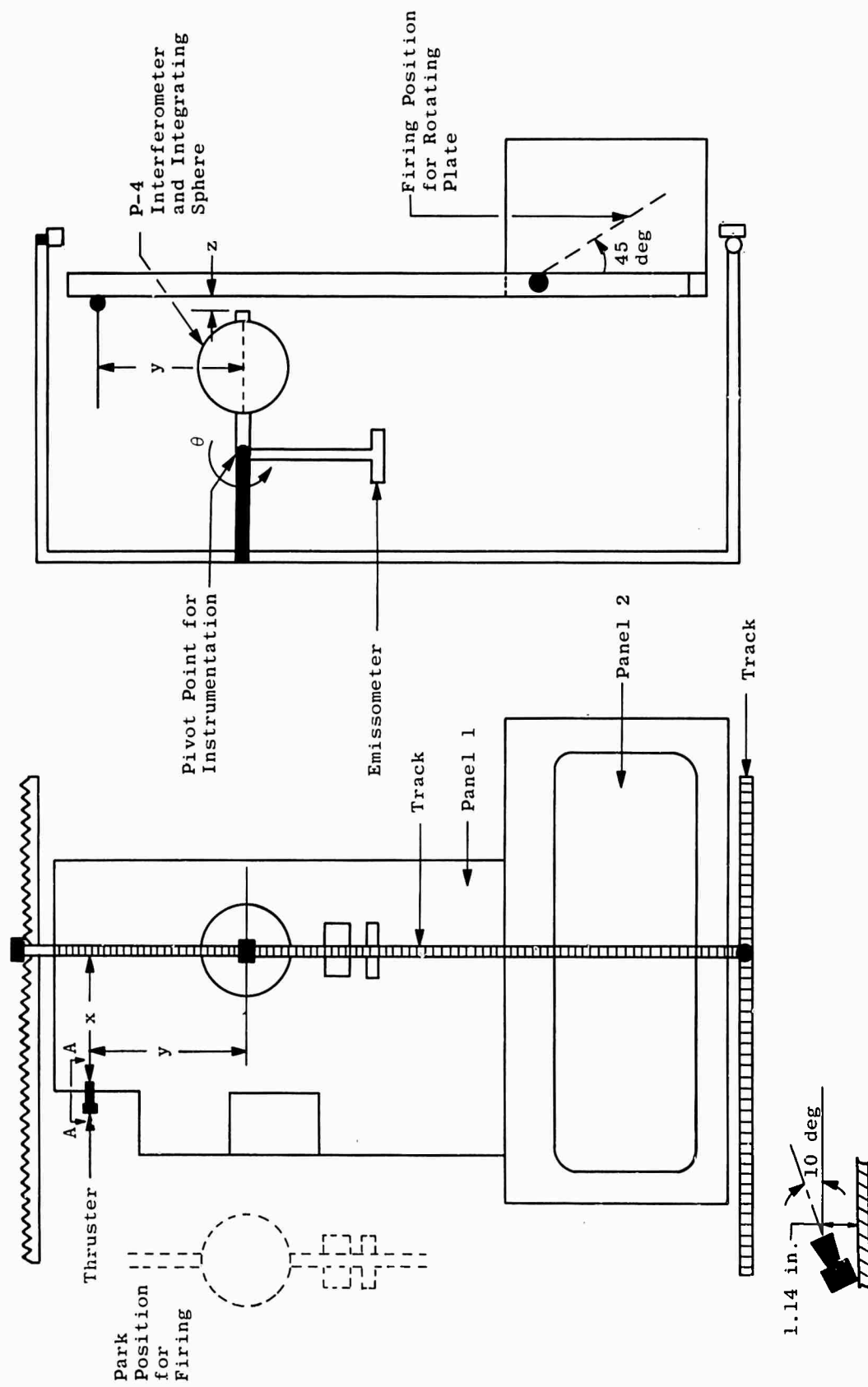


Fig. 10 Scanner Mechanism with Instrumentation

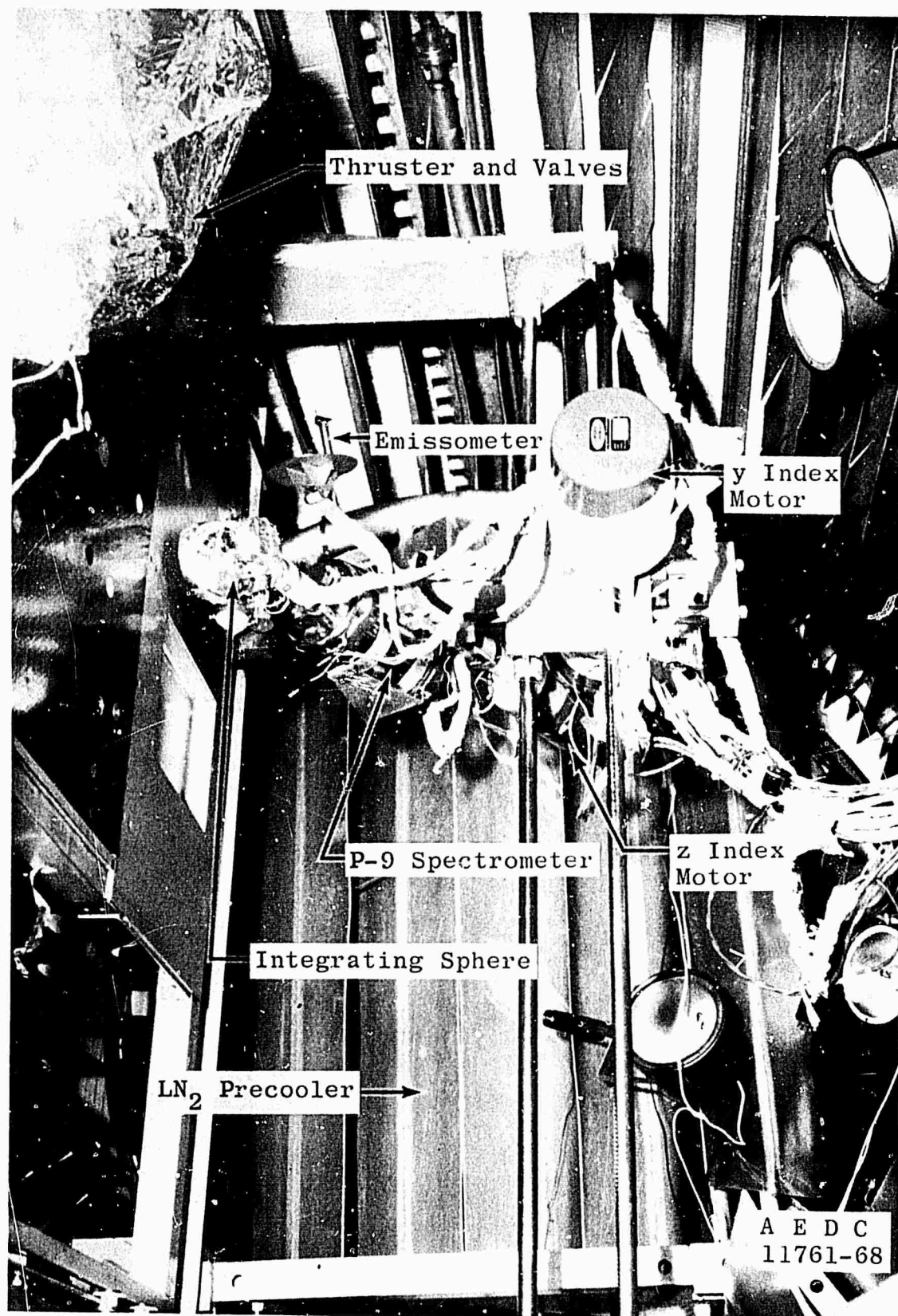


Fig. 11 Test Installation of In Situ Instrumentation

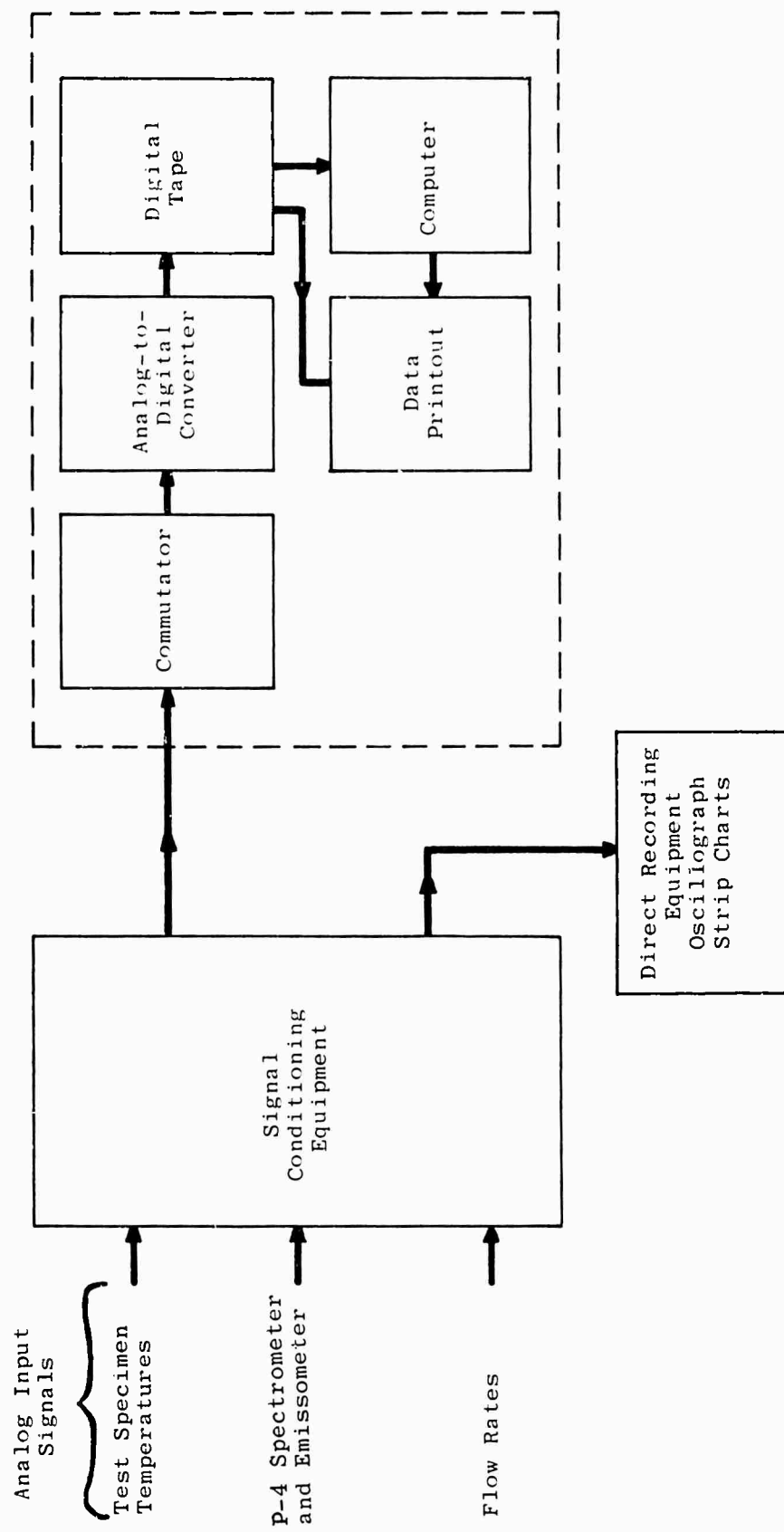


Fig. 12 Test Data System

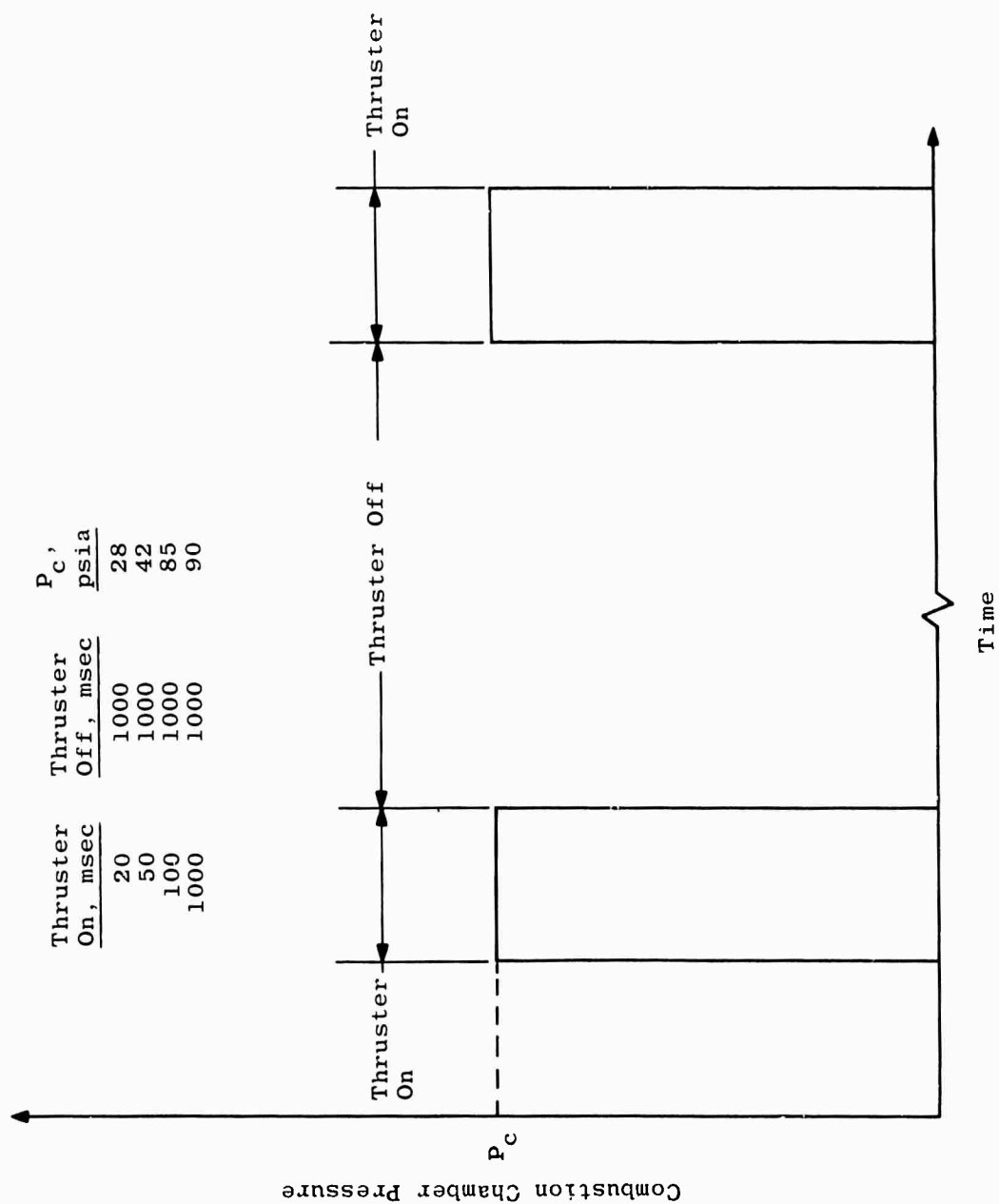


Fig. 13 Combustion Chamber Pressure versus Engine Firing Time

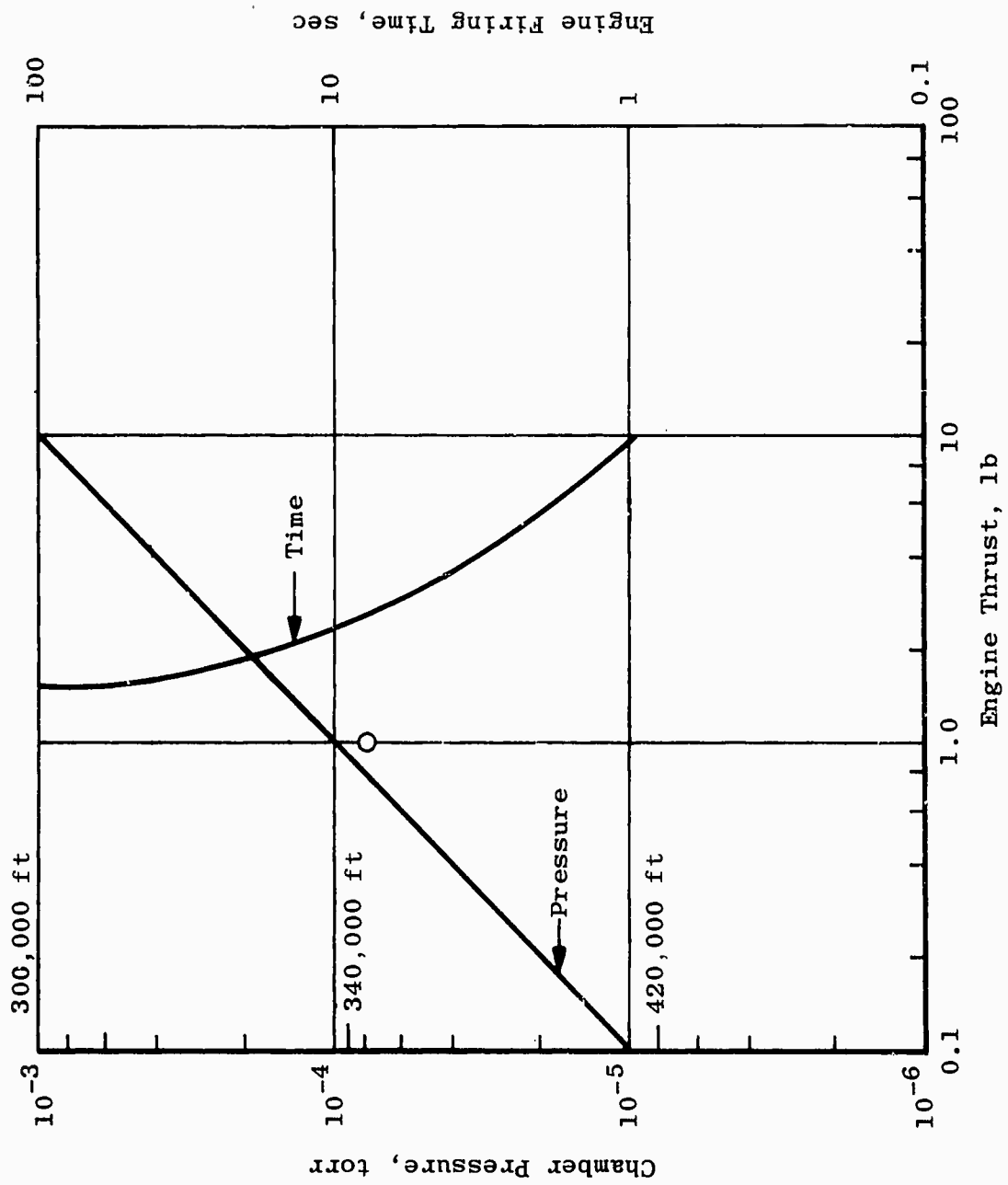


Fig. 14 Predicted ARC 8V Chamber Performance

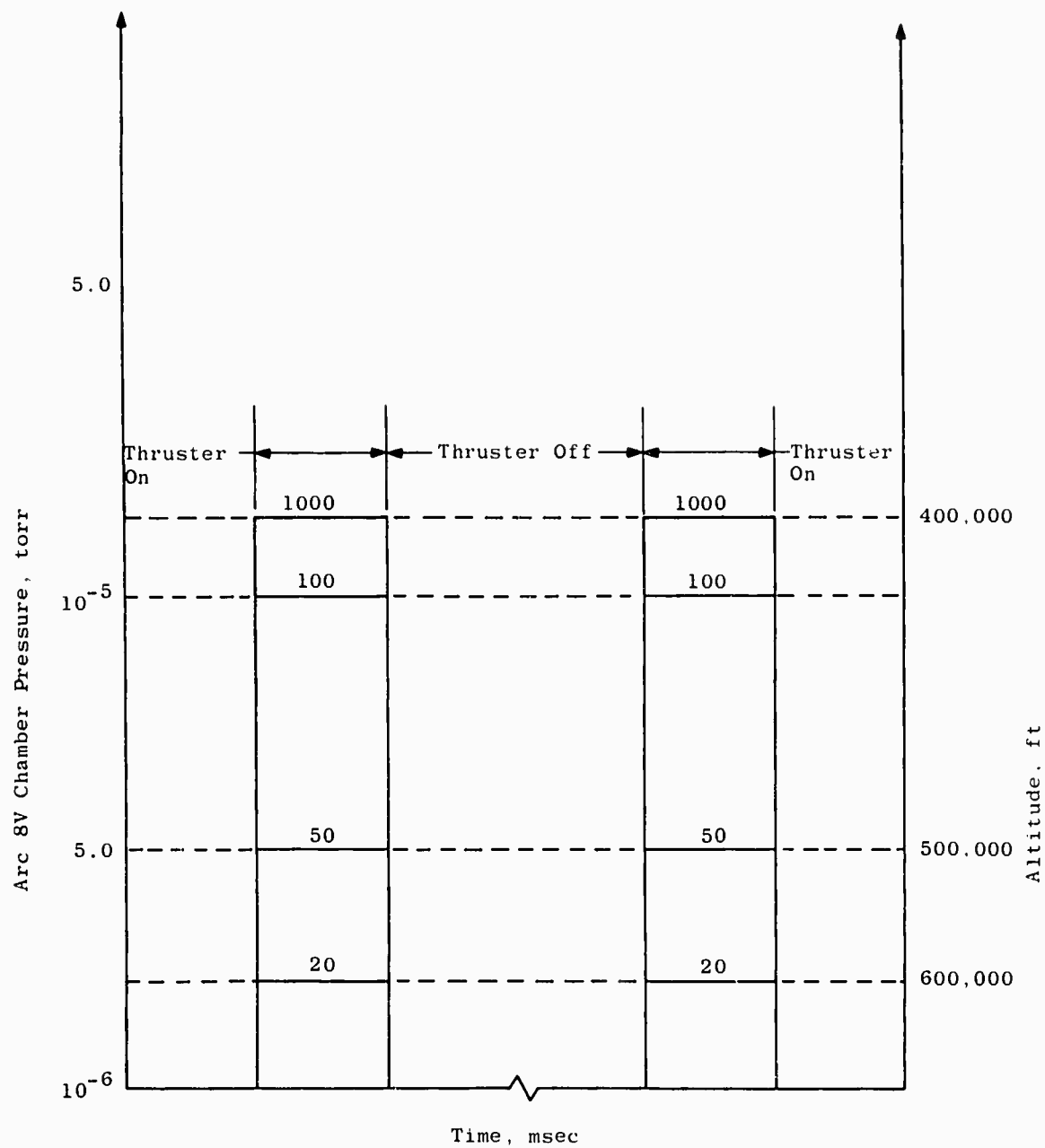


Fig. 15 ARC 8V Chamber Pressure versus Engine Firing Time

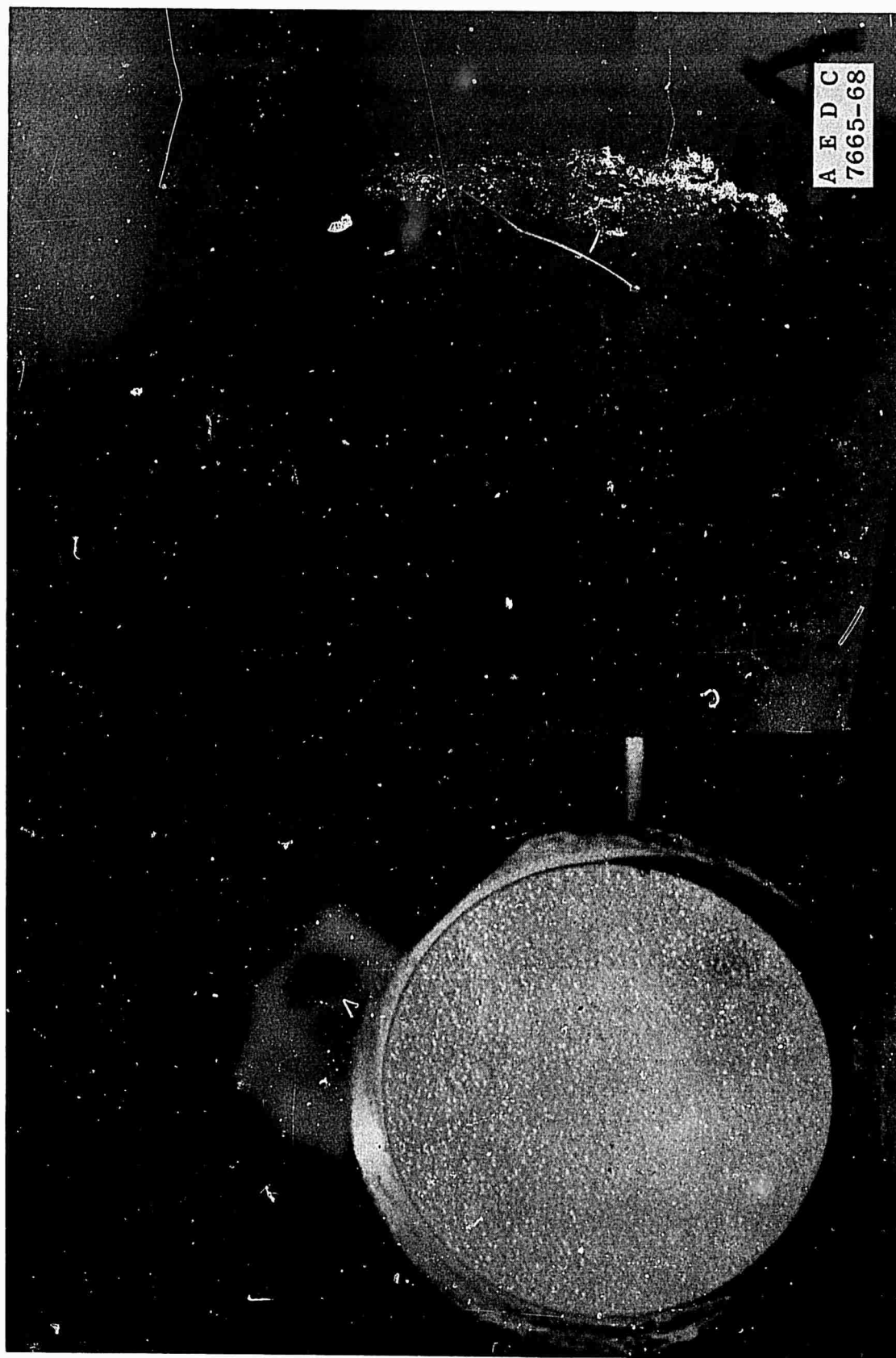
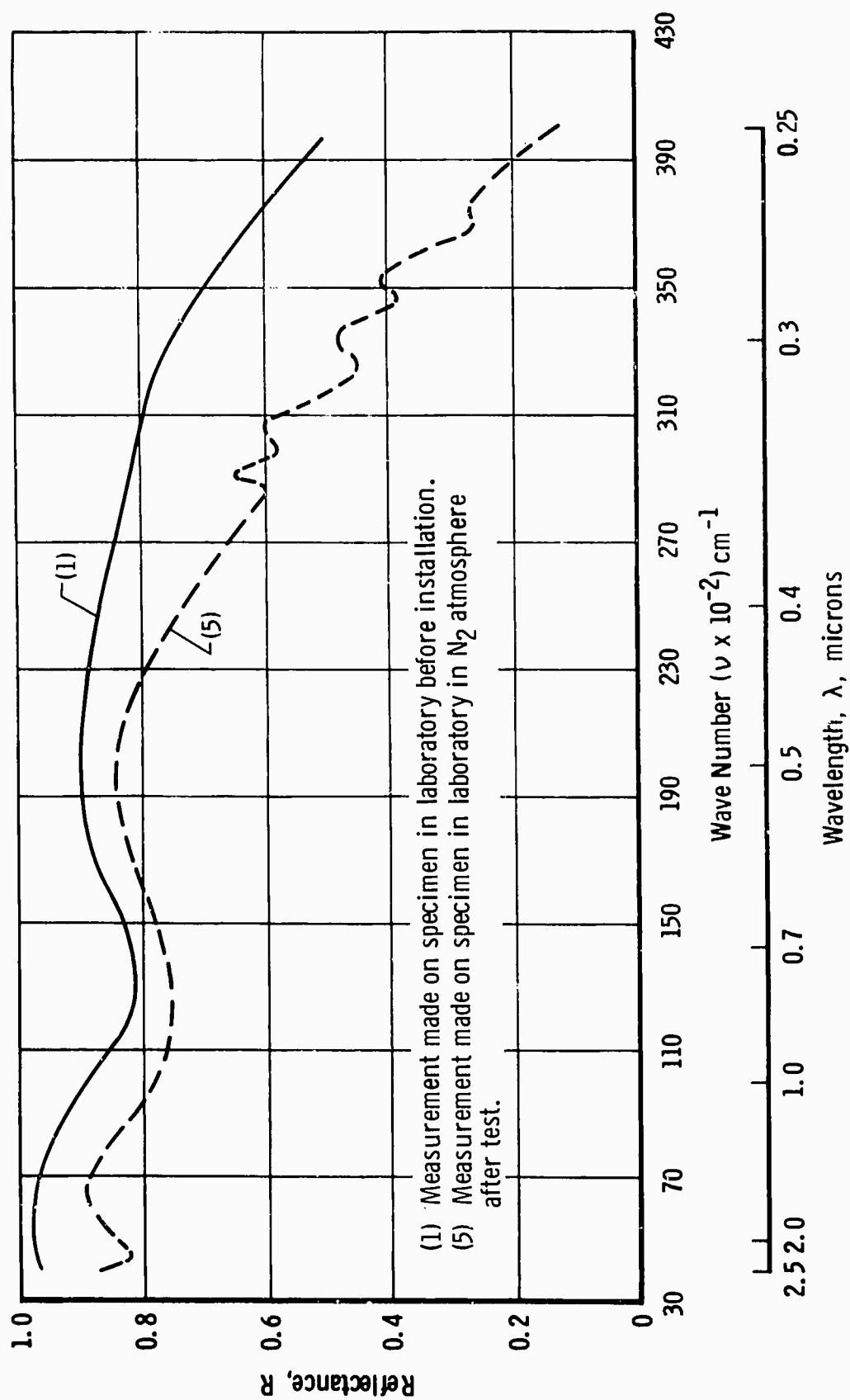
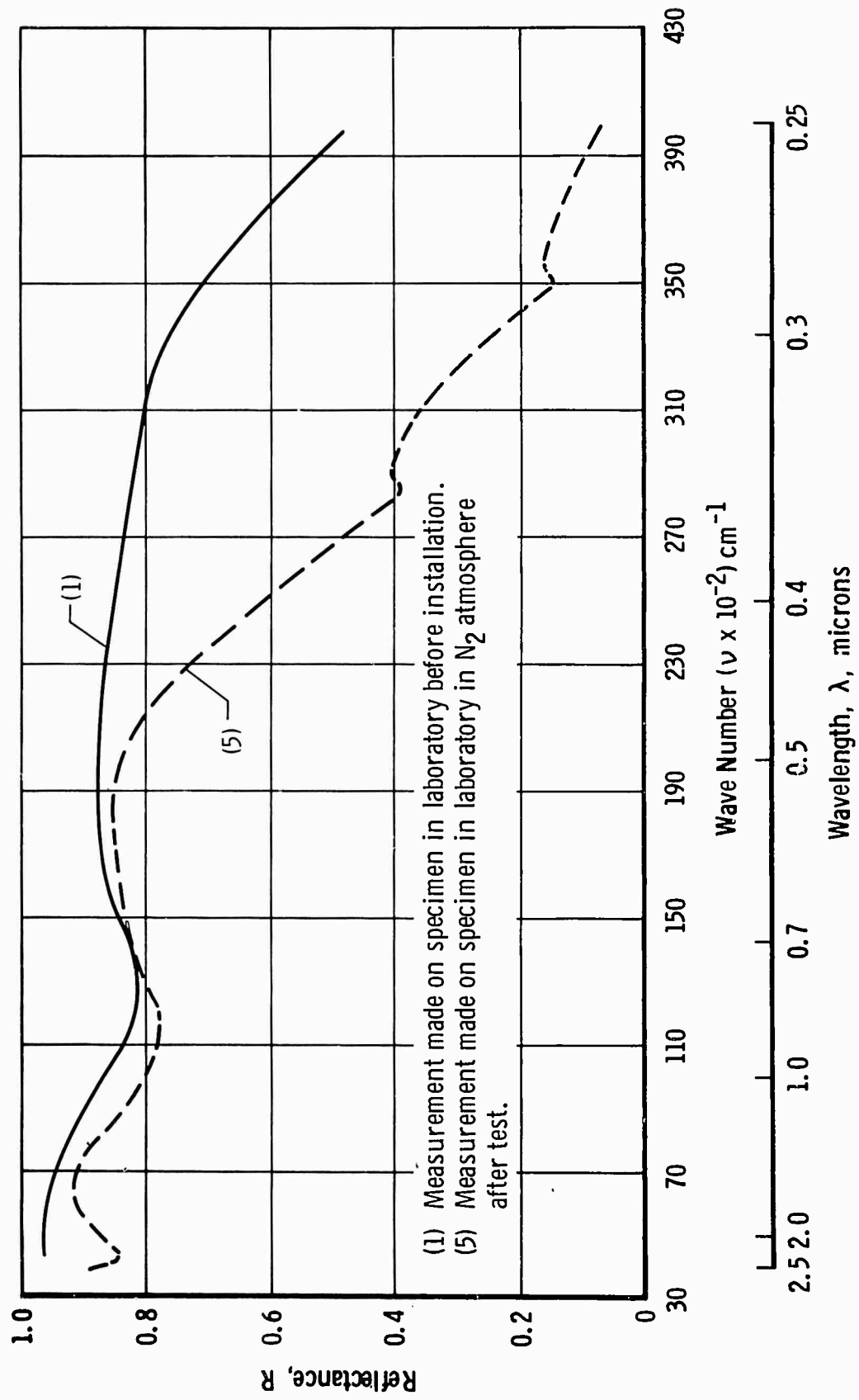


Fig. 16 Chemical Corrosion on Specimen, Location S_5 , Type A, after Test 7

Fig. 17 Test 7-Reflectance Measurements on Specimen, Location S₁, Type C

Fig. 18 Test 7—Reflectance Measurements on Specimen, Location S_2 , Type C

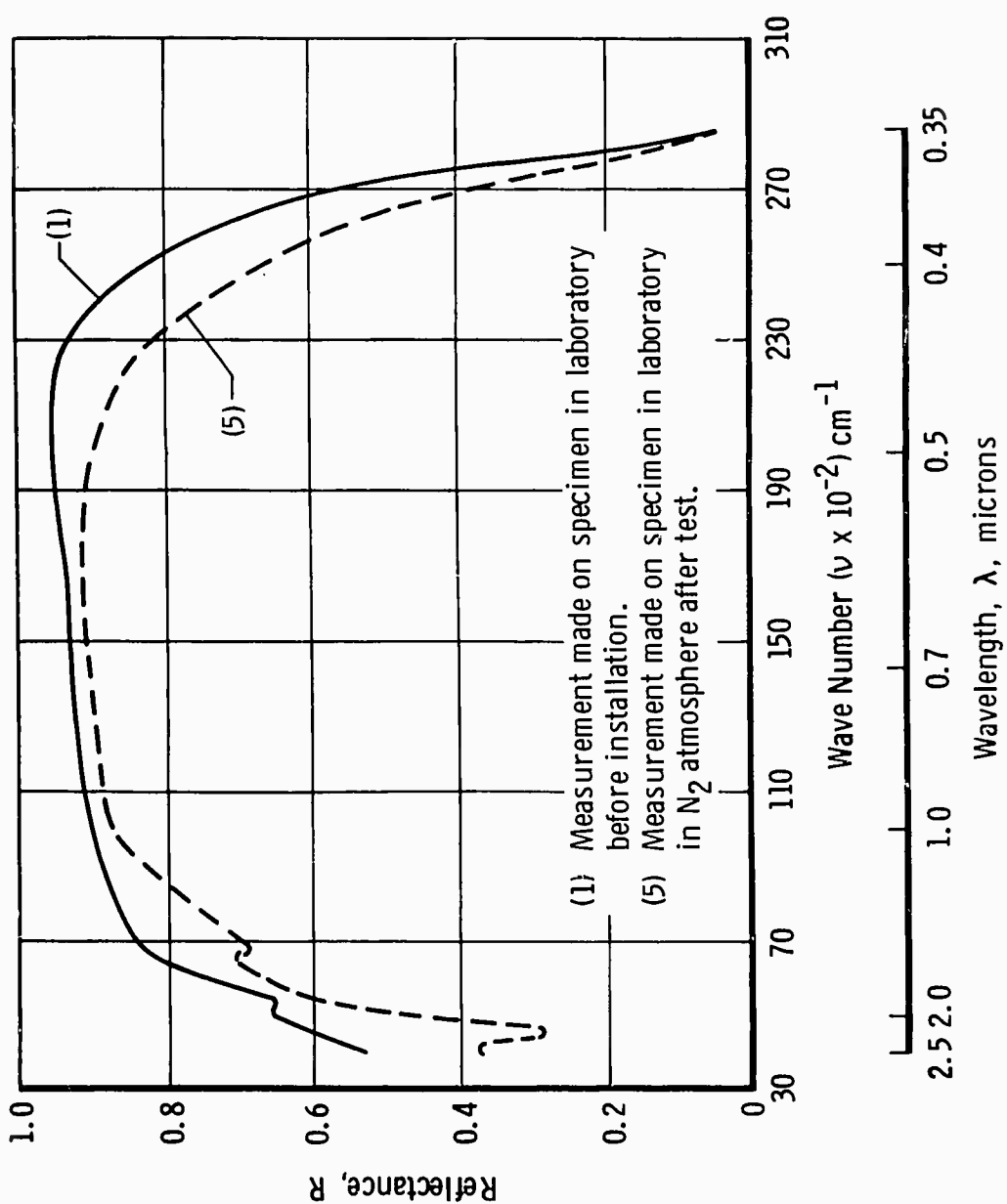


Fig. 19 Test 7—Reflectance Measurements on Specimen, Location S₅, Type A

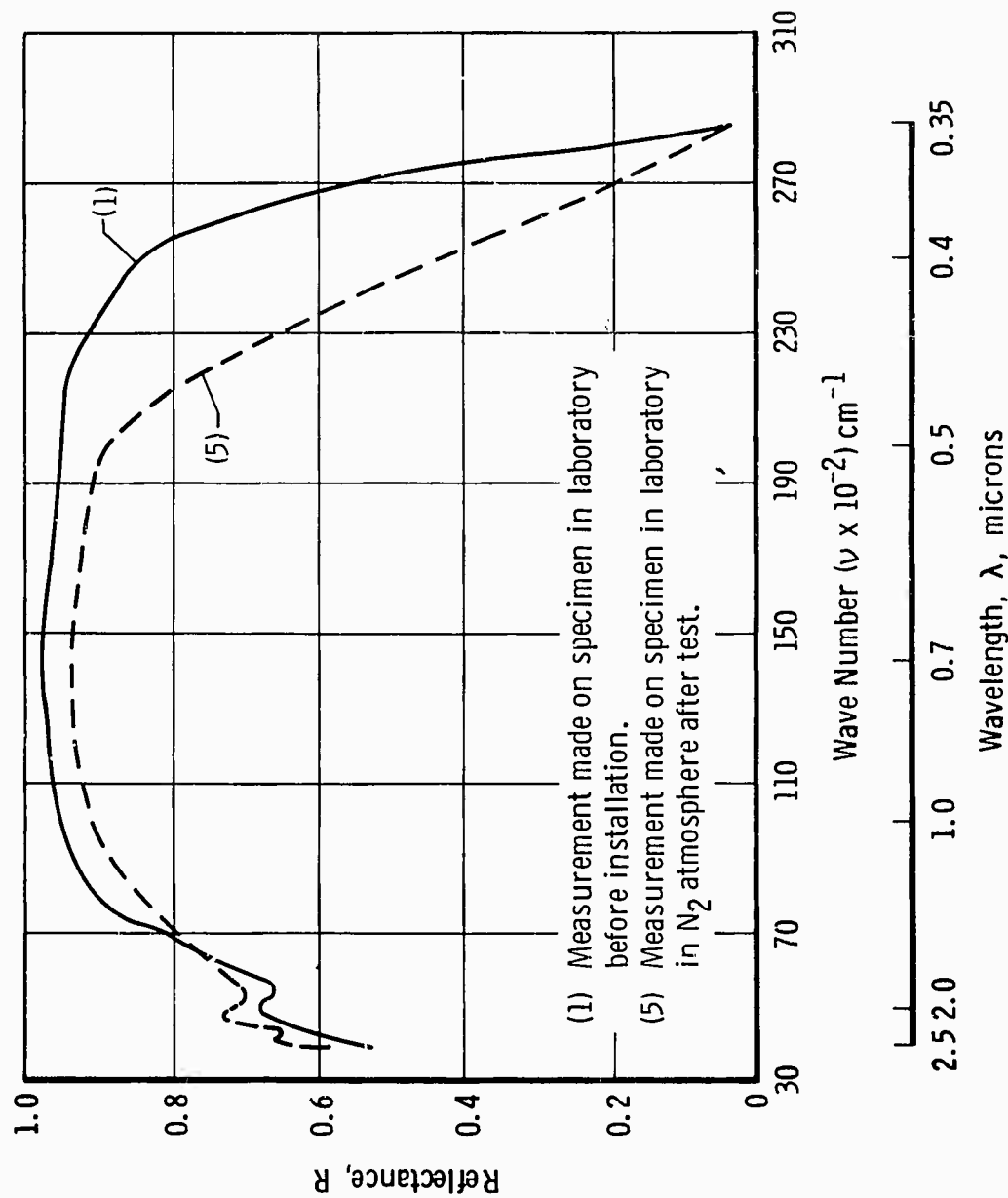


Fig. 20 Test 7—Reflectance Measurements on Specimen, Location S₆, Type A

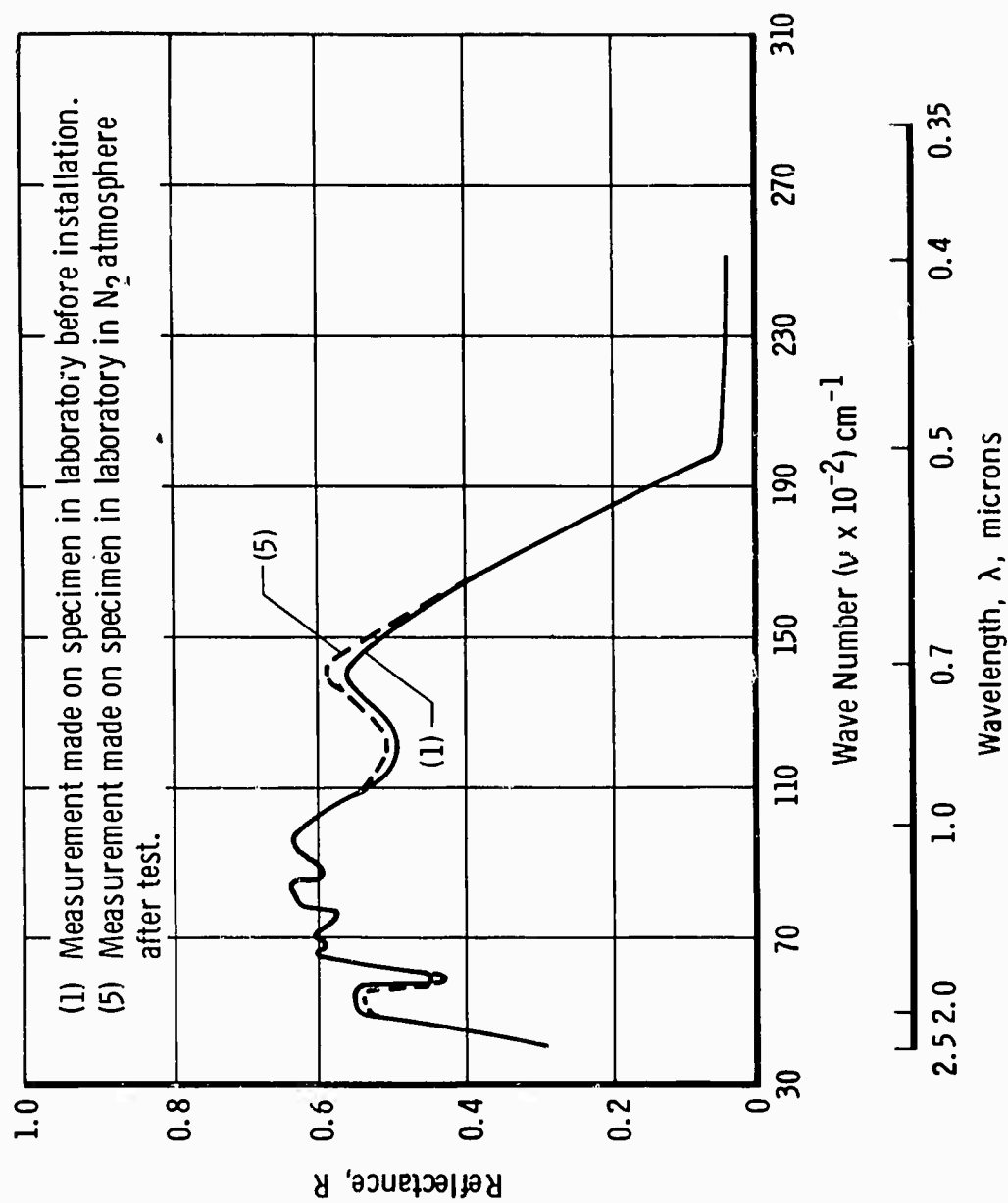


Fig. 21 Test 7—Reflectance Measurements on Specimen, Location S_9 , Type E

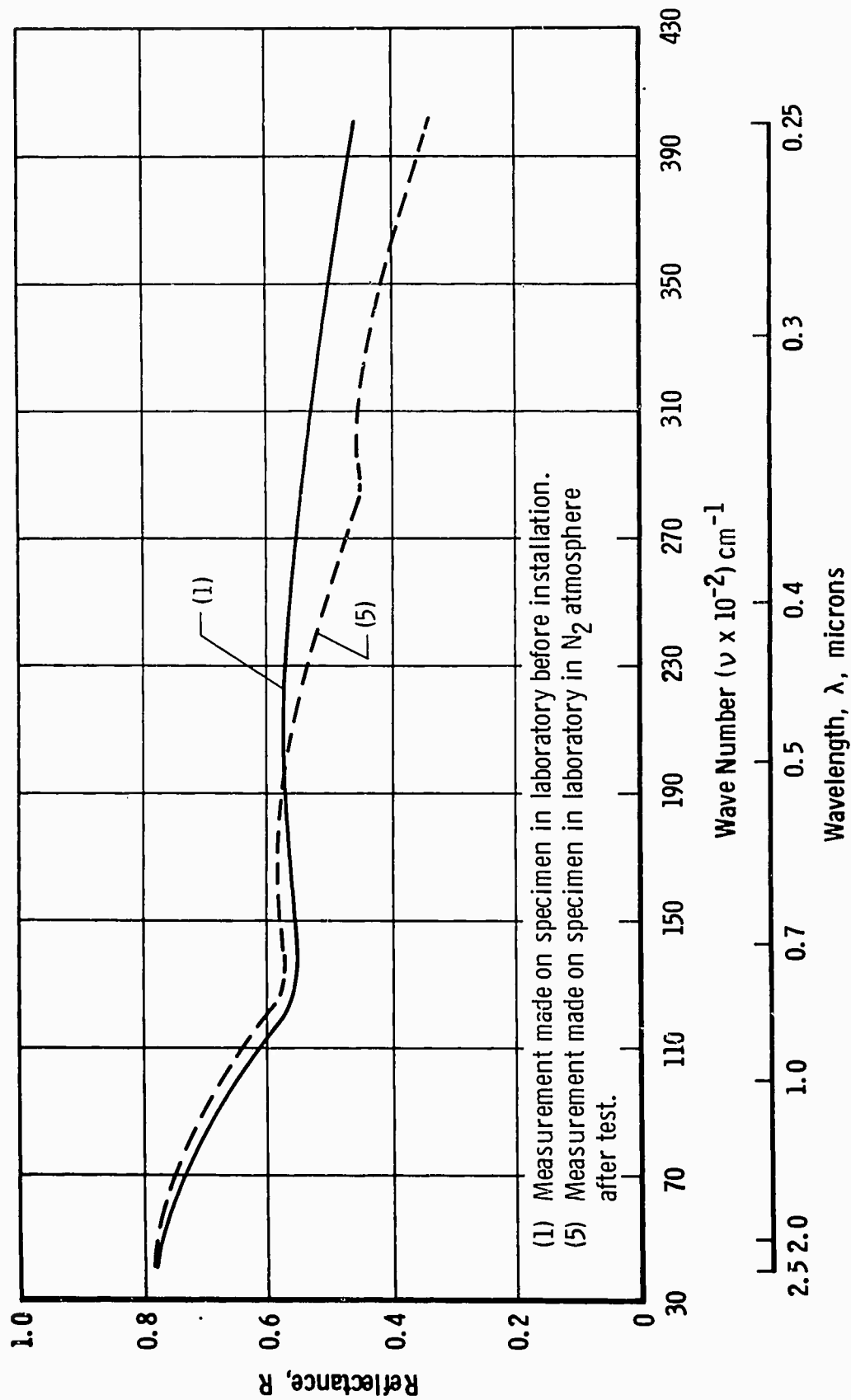


Fig. 22 Test 7—Reflectance Measurements on Specimen, Location S₁₄, Type E

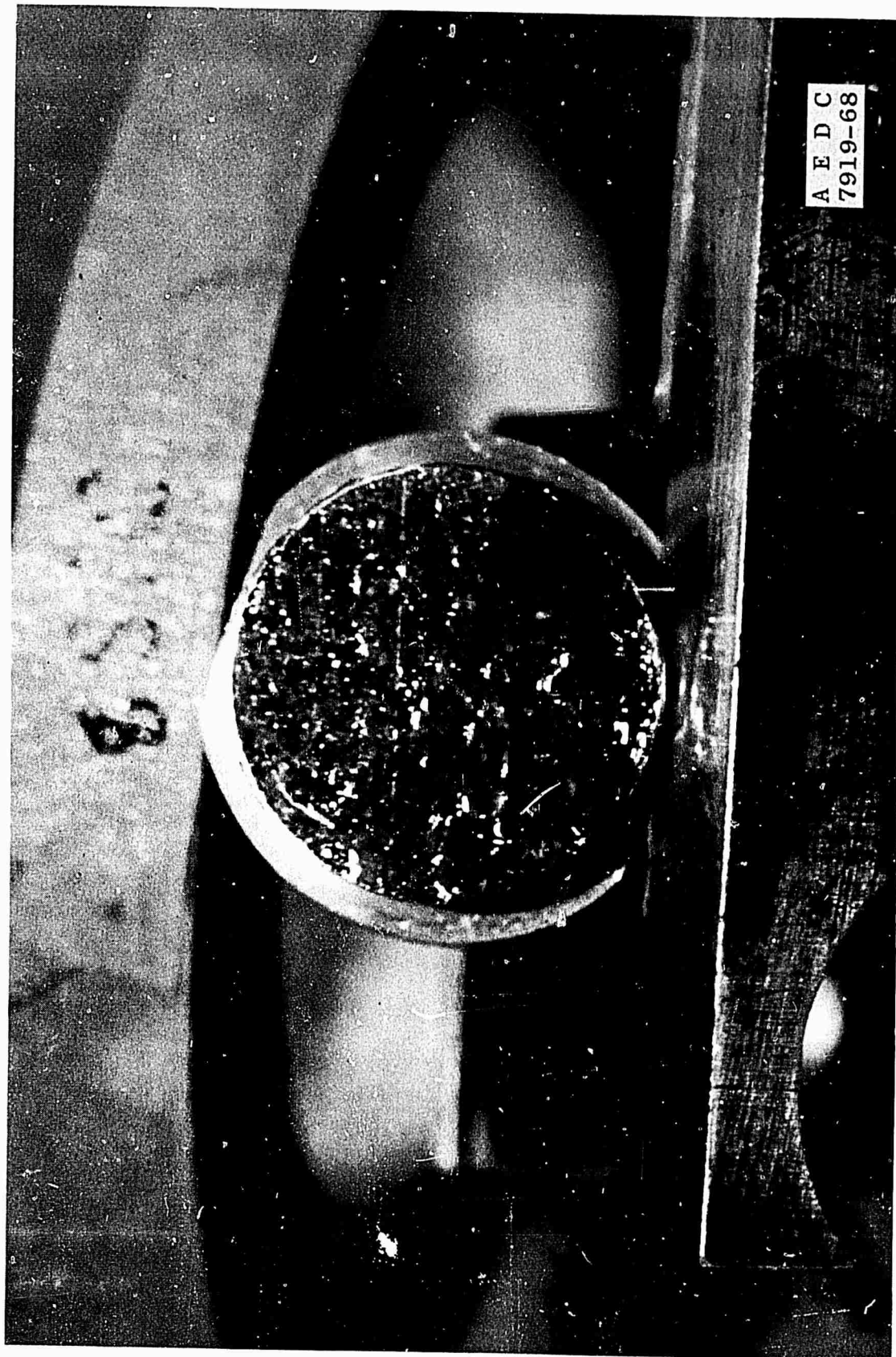


Fig. 23 Test 8—Contamination on Specimen, Location S₁, Type C, after Test

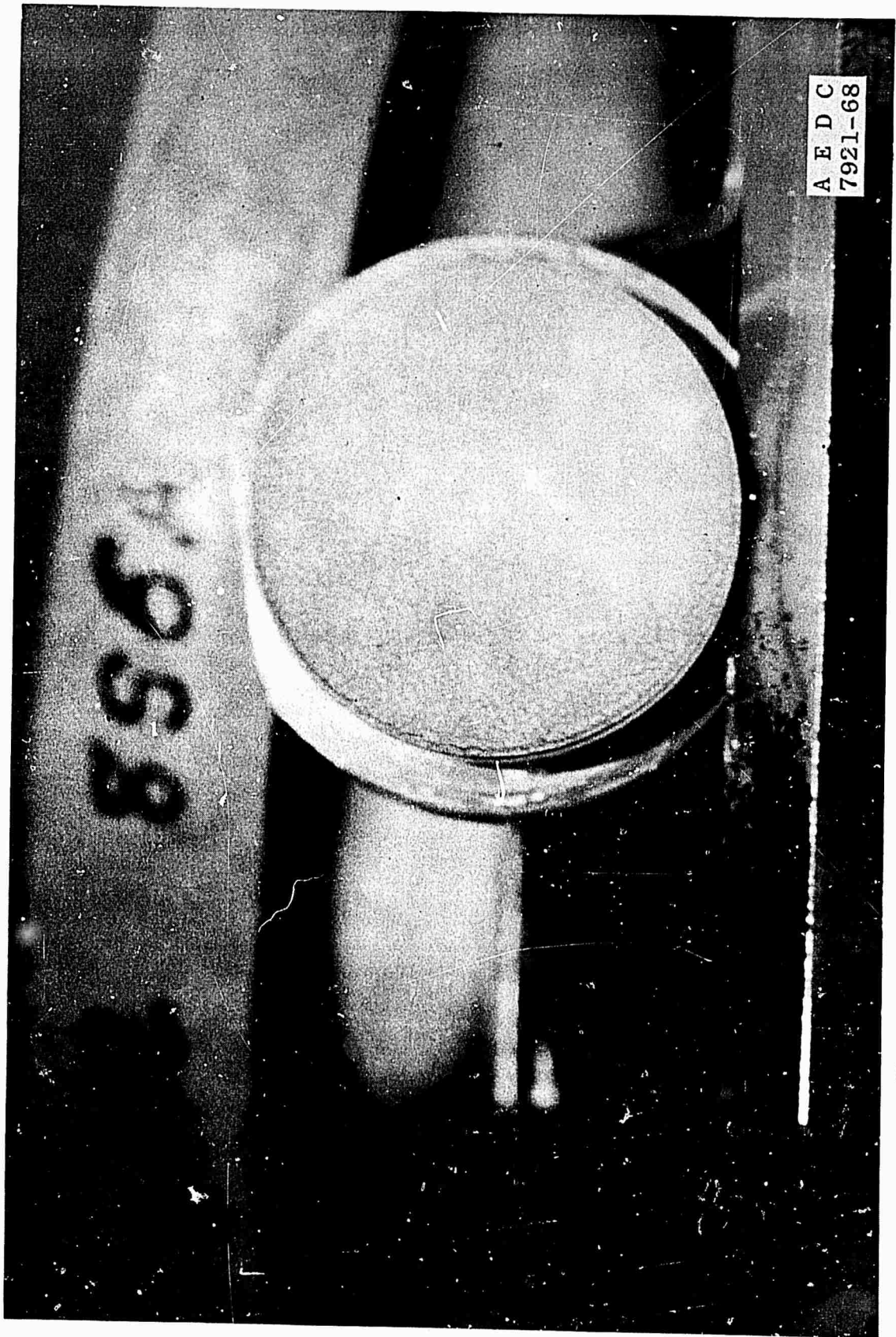


Fig. 24 Test 8—Contamination on Specimen, Location S₆, Type A, after Test

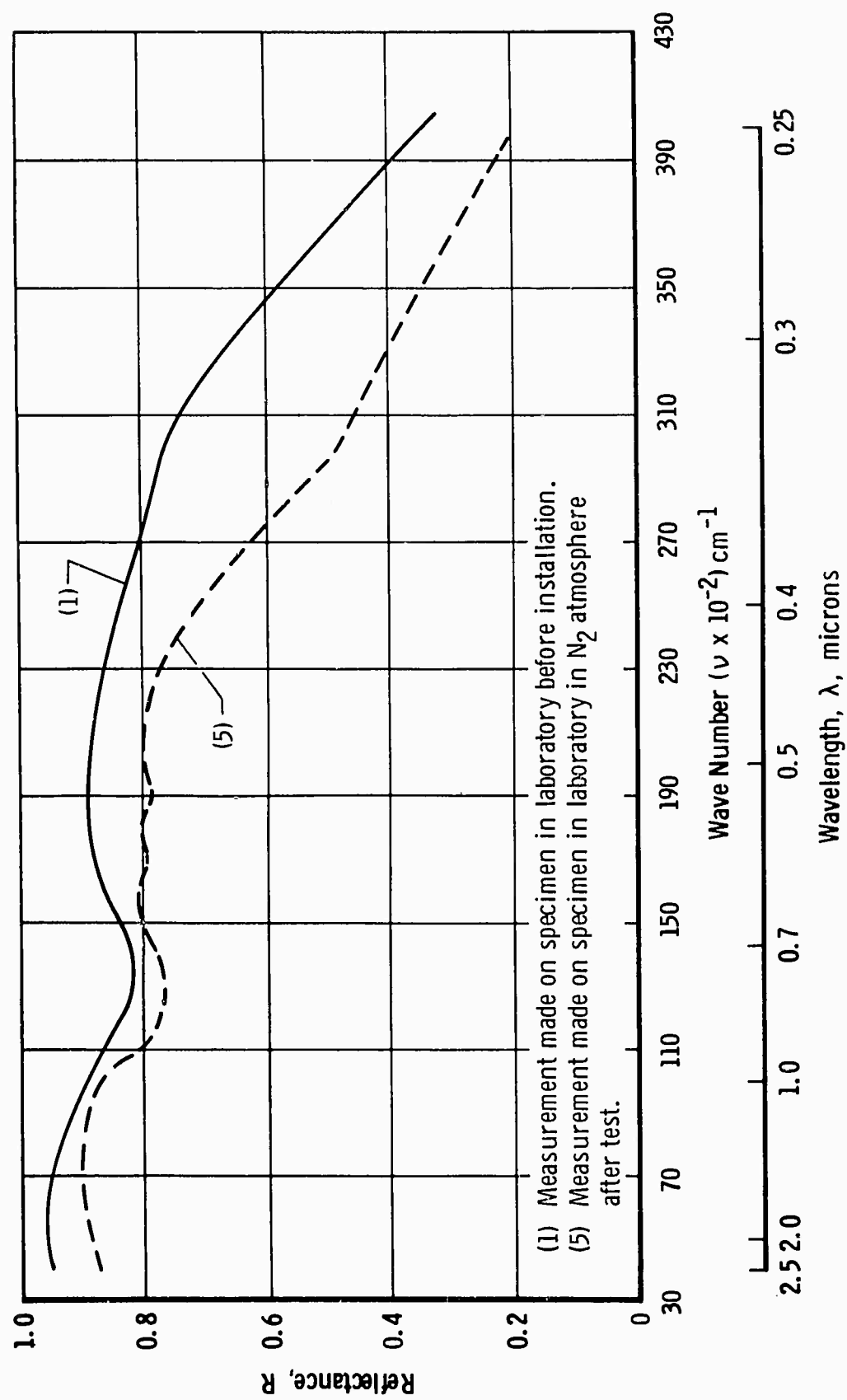


Fig. 25 Test 8—Reflectance Measurements on Specimen, Location S₁, Type C

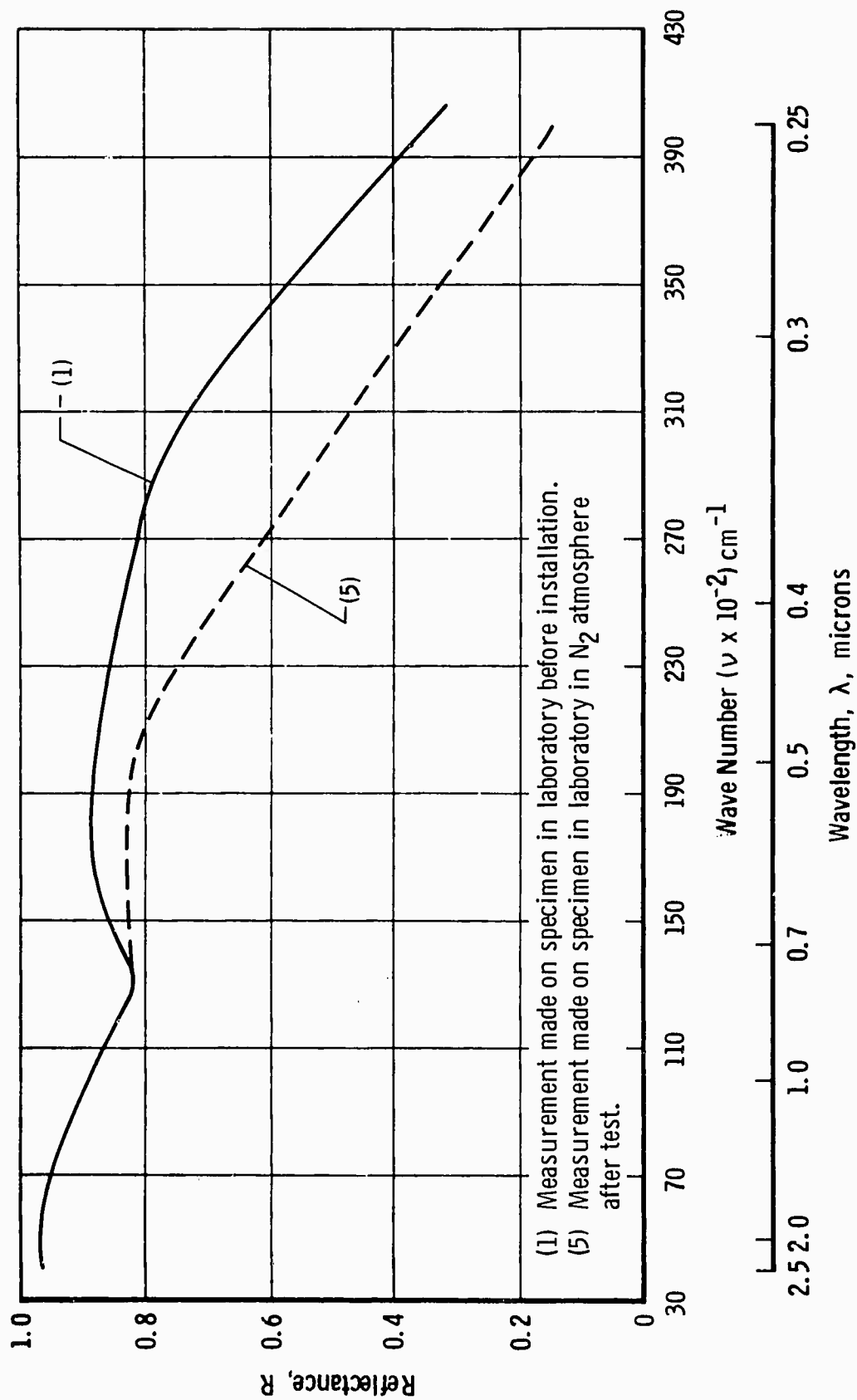


Fig. 26 Test 8—Reflectance Measurements on Specimen, Location S_2 , Type C

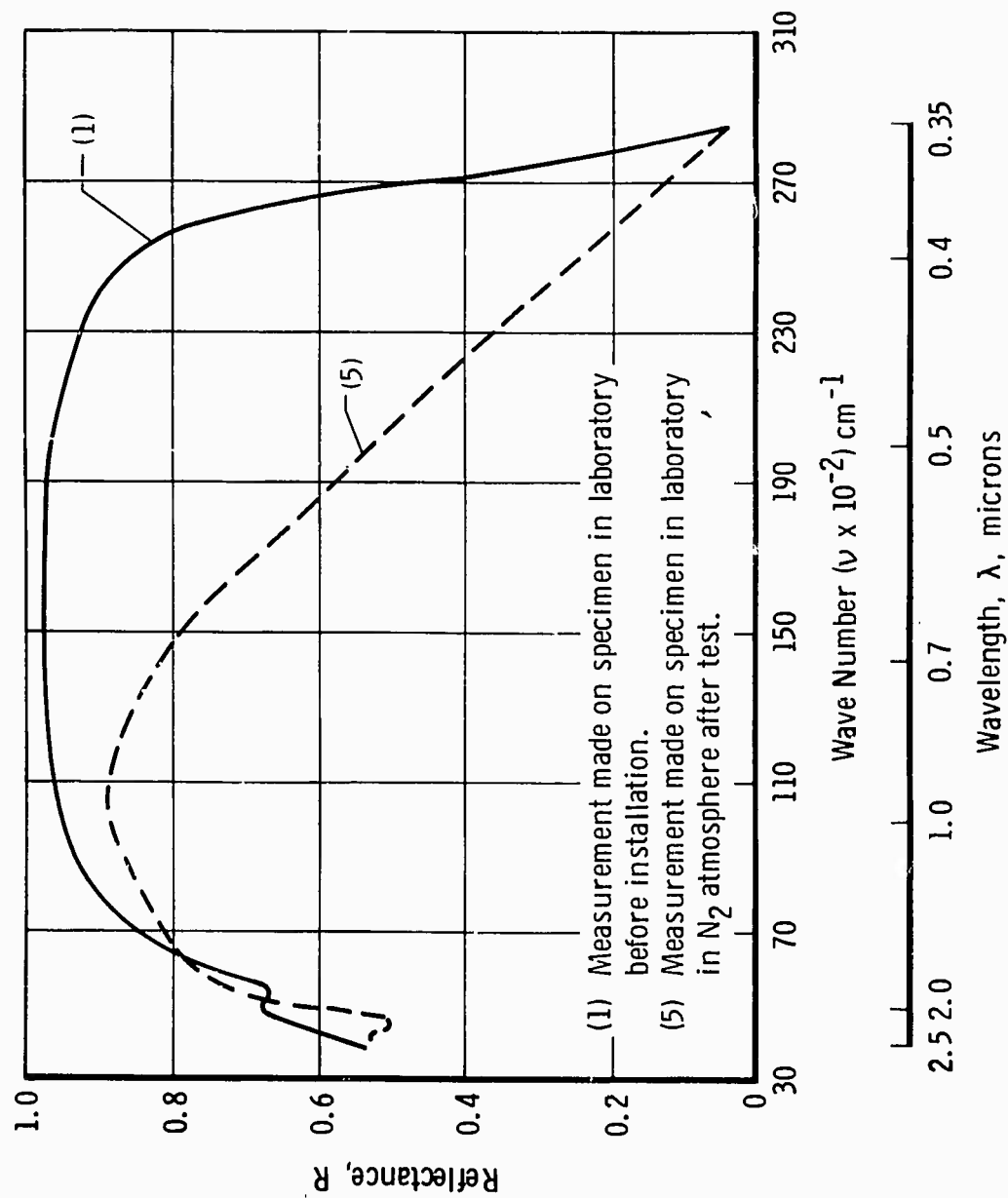
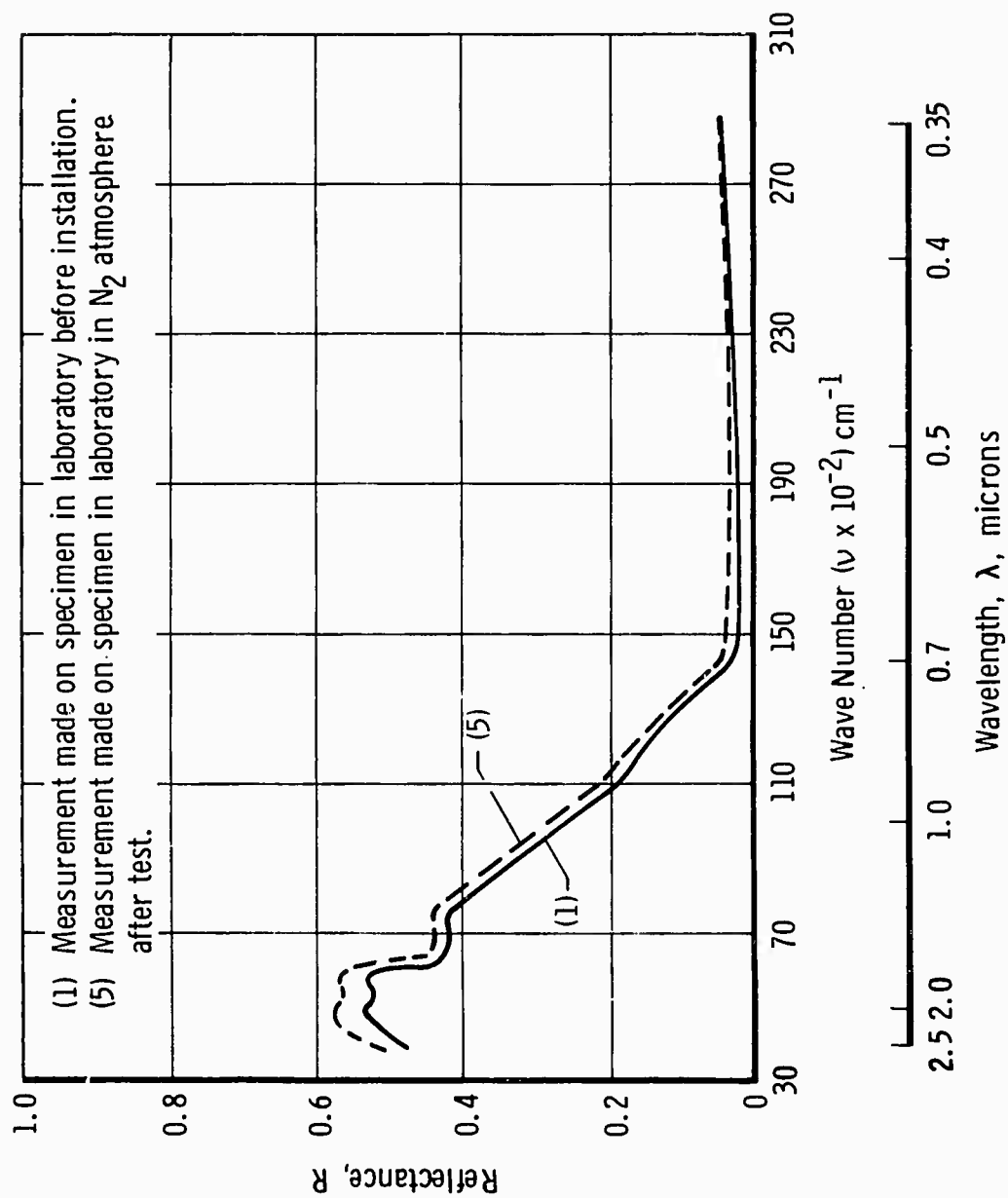


Fig. 27 Test 8—Reflectance Measurements on Specimen, Location S_6 , Type A

Fig. 28 Test 8—Reflectance Measurements on Specimen, Location S₁₀, Type K

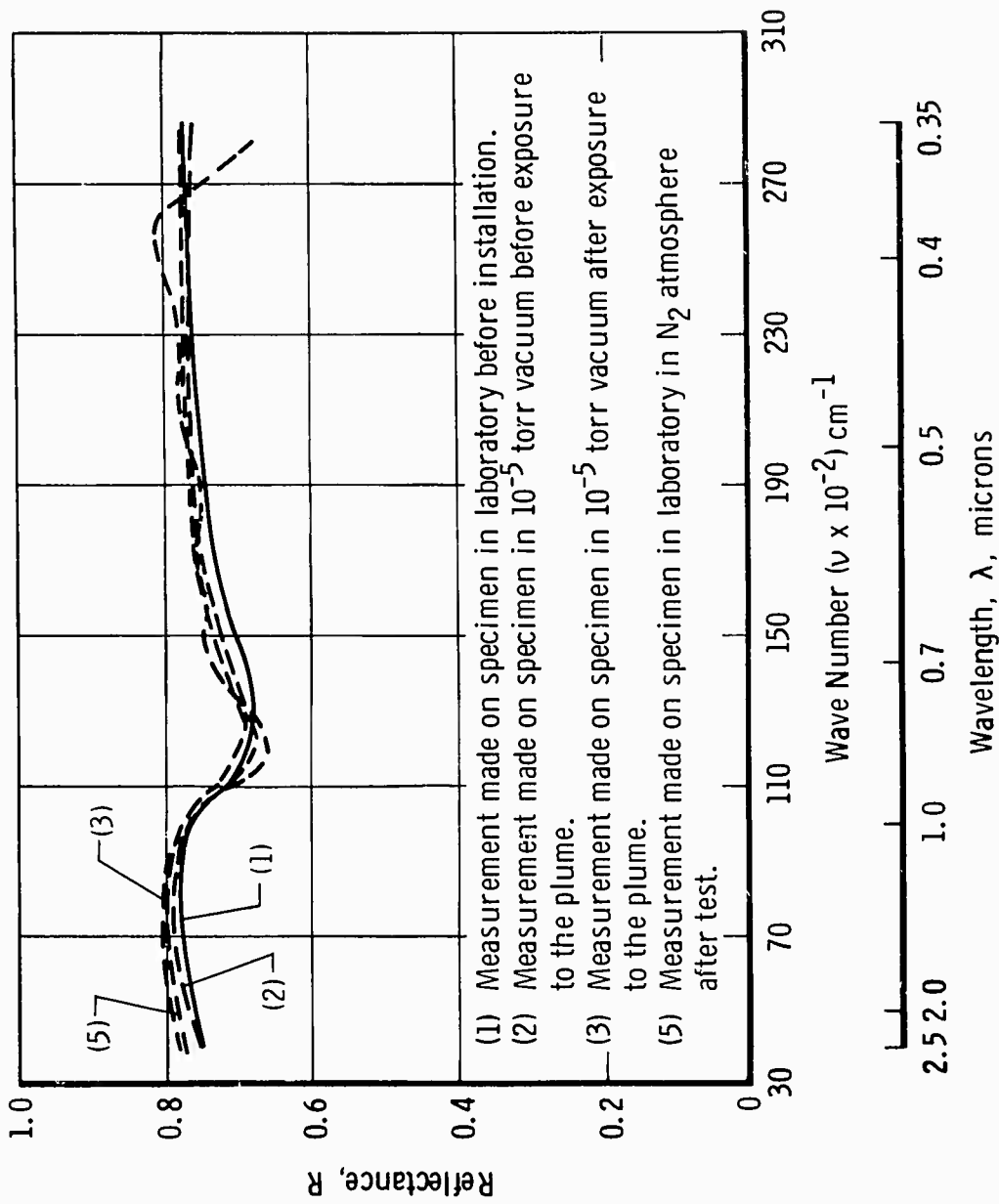


Fig. 29 Test 8—Reflectance Measurements on Specimen, Location S₁₉, Type B

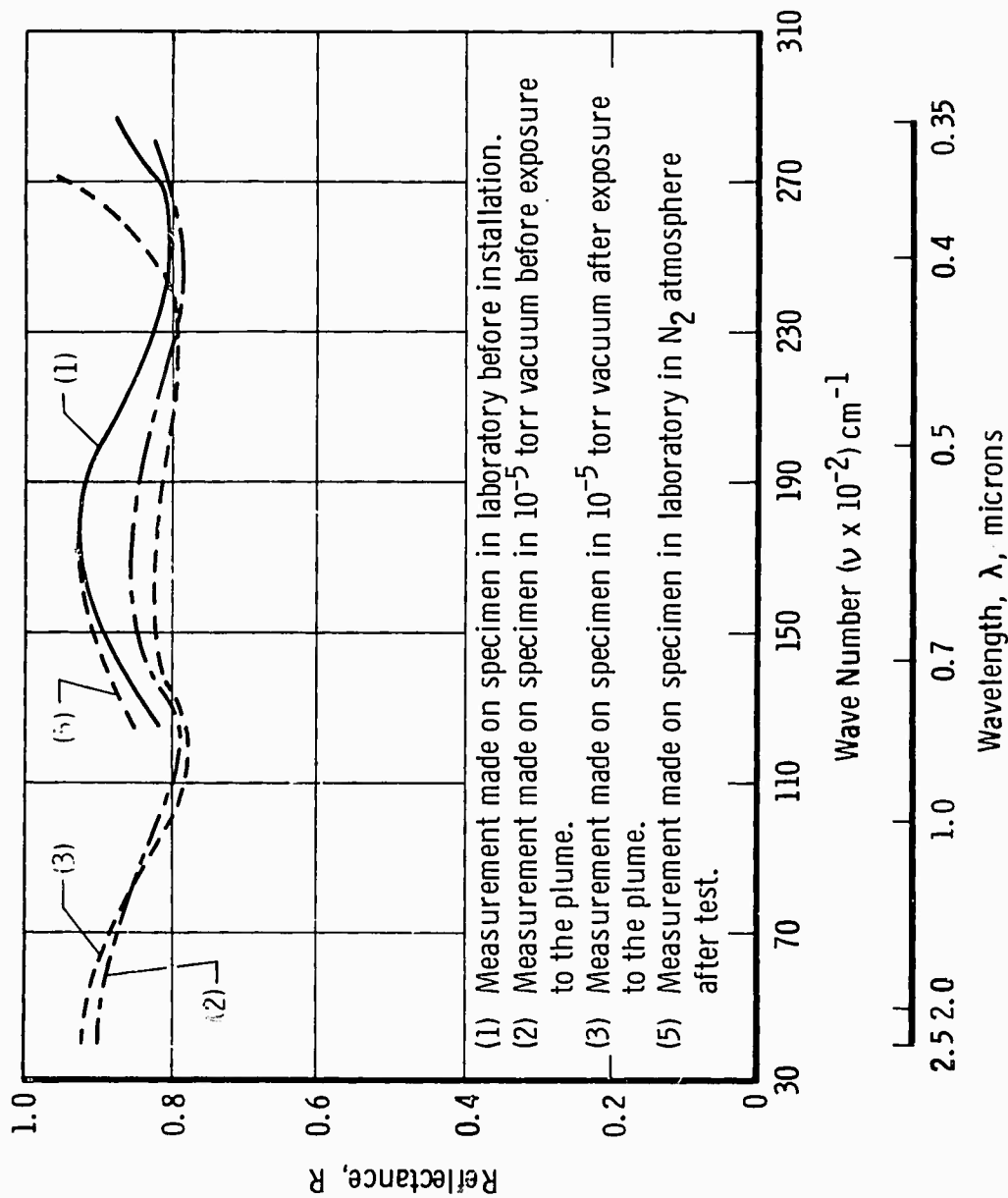
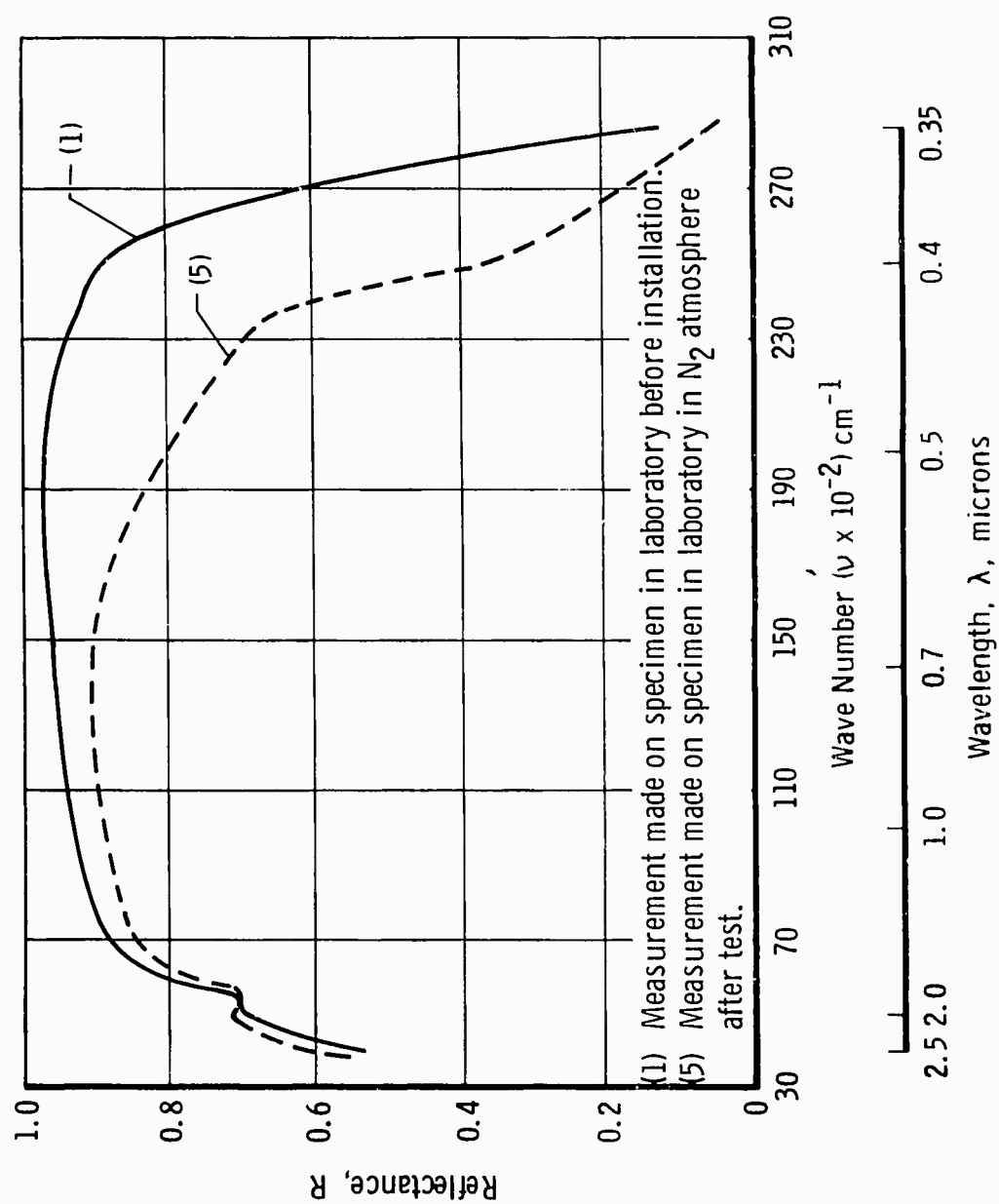


Fig. 30 Test 8—Reflectance Measurements on Specimen, Location S₂₅, Type M

Fig. 31 Test 9—Reflectance Measurements on Specimen, Location S_g , Type A

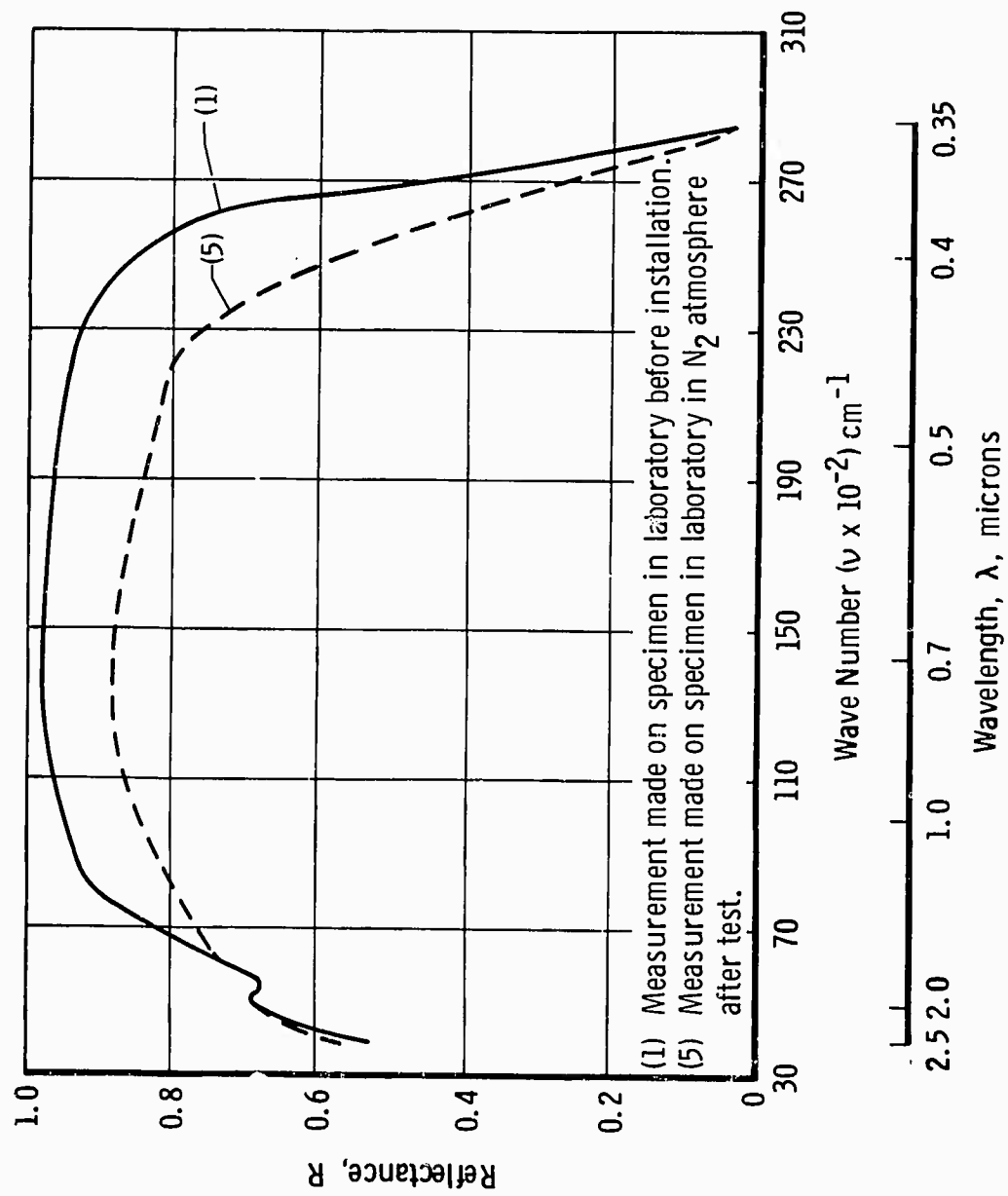
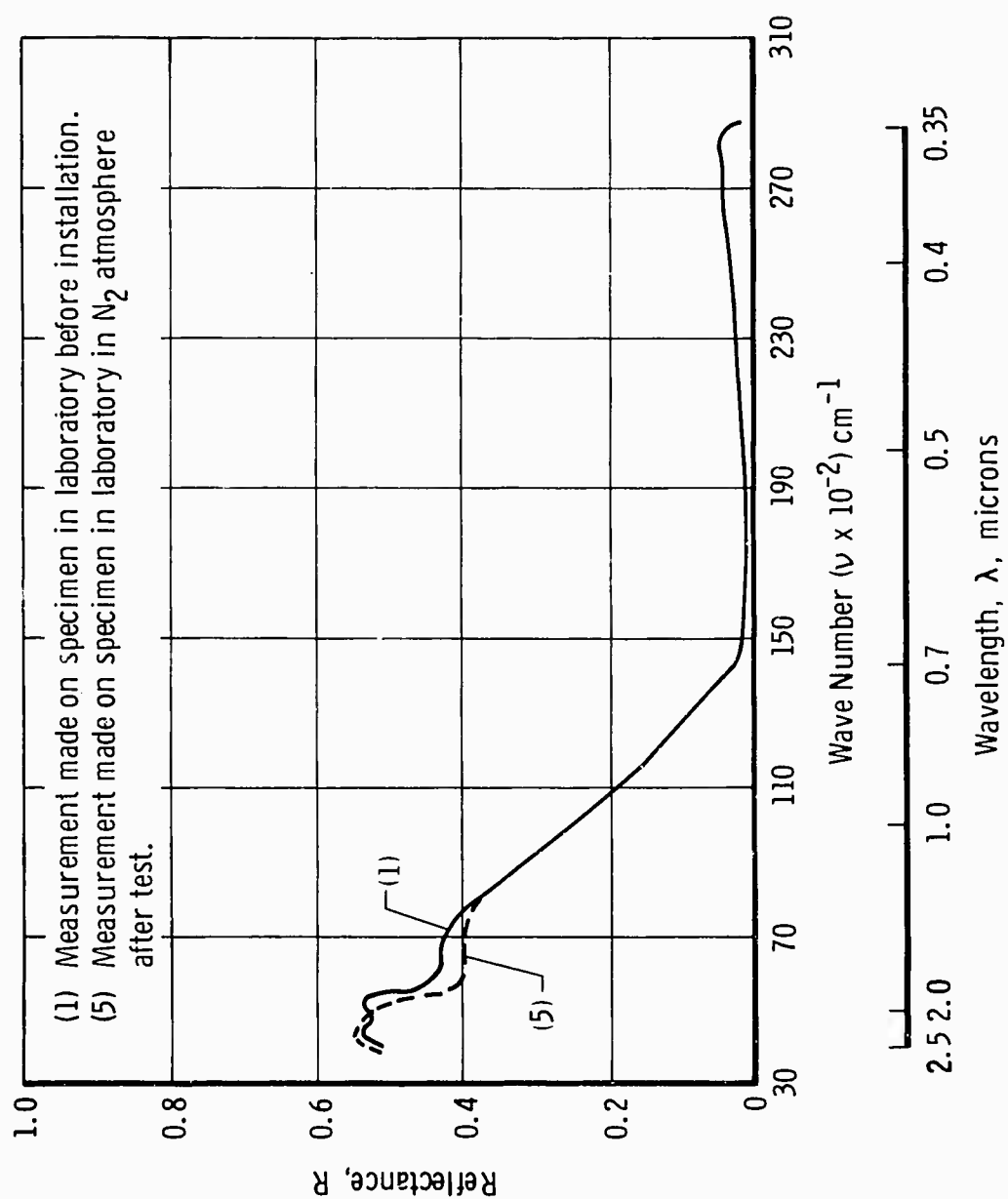
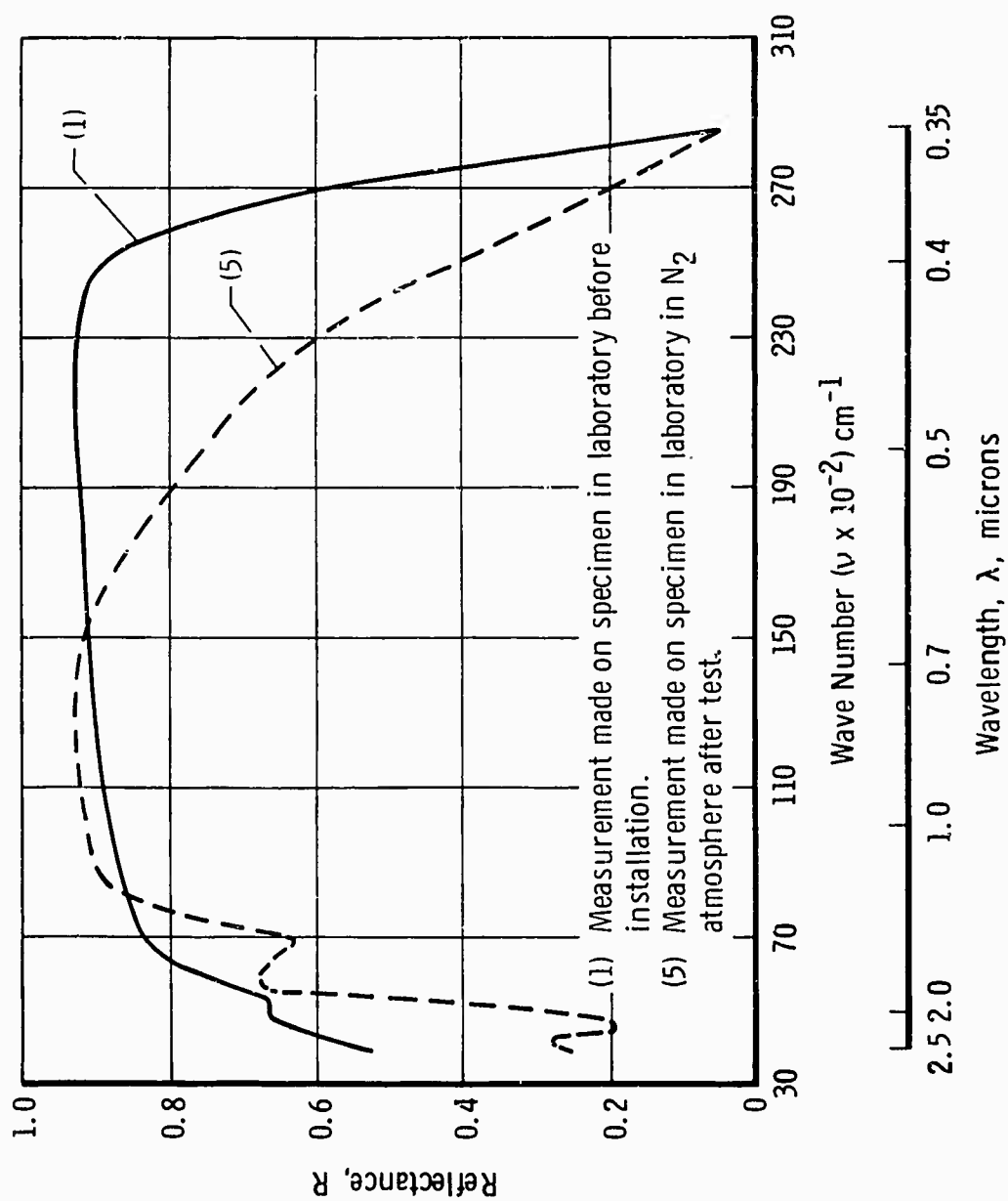
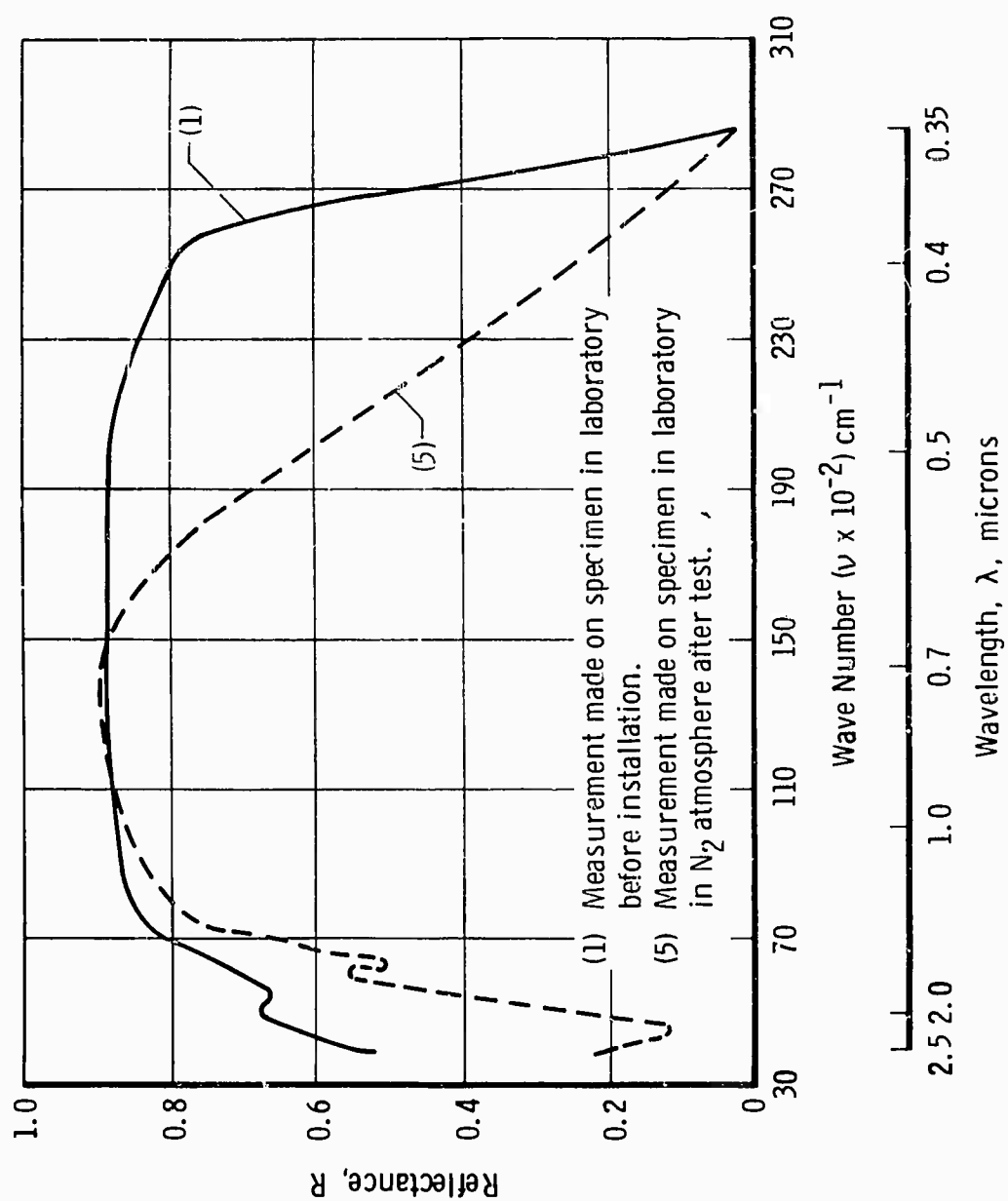
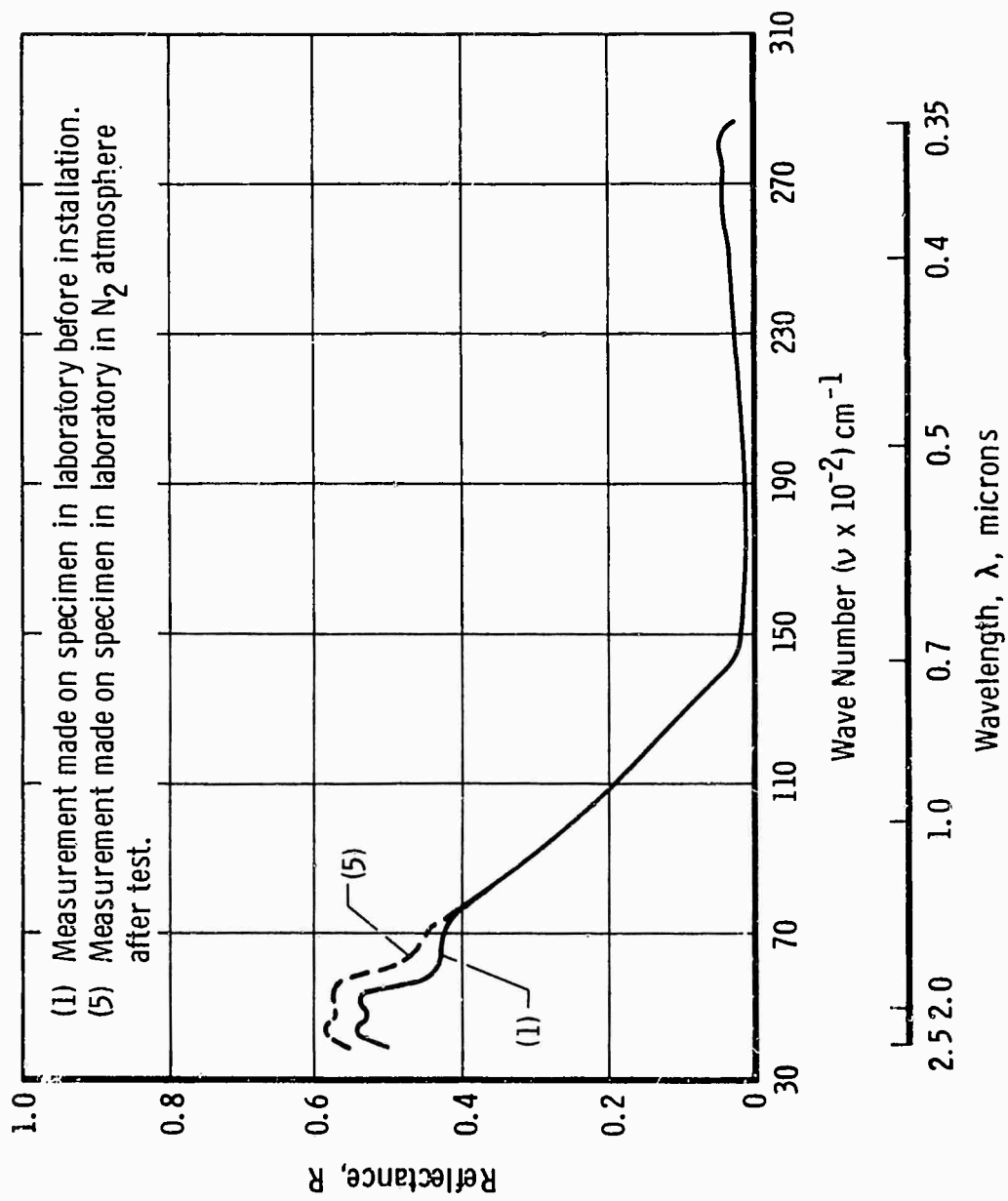


Fig. 32 Test 9—Reflectance Measurements on Specimen, Location S_6 , Type A

Fig. 33 Test 9—Reflectance Measurements on Specimen, Location S_{10} , Type K

Fig. 34 Test 10B—Reflectance Measurements on Specimen, Location S_6 , Type A

Fig. 35 Test 10B—Reflectance Measurements on Specimen, Location S₆, Type A

Fig. 36 Test 10B—Reflectance Measurements on Specimen, Location S_{10} , Type K

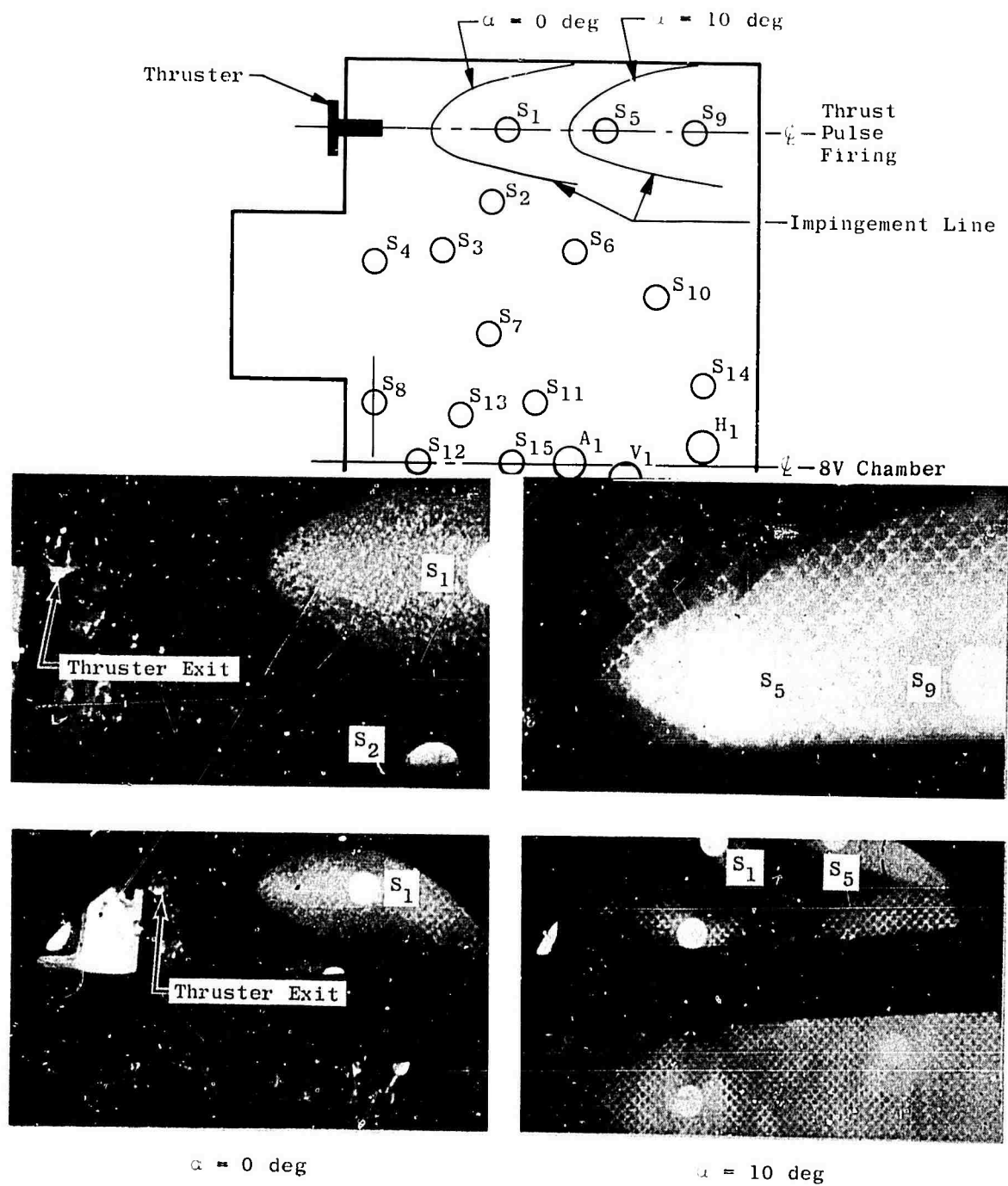
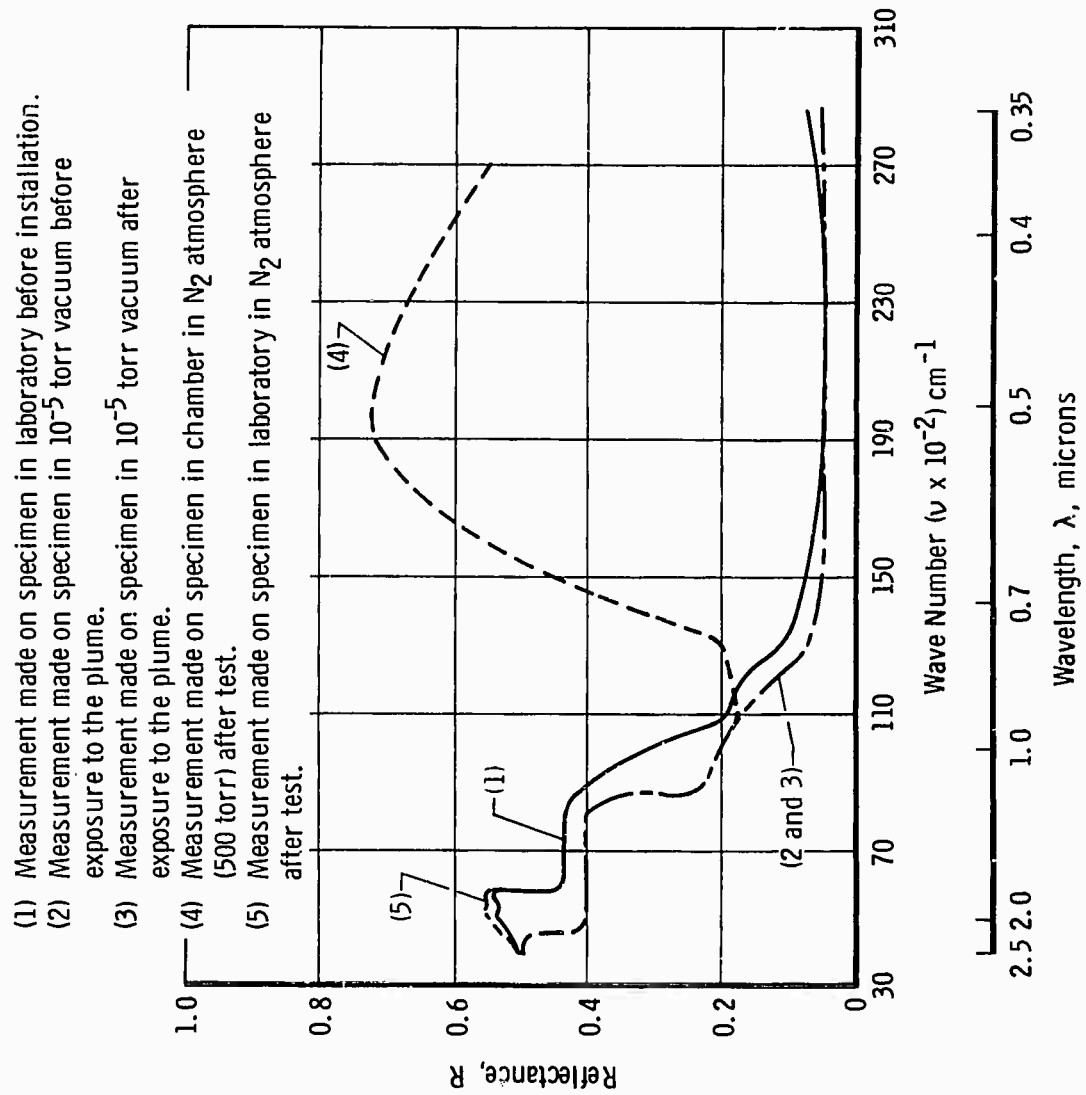
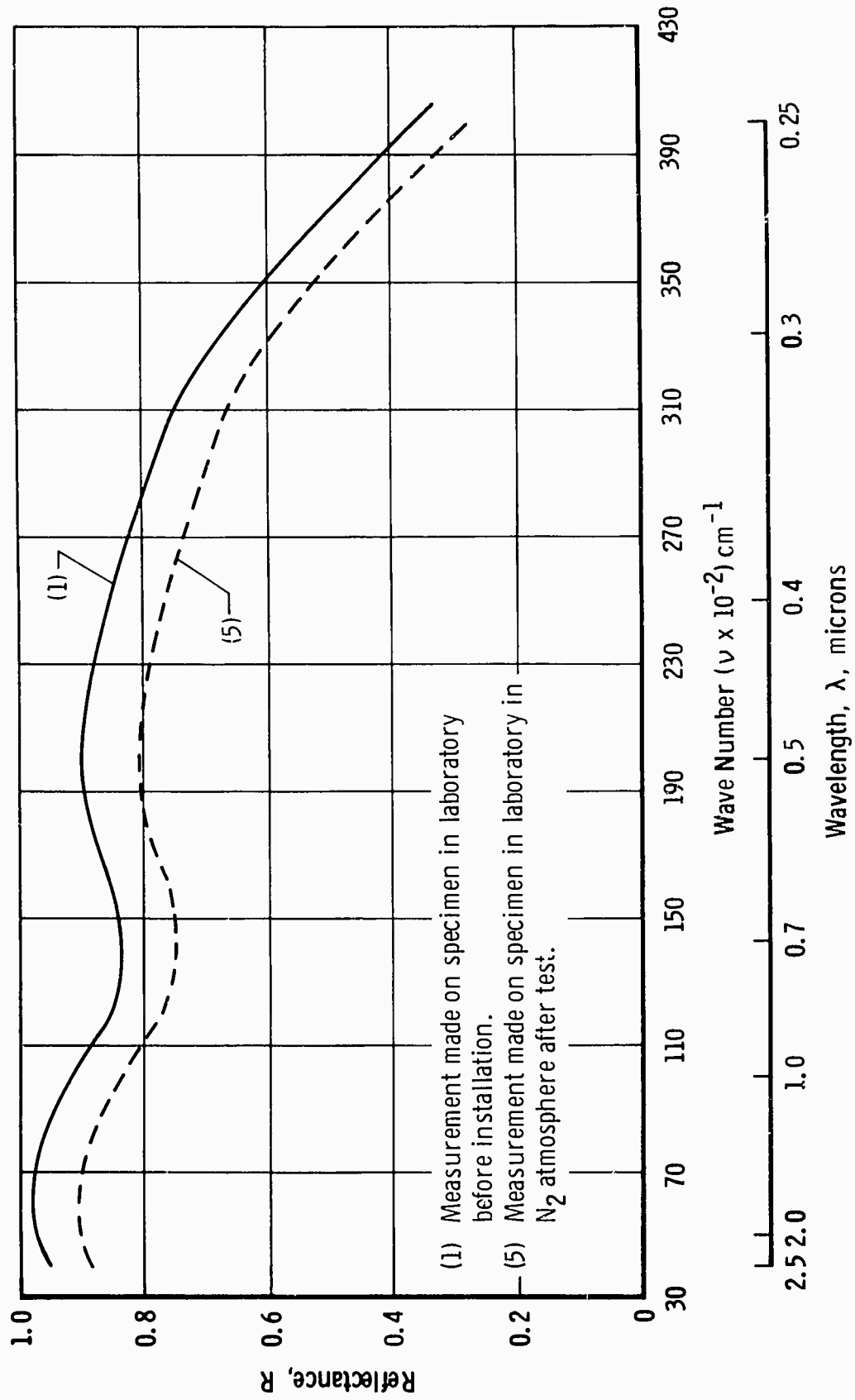


Fig. 37 Impingement Patterns on Panel 1 for 0- and 10-deg Thruster Angle

Fig. 38 Test 11—Reflectance Measurements on Specimen, Location S_{10} , Type K

Fig. 39 Test 11—Reflectance Measurements on Specimen, Location S_1 , Type C

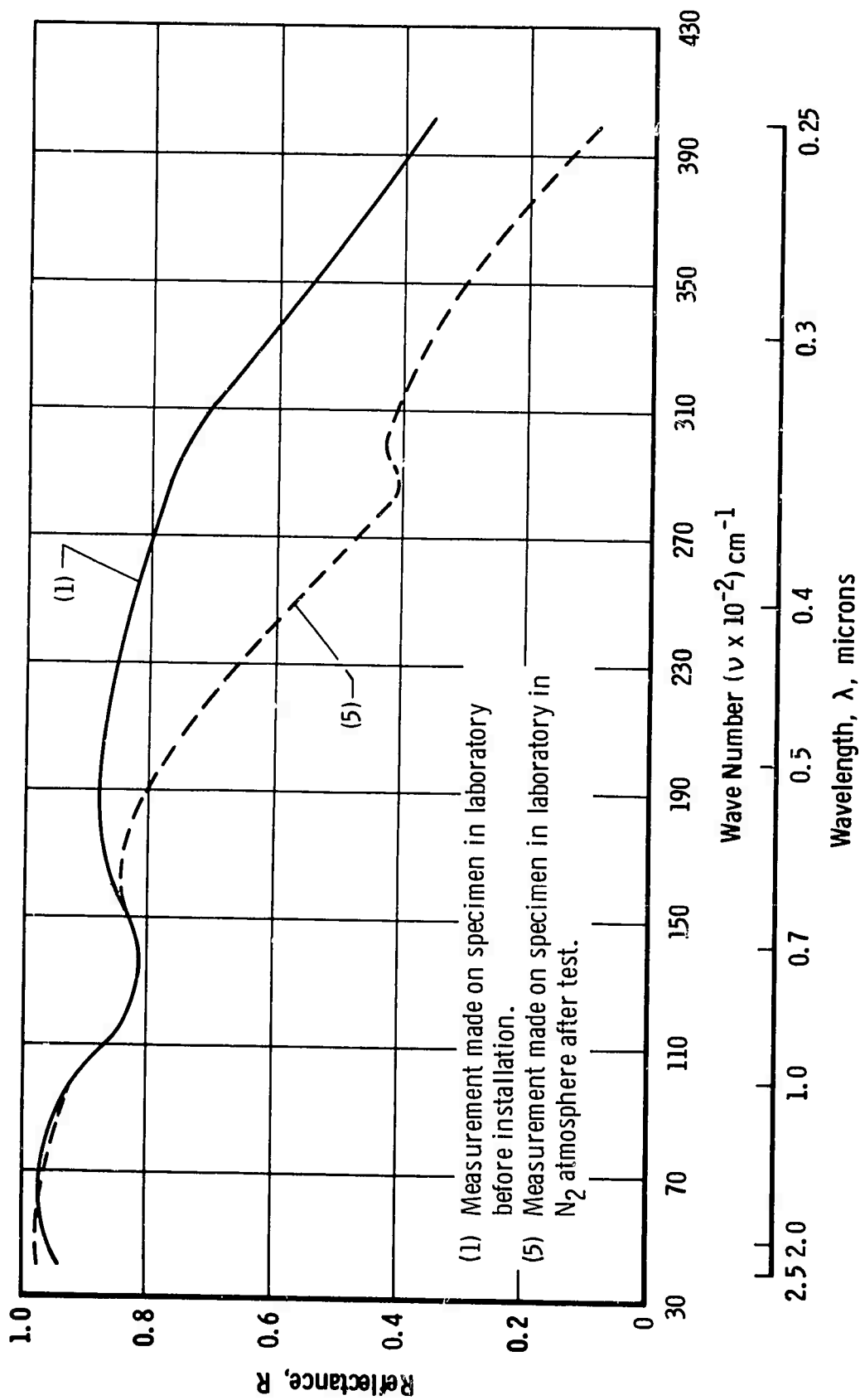
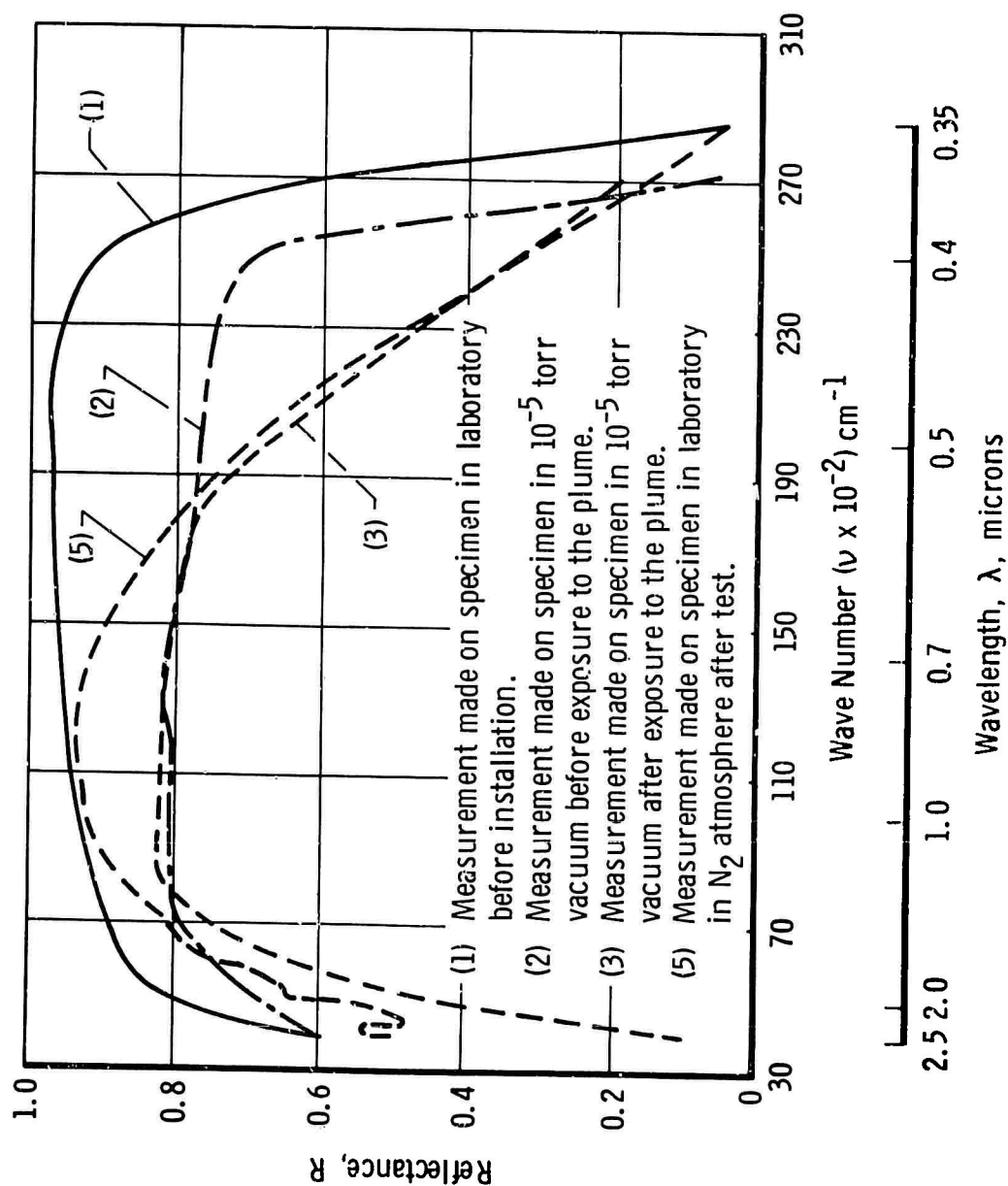
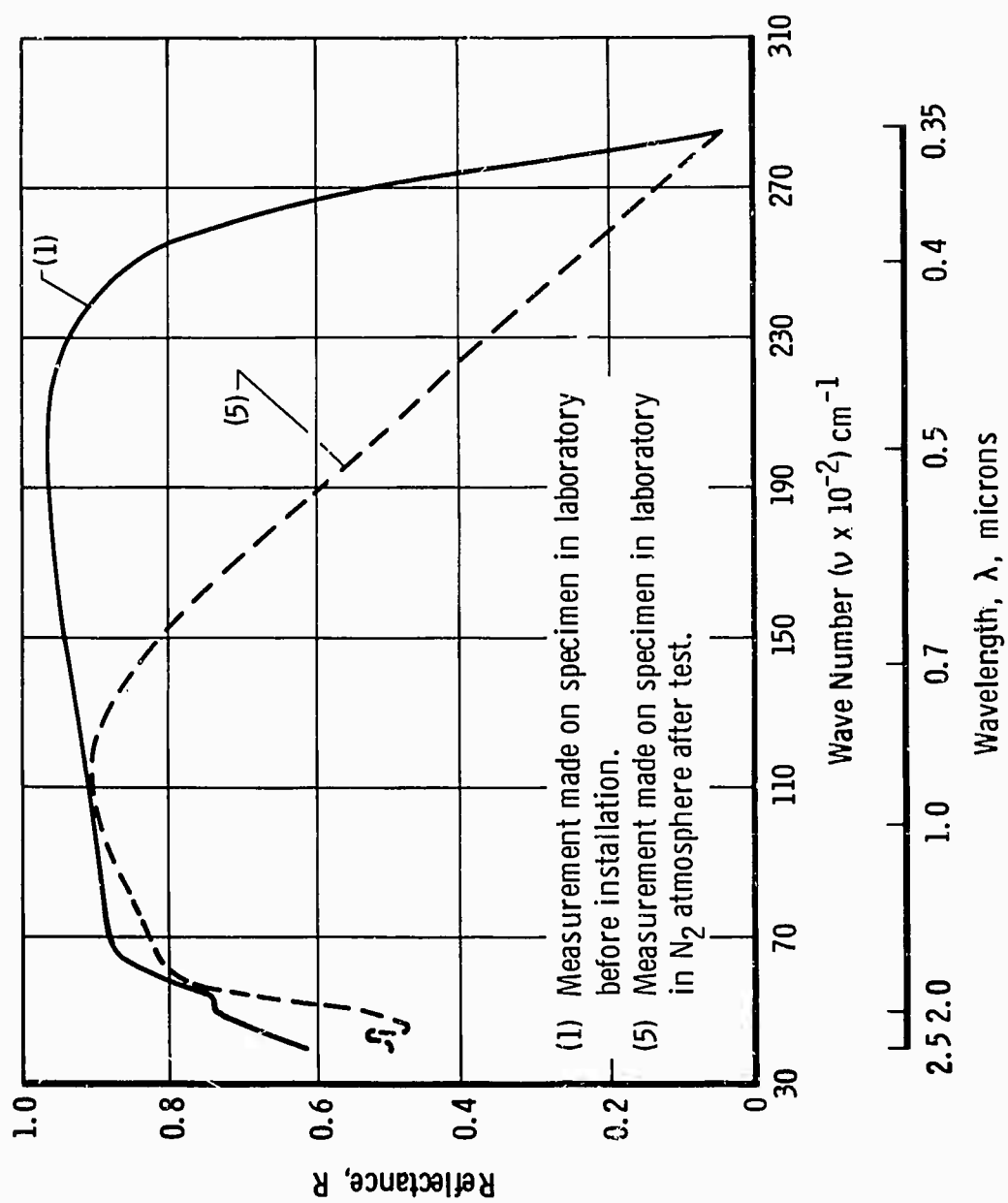


Fig. 40 Test 11—Reflectance Measurements on Specimen, Location S_2 , Type C

Fig. 41 Test 11—Reflectance Measurement on Specimen, Location S_g , Type A

Fig. 42 Test 11—Reflectance Measurement on Specimen, Location S_e , Type A

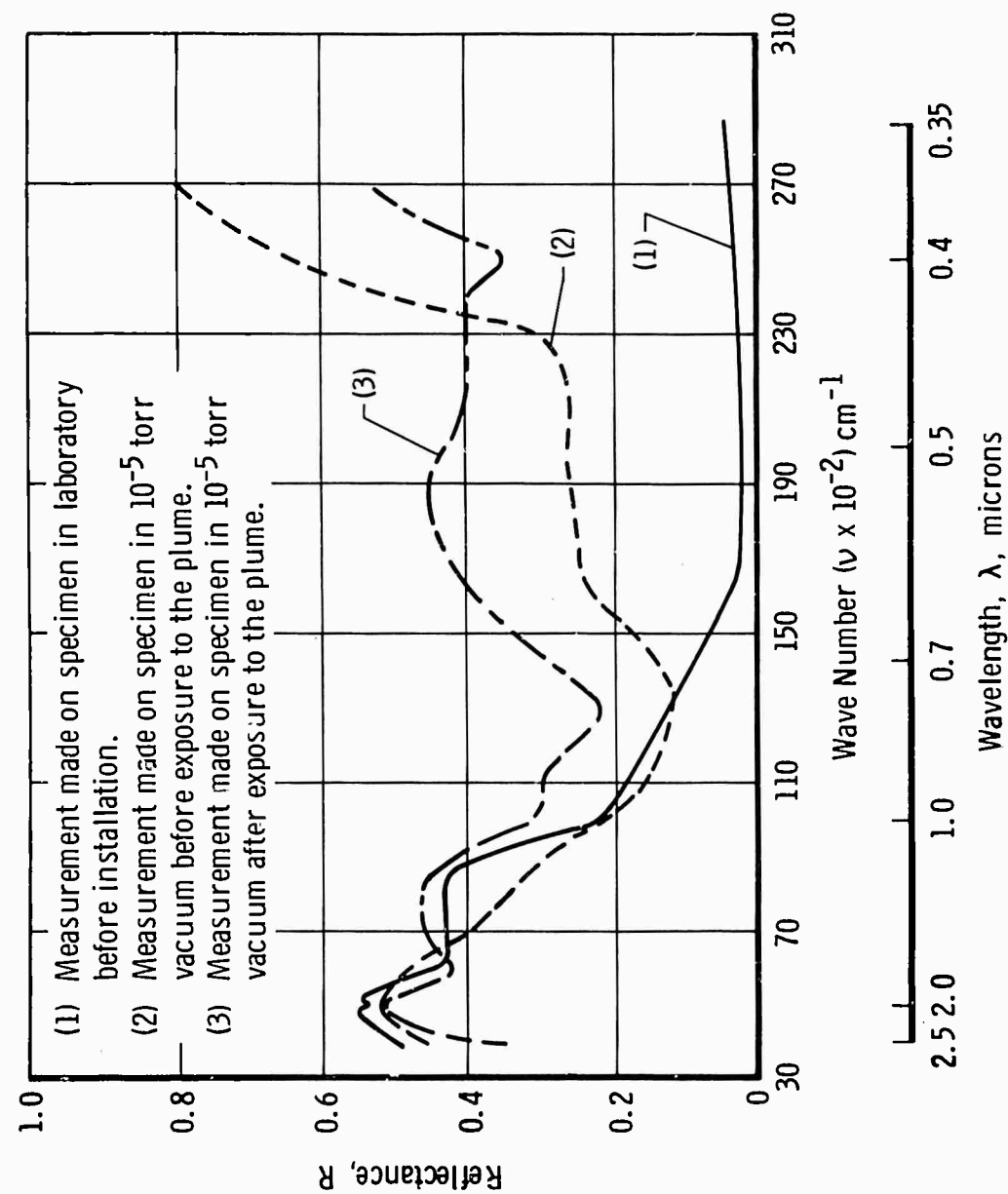
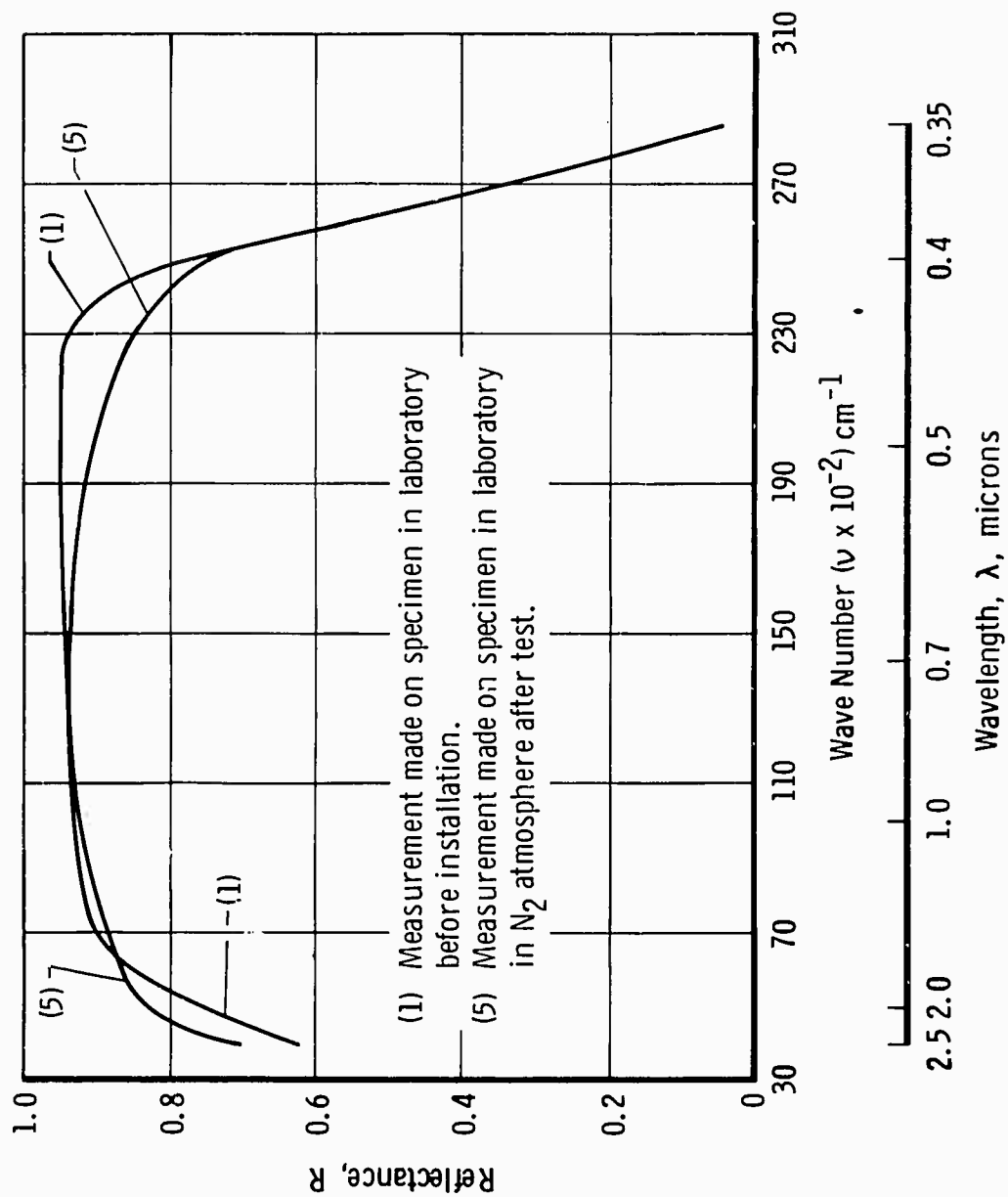
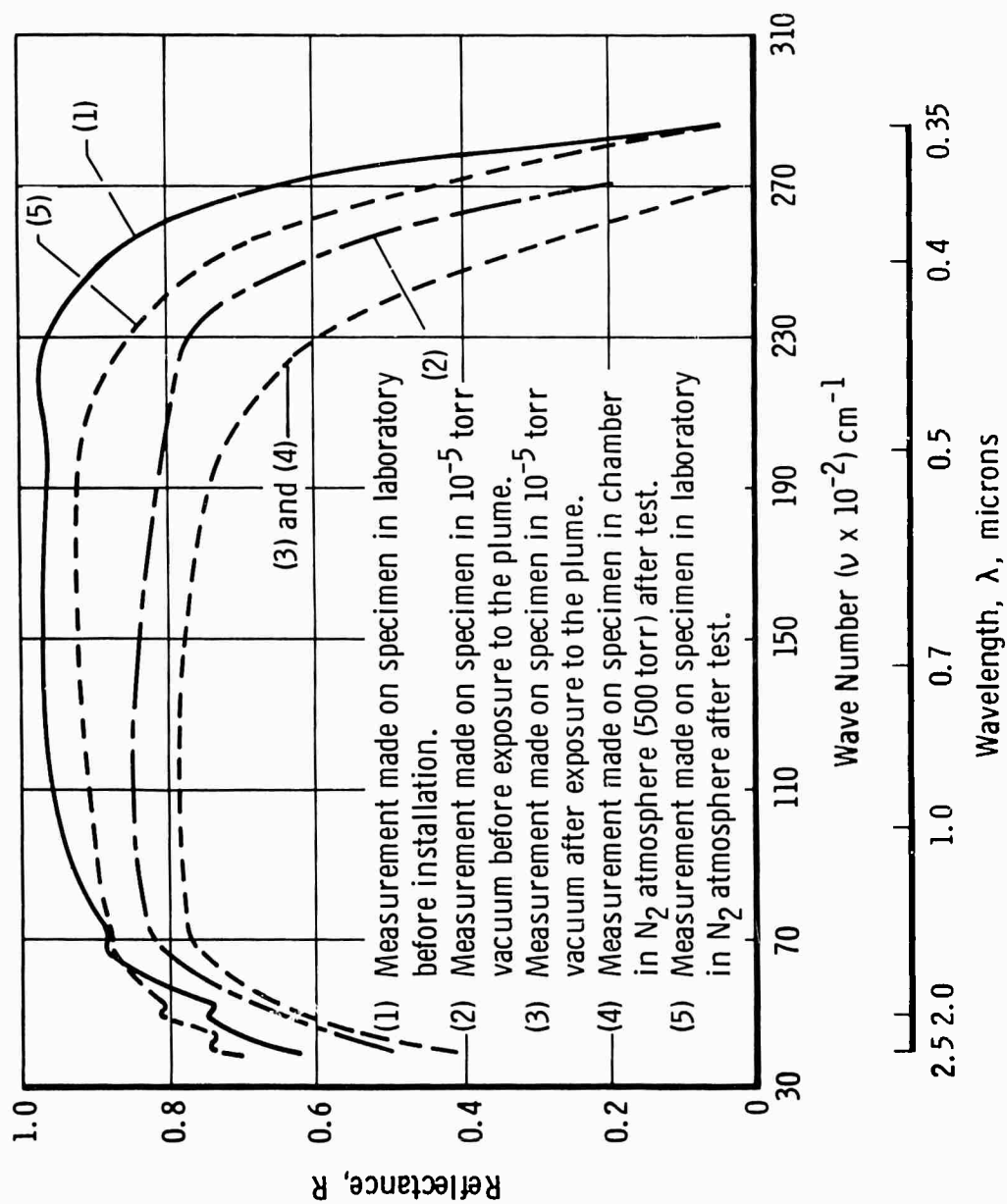


Fig. 43 Test 12—Reflectance Measurement on Specimen, Location S_5 , Type K

Fig. 44 Test 16—Reflectance Measurements on Specimen, Location S_1 , Type A

Fig. 45 Test 16—Reflectance Measurements on Specimen, Location S_2 , Type A

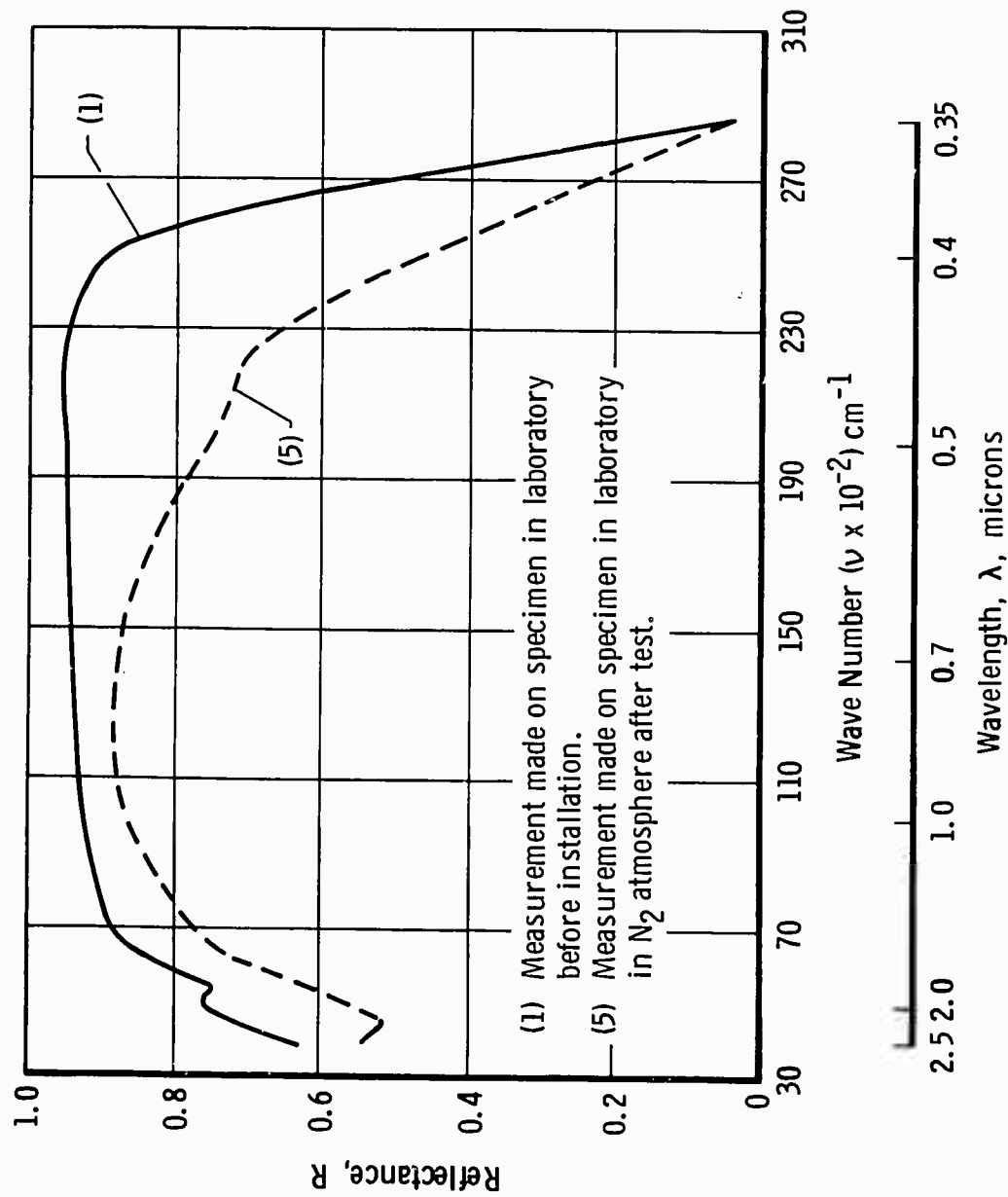
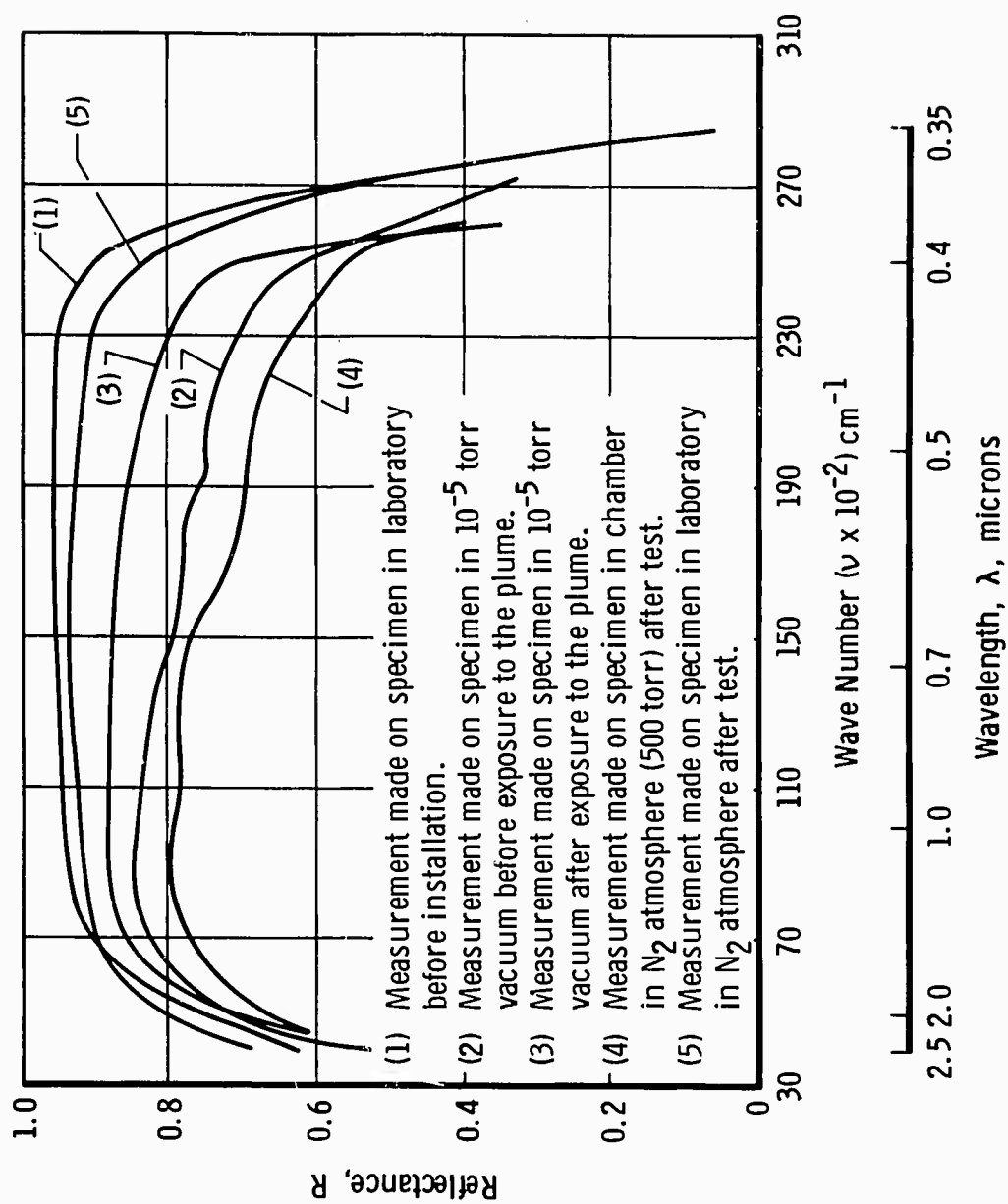
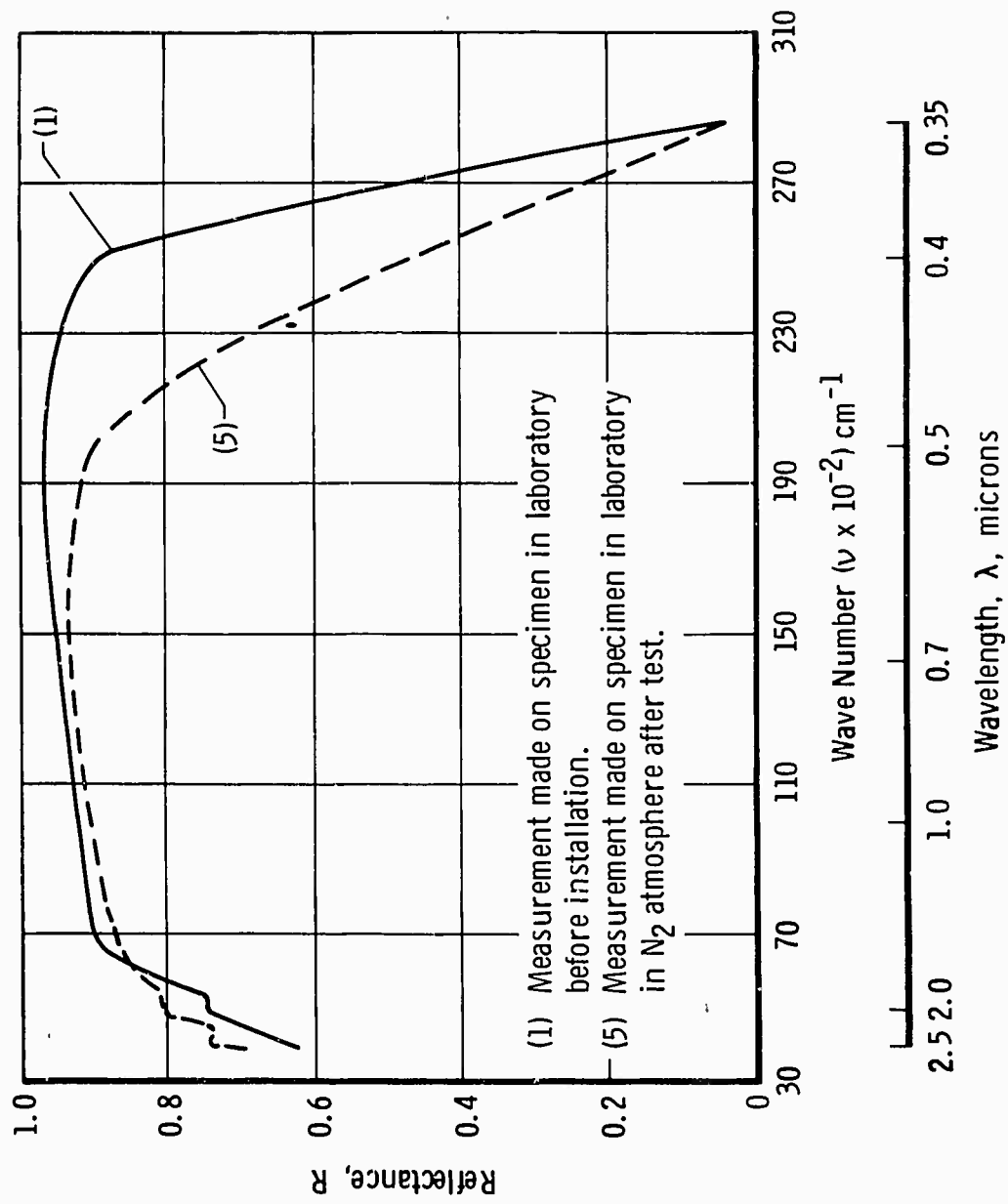
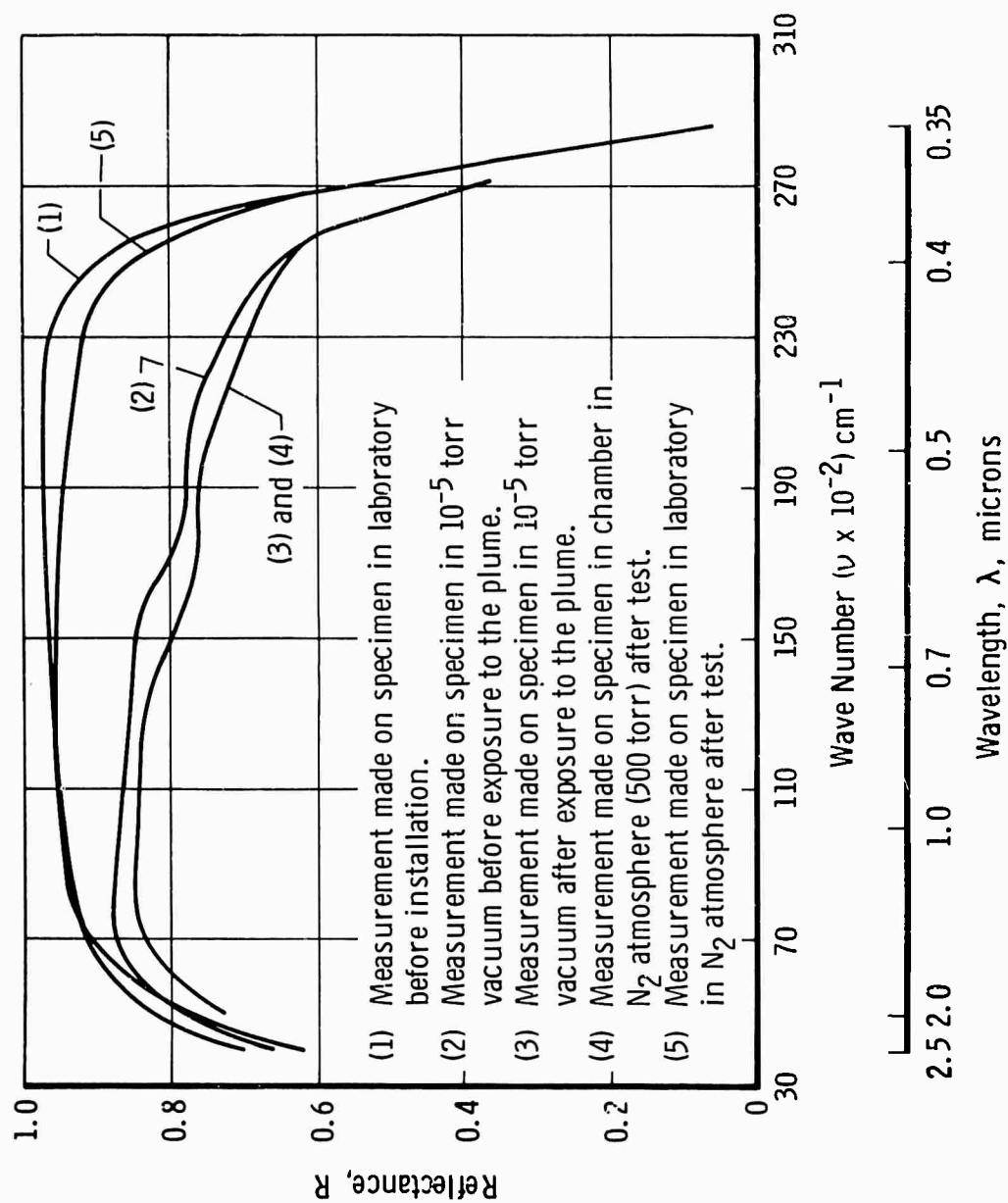


Fig. 46 Test 16—Reflectance Measurements on Specimen, Location S₅, Type A

Fig. 47 Test 16—Reflectance Measurements on Specimen, Location S_6 , Type A

Fig. 48 Test 16—Reflectance Measurements on Specimen, Location S₉, Type A

Fig. 49 Test 16—Reflectance Measurements on Specimen, Location S₁₀, Type A

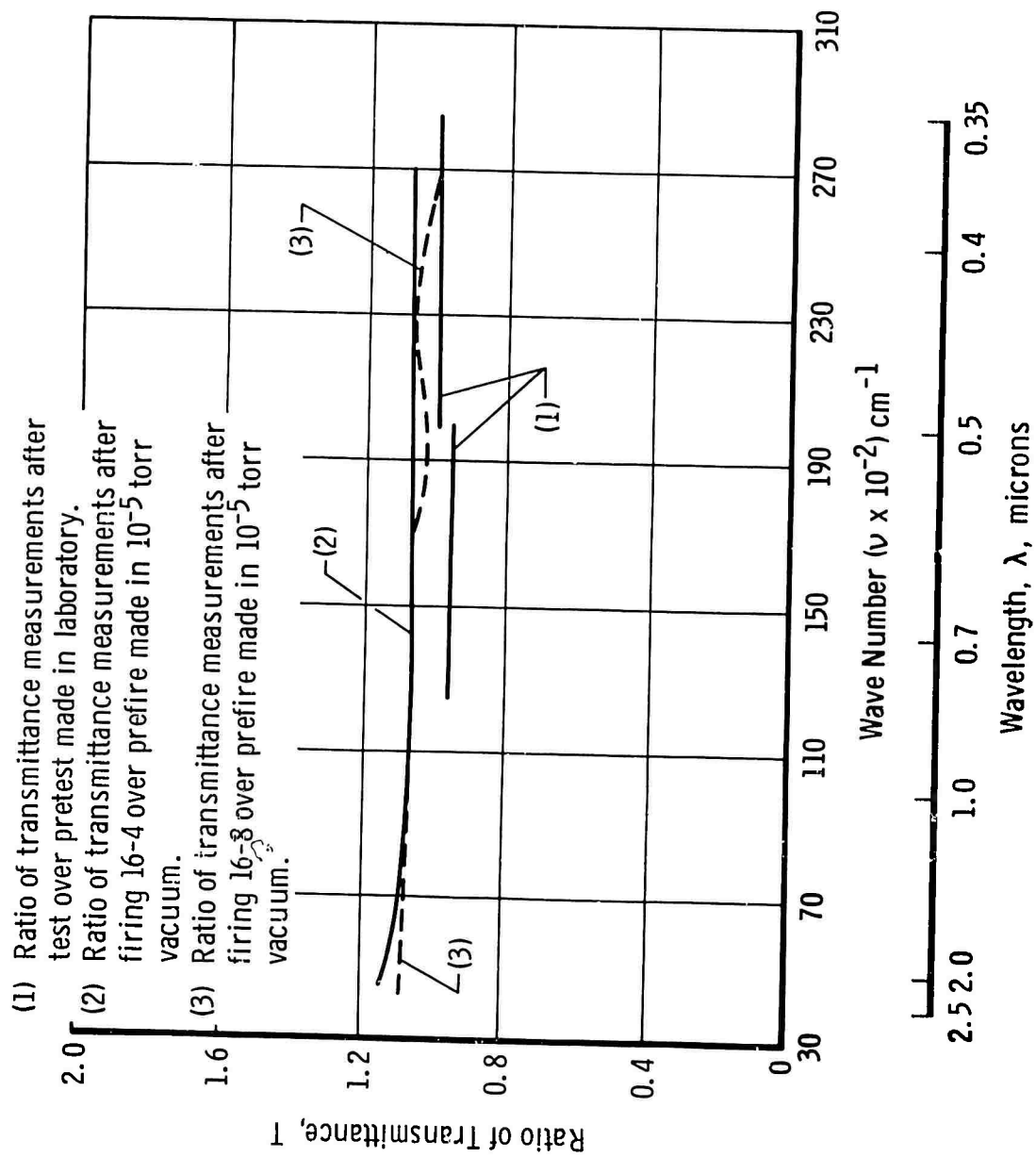


Fig. 50 Test 16—Transmittance Measurements on Specimen, Location S_{23} , Type W

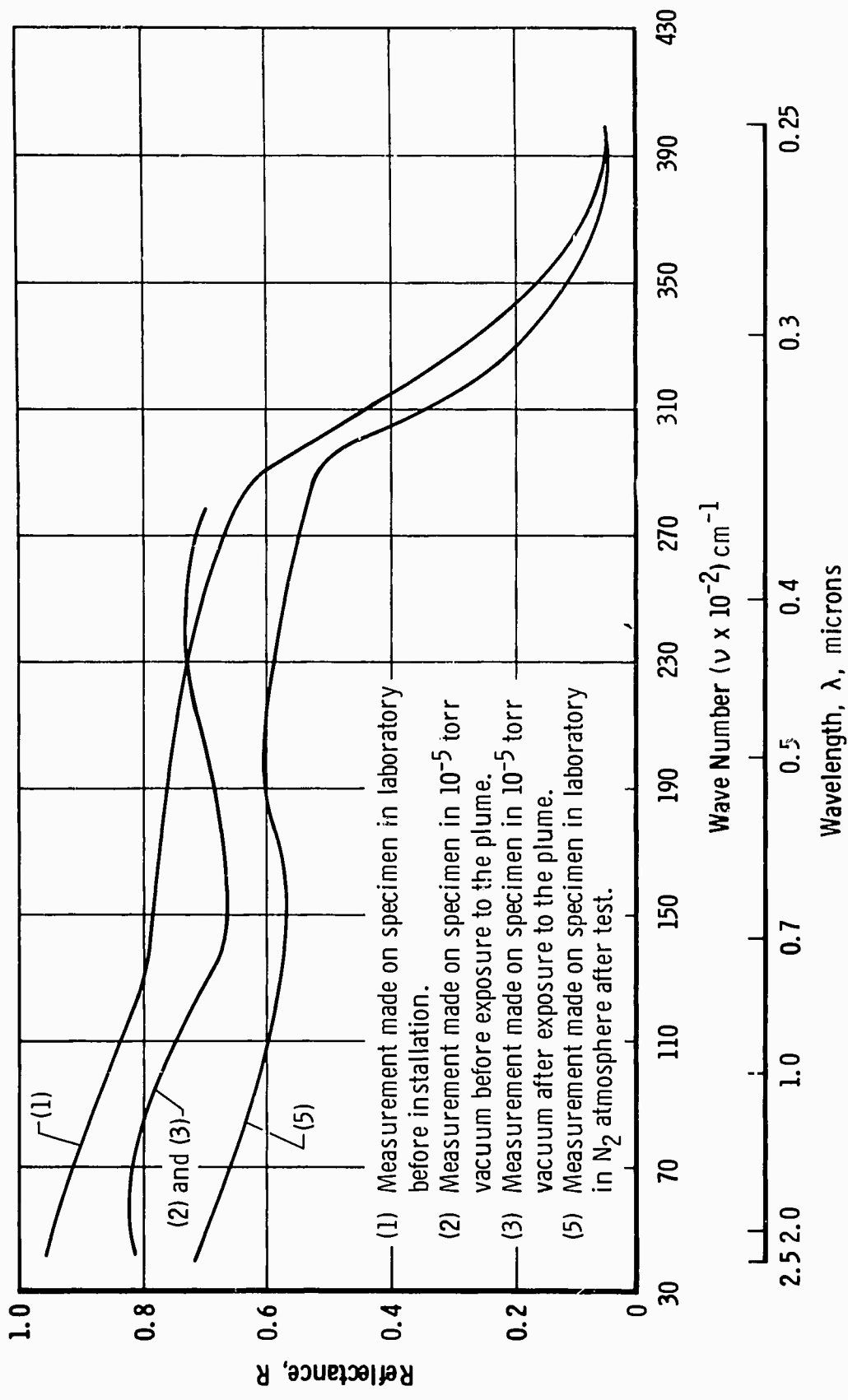


Fig. 51 Test 16—Reflectance Measurements on Specimen, Location S₂₇, Type T₂

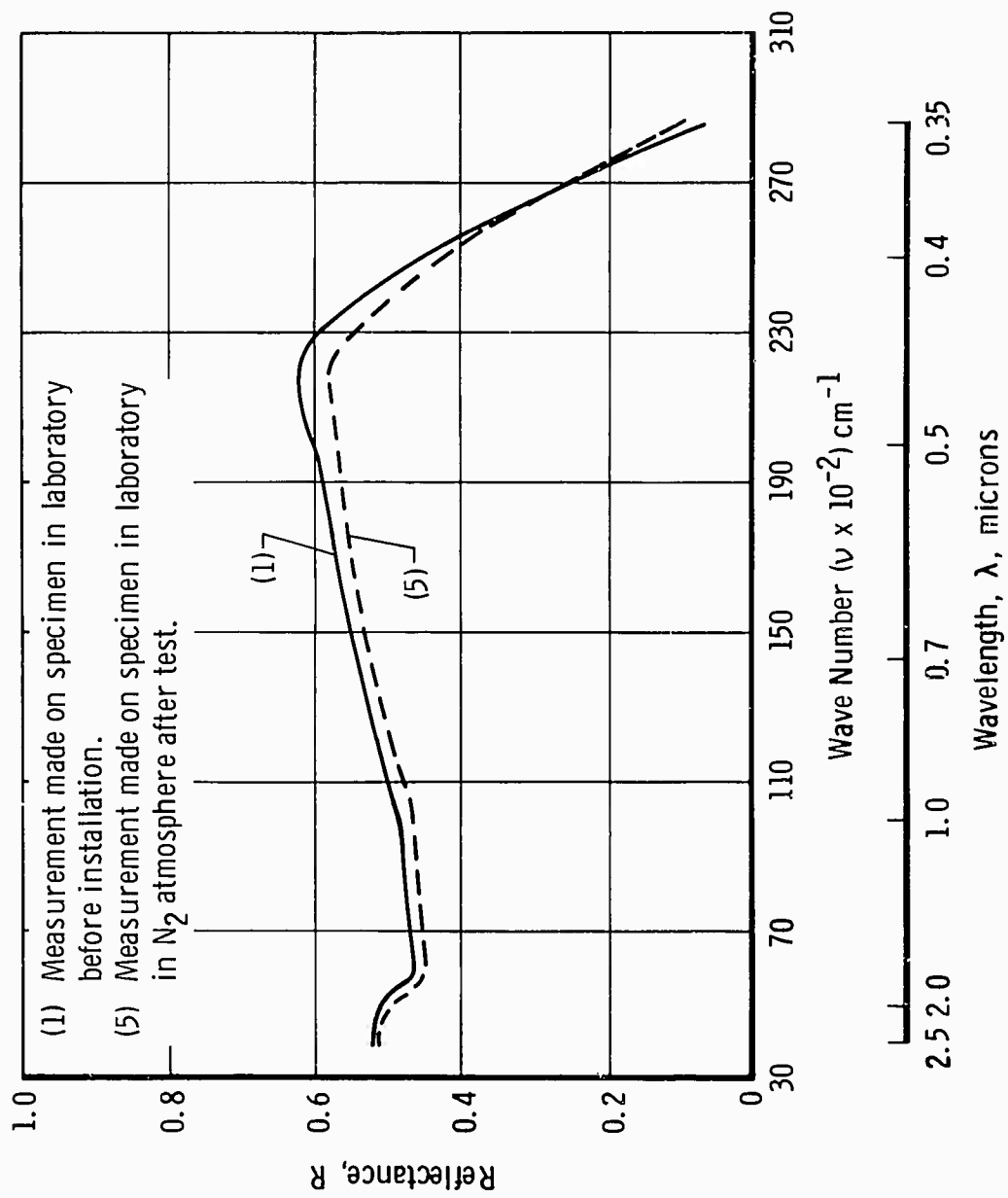


Fig. 52 Test 16—Reflectance Measurements on Specimen, Location H₁, Cube, Type T₁

APPENDIX II TEST LOG

TEST 7

TANGENTIAL THRUSTER (PULSE FIRING)

OBJECTIVE: Determine if contamination is generated by thruster.

RESULTS: Very significant amounts of contamination deposited on panel 1 in vicinity of thruster exit. Contamination decreased as thruster pulse duration increased, i.e., 20 to 1000 msec.

TEST HARDWARE: Contamination Test Panels 1 and 2
Surface Coating Specimens
View Port Specimen
Horizon Sensor Specimen
Mirror and Window Specimens

TEST CONDITIONS: $h = 1.14$ in., $\alpha = 10$ deg, $P_{OX} = 150$ psia,
 $P_F = 125$ psia, Altitude = 400,000 to 600,000 ft

Run No.	Pulsing Mode on / off / No. of (msec)/(msec)/Pulses	Specimen Measurement Sequence	Photographic Coverage
7-1	20/1000/862	Pretest Laboratory Prefire In Situ	Motion Pictures
7-2	20/1000/80		
7-3	20/1000/1000		
7-4	20/1000/1058	Postfire In Situ	Motion Pictures
7-5	20/1000/186		
7-6	20/1000/1814		
7-7	20/1000/3000	Postfire In Situ Prefire In Situ	Motion Pictures
7-8	50/1000/1466		
7-9	50/1000/934		
7-10	100/1000/884	Postfire In Situ Posttest Laboratory	Motion Pictures
7-11	100/1000/323		
7-12	1000/1000/120		

Test 7

Specimen Location	Type	Pre Lab	In Situ							Post Lab
			Pre	Post 4	Post 7	Post 8	Post 12	Post	Post S. L.	
S1	C	R								R
S2	C	R								R
S3	C	R								R
S4	C	R								R
S5	A	R								R
S6	A	R								R
S7	A	R	R, c	R, c	R, c	R, c				R
S8	A	R	R, c	R, c	R, c	R, c				R
S9	E	R								R
S10	K	R								R
S11	K	R								R
S12	K	R								R
S13	A	R								R
S14	D	R								R
S15	B	R	R, c	R, c	R, c	R, c				R
S16	D	R								R
S17	D	R								R
S18	A	R								R
S19	B	R	R, c	R, c	R, c	R, c				R
S20	A	R								R
S21	D	R								R
S22	A	R								R
S23										
S24	D									
S25	B	R	R, c	R, c	R, c	R, c				R
S26	A	R								R
S27	W	T	T	T	T	T	T			T
S28	A	R	R, c	R, c	R, c	R, c				R
H1	Emcal									
V1										
H2	H									T
V2	V		T	T	T	T	T			T
G1	W	T								T
G2	M	R								R
G3	W	T	T	T	T	T	T			T
G4	M	R	R							R
G5										
G6										
G7										
G8										
G9	M	R	R	R		R				R
G10										
G11										
G12	M	R								R

TEST 8

TANGENTIAL THRUSTER (PULSE FIRING)

OBJECTIVE: Investigate feasibility of heated shroud for capturing and decomposing the contamination generated by thruster; therefore, reducing amount deposited on panel.

RESULTS: The 800°F shroud reduced significantly the amount of contamination on the panel that previously had been observed.

TEST HARDWARE: Contamination Test Panels 1 and 2
 Surface Coating Specimens
 View Port Specimen
 Horizon Sensor Specimen
 Mirror and Window Specimens
 Shroud with Flask for Capturing Contamination

TEST CONDITIONS: $h = 1.14$ in., $\alpha = 10$ deg, $P_{ox} = 150$ psia,
 $P_F = 125$ psia, Altitude = 400,000 to 600,000 ft

Run No.	Pulsing Mode on / off / No. of (msec)/(msec)/Pulses	Specimen Measurement Sequence	Photographic Coverage
8-1	20/1000/1000	Pretest Laboratory Prefire In Situ	Motion Pictures ↓
8-2	20/1000/604		
8-3	20/1000/396		
8-4	20/1000/1000	Postfire In Situ	
8-5	50/1000/2400	Postfire In Situ	
8-6	100/1000/1260	Postfire In Situ	
8-7	1000/1000/120	Postfire In Situ Posttest Laboratory	

Test 8

Specimen Location	Type	Pre Lab	In Situ							Post Lab
			Pre	Post 4	Post 5	Post 6	Post 7	Post	Post S. L.	
S1	C	R								R
S2	C	R								R
S3	C	R								R
S4	C	R								R
S5	A	R	R, ε	R, ε	R, ε	R, ε	ε			R
S6	A	R								R
S7	A	R	R, ε	R, ε	R, ε	R, ε	ε			R
S8	A	R								R
S9	E									
S10	K	R								R
S11	K	R								R
S12	K	R	R, ε	R, E			ε			R
S13	A	R								R
S14	B	R								R
S15	B	R	R, ε	R, ε	R, ε	R, ε	ε			R
S16	D									
S17	A	R								R
S18	A	R								R
S19	B	R	R, ε	R, ε	R, ε		ε			R
S20	A	R								R
S21	D									
S22										
S23										
S24	D									
S25	M	R	R	R	R					R
S26	A	R								R
S27	W	T	T	T	T	T	T			T
S28	A	R	R, ε	R, ε			ε			R
H1	Emcal									
V1										
H2	H									
V2	V		T	T	T	T				T
G1										
G2										
G3	M	R	R	R						R
G4	W	T	T	T		T	T			T
G5	M	R								R
G6										
G7										
G8										
G9	M	R	R	R						R
G10										
G11	W	T								T
G12										

TEST 9

TANGENTIAL THRUSTER (PULSE FIRING)

OBJECTIVE: Determine if fences were effective in shielding specimens from plume contamination.

RESULTS: Large amounts of contamination deposited on shielded specimens.

TEST HARDWARE: Contamination Test Panels 1 and 2
 Surface Coating Specimens
 View Port Specimen
 Horizon Sensor Specimen
 Mirror and Window Specimens
 4-in. Movable Fence Shielding Specimens S23 and S25
 1.5-in. Movable Fence Located Downstream of
 Thruster with Flask for Capturing Contamination

TEST CONDITIONS: $h = 1.14$ in., $\alpha = 10$ deg, $P_{ox} = 150$ psia,
 $P_F = 125$ psia, Altitude = 400,000 to 600,000 ft

Run No.	Pulsing Mode on / off / No. of (msec)/(msec)/Pulses	Specimen Measurement Sequence	Photographic Coverage
9-1	20/1000/1000	Pretest Laboratory	Motion Pictures ↓
9-2	20/1000/1000		
9-3	20/1000/1000		
9-4	50/1000/2400		
9-5	100/1000/1200		
9-6	1000/1000/120		
		Posttest Laboratory	

Test 9

Specimen Location	Type	Pre Lab	In Situ							Post Lab
			Pre	Post	Post	Post	Post	Post	Post S. L.	
S1										
S2										
S3										
S4										
S5	A	R								R
S6	A	R								R
S7	A	R								R
S8	A	R								R
S9	D									
S10	K	R								R
S11	K	R								R
S12	K	R								R
S13	A	R								R
S14	B	R								R
S15	B	R								R
S16	D									
S17	A	R								R
S18	A	R								R
S19	B	R								R
S20	A	R								R
S21	D									
S22										
S23	W	T								T
S24	D									
S25	M	R								R
S26	A	R								R
S27	W	T								T
S28	A	R								R
H1	Emcal									
V1										
H2	H									
V2	V									T
G1										
G2										
G3	M	R								R
G4	W	T								T
G5	M	R								R
G6										
G7										
G8										
G9	M	R								R
G10										
G11										
G12										

TEST 10A

TANGENTIAL THRUSTER (PULSE FIRING)

OBJECTIVE: Using slightly modified shroud, verify results of test 8.
Investigate contamination from a heated and unheated shroud.

RESULTS: Test terminated because of instrumentation problems.

TEST HARDWARE: Contamination Test Panels 1 and 2
Surface Coating Specimens
View Port Specimen
Horizon Sensor Specimen
Mirror and Window Specimens
4-in. Movable Fence Shielding Specimens S23 and S25
Heated Shroud with Flask for Capturing Contamination

TEST CONDITIONS: $h = 1.14$ in., $\alpha = 10$ deg, $P_{OX} = 150$ psia,
 $P_F = 125$ psia, Altitude = 400,000 to 600,000 ft

Run No.	Pulsing Mode on / off / No. of (msec)/(msec)/Pulses	Specimen Measurement Sequence	Photographic Coverage
		None	Motion Pictures
Heated Shroud to 750°F 10A-1	20/1000/1000		↓
Heated Shroud to 750°F 10A-2	20/1000/1000		
Heated Shroud to 750°F 10A-3	20/1000/1000		
Heated Shroud to 750°F 10A-4	50/1000/1976		
Unheated Shroud 10A-5	20/1000/537		

TEST 10B

TANGENTIAL THRUSTER (PULSE FIRING)

OBJECTIVE: Same as 10A

RESULTS: Modified heated shroud was more effective than previous shroud.
Modified unheated shroud did not capture any contamination.TEST HARDWARE: Contamination Test Panels 1 and 2
Surface Coating Specimens
View Port Specimen
Horizon Sensor Specimen
Mirror and Window Specimens
4-in. Movable Fence Shielding Specimens S23 and S25
Heated Shroud with Flask for Capturing ContaminationTEST CONDITIONS: $h = 1.14$ in., $\alpha = 10$ deg, $P_{ox} = 150$ psia,
 $P_F = 125$ psia, Altitude = 400,000 to 600,000 ft

Run No.	Pulsing Mode on / off / No. of (msec)/(msec)/Pulses	Specimen Measurement Sequence	Photographic Coverage
		Pretest Laboratory	
Heated Shroud to 800°F 10B-1	20/1000/3000		Motion Pictures
Heated Shroud to 800°F 10B-2	50/1000/2400		
Unheated Shroud 10B-3	50/1000/2400		
Unheated Shroud 10B-4	1000/1000/240		
Heated Shroud to 800°F 10B-5	1000/1000/240		
		Posttest Laboratory	

Test 10B

Specimen Location	Type	Pre Lab	In Situ							Post Lab
			Pre	Post	Post	Post	Post	Post	Post S.I.	
S1	A	R								R
S2	B	R								R
S3	A	R								R
S4	B									
S5	A	R								R
S6	A	R								R
S7	A	R								R
S8	A	R								R
S9	E									
S10	K	R								R
S11	K	R								R
S12	K	R								R
S13	A	R								R
S14	B	R								R
S15	B	R								R
S16	D									
S17	A	R								R
S18	A	R								R
S19	B	R								R
S20	A	R								R
S21	D									
S22										
S23	W	T								T
S21	D									
S25	M	R								R
S26	A	R								R
S27	W	T								T
S28	A	R								R
H1	Emcal									
V1										
H2	H									
V2	V									T
G1										
G2										
G3	M	R								R
G4	W	T								T
G5	M	R								R
G6										
G7										
G8										
G9	M	R								R
G10										
G11										
G12										

TEST 11

TANGENTIAL THRUSTER (PULSE FIRING)

OBJECTIVE: Determine feasibility of heated and unheated modified shroud to reduce contamination on test panel.

RESULTS: Wire mesh became saturated; therefore, contamination increased on test panel. Contamination was similar to that of test 7.

TEST HARDWARE: Contamination Test Panels 1 and 2
 Surface Coating Specimens
 View Port Specimen
 Horizon Sensor Specimen
 Mirror and Window Specimens
 4-in. Movable Fence Shielding Specimens S₂₃ and S₂₅
 Heated Shroud with Stainless Steel Mesh between
 Shroud and Nozzle, and Flask.

TEST CONDITIONS: $h = 1.14$ in., $\alpha = 10$ deg, $P_{ox} = 150$ psia,
 $P_F = 125$ psia, Altitude = 400,000 to 600,000 ft

Run No.	Pulsing Mode on / off / No. of (msec)/(msec)/Pulses	Specimen Measurement Sequence	Photographic Coverage
		Pretest Laboratory Prefire In Situ	Motion Pictures ↓
Heated Shroud to 800°F 11-1	20/1000/3000	Postfire In Situ	
Heated Shroud to 800°F 50/1000/2400		Postfire In Situ	
Unheated Shroud 11-3	50/1000/2400	Postfire In Situ	
Unheated Shroud 11-4	1000/1000/240	Postfire In Situ	
Heated Shroud to 800°F 11-5	1000/1000/240	Postfire In Situ	
		Sea Level In Situ	
		Posttest Laboratory	

Test 11

Specimen Location	Type	Pre Lab	In Situ							Post Lab
			Pre	Post 1	Post 2	Post 3	Post 4	Post 5	Post S. L.	
S1	C	R								R
S2	C	R								R
S3	C	R								R
S4	C	R								R
S5	A	R	R, ϵ	R, ϵ	R, ϵ	R, ϵ				R
S6	A	R								R
S7	A	R	R, ϵ	R, ϵ	R, ϵ	R, ϵ	R, ϵ	R, ϵ	R	R
S8	A	R								R
S9	D									
S10	K	R	R, ϵ	R, ϵ	R, ϵ	R, ϵ	R, ϵ	R, ϵ	R	R
S11	K	R								R
S12	K	R	R, ϵ	R, ϵ	R, ϵ	R, ϵ	R, ϵ	R, ϵ	R	R
S13	A	R								R
S14	B	R								R
S15	B	R	R, ϵ	R, ϵ	R, ϵ	R, ϵ	R, ϵ	R, ϵ	R	R
S16	D									
S17	A	R								R
S18	A	R								R
S19	B	R								R
S20	A	R								R
S21	D									
S22										
S23	W	T	T	T	T	T	T	T	T	T
S24	D									
S25	M	R	R	R	R	R	R	R	R	R
S26	A	R								R
S27	W	T	T	T	T	T	T	T	T	T
S28	A	R	R, ϵ	R, ϵ	R, ϵ	R, ϵ	R, ϵ	R, ϵ	R	R
H1	Emcal									
V1										
H2	H									
V2	V		T	T	T	T	T	T	T	T
G1										
G2										
G3	M	R	R	R	R	R	R	R	R	R
G4	W	T								T
G5	M	R	R	R	R	R	R	R	R	R
G6										
G7										
G8										
G9	M	R	R	R	R	R	R	R	R	R
G10										
G11										
G12										

TEST 12

TANGENTIAL THRUSTER (PULSE FIRING)

OBJECTIVE: Determine feasibility of reducing contamination by heating combustion chamber, varying oxidizer-to-fuel ratio, and heating oxidizer and fuel lines.

RESULTS: None of these methods proved to be effective in decreasing contamination generated by thruster.

TEST HARDWARE: Contamination Test Panels 1 and 2
 Surface Coating Specimens
 View Port Specimen
 Horizon Sensor Specimen
 Mirror and Window Specimens
 4-in. Movable Fence Shielding Specimens S₂₃ and S₂₅
 Heated Nozzle and Heated Propellants

TEST CONDITIONS: $h = 1.14$ in., $\alpha = 10$ deg, $P_{ox} = 150$ psia,
 $P_F = 125$ psia, Altitude = 400,000 to 600,000 ft

Run No.	Pulsing Mode on / off / No. of (msec)/(msec)/Pulses	Specimen Measurement Sequence	Photographic Coverage
		Pretest Laboratory Prefire In Situ	
Heated Nozzle to 200°F 12-1	20/1000/3000	Postfire In Situ	Motion Pictures ↓
O/F Ratio of 2.0 12-2	20/1000/609		
O/F Ratio of 1.2 12-3	20/1000/600		
Heated Propellants Oxidizer - 100°F Fuel - 120°F 12-4	20/1000/600		

Test 12

Specimen Location	Type	Pre Lab	In Situ							Post Lab
			Pre	Post	Post	Post	Post	Post	Post S. I.	
S1	C	R								
S2										
S3										
S4										
S5	K	R	R, ϵ	R, ϵ						
S6	A	R								
S7	A	R	R, ϵ	R, ϵ						
S8	A	R								
S9	D									
S10	K	R	R	R						
S11	K	R								
S12	A	R		R, ϵ						
S13	A	R								
S14	B	R								
S15	B	R	R	R						
S16	D									
S17	A	R								
S18	A	R								
S19	B	R								
S20	A	R								
S21	D	R								
S22										
S23	W	T	T	T						
S24	D									
S25	M	R	R	R						
S26	A	R								
S27	W	T	T	T						
S28	A	R	R, ϵ	R, ϵ						
H1	Emcal									
V1										
H2	H									
V2	V		T	T						
G1										
G2										
G3	M	R	R	R						
G4	W	T								
G5	M	R	R	R						
G6										
C7										
G8										
G9	M	R	R	R						
G10										
G11										
G12										

TEST 16

TANGENTIAL THRUSTER (PULSE FIRING)

OBJECTIVE: Determine minimum temperature of the nozzle shroud in decomposing contamination.

RESULTS: The minimum shroud temperature was observed to be 300°F.

TEST HARDWARE: Contamination Test Panels 1 and 2
 Surface Coating Specimens
 View Port Specimen
 Horizon Sensor Specimen with Ramp
 Mirror and Window Specimens
 4-in. Movable Fence Shielding Specimens S₂₃ and S₂₅
 Heated Shroud with Flask for Capturing Contamination
 Cube with Specimen Located at H₁

TEST CONDITIONS: $h = 1.14$ in., $\alpha = 10$ deg, $P_{ox} = 150$ psia,
 $P_F = 125$ psia, Altitude = 400,000 to 600,000 ft

Run No.	Pulsing Mode on / off / No. of (msec)/(msec)/Pulses	Specimen Measurement Sequence	Photographic Coverage
		Pretest Laboratory Prefire In Situ	Motion Pictures ↓
Heated Shroud to 200°F			
16-1	20/1000/97		
16-2	20/1000/903		
Heated Shroud to 300°F			
16-3	20/1000/1000		
Heated Shroud to 400°F			
16-4	20/1000/1000	Postfire In Situ	
Heated Shroud to 500°F			
16-5	20/1000/1000		
Heated Shroud to 600°F			
16-6	20/1000/1000		
Heated Shroud to 700°F			
16-7	20/1000/1000	Postfire In Situ	
Unheated Shroud			
16-8	20/1000/1000	Postfire In Situ	
Heated Panel to 130°F			
		Prefire In Situ	
Heated Shroud to 200°F			
16-9	20/1000/1000	Postfire In Situ Sea-Level In Situ Posttest Laboratory	

Test 16

Specimen Location	Type	Pre Lab	In Situ							Post Lab
			Pre	Post 4	Post 7	Post 8	Post 9	Post 9	Post S. L.	
S1	A	R								R
S2	A	R	R, ϵ	R, ϵ	R, ϵ	R, ϵ	R, ϵ	R, ϵ	R	R
S3										
S4	A	R								R
S5	A	R								R
S6	A	R	R, ϵ	R, ϵ	R, ϵ	R, ϵ	R, ϵ	R, ϵ	R	R
S7	A	R	R, ϵ	R, ϵ	R, ϵ	R, ϵ	R, ϵ	R, ϵ	R	R
S8	A	R								R
S9	A	R								R
S10	A	R	R, ϵ	R, ϵ	R, ϵ	R, ϵ	R, ϵ	R, ϵ	R	R
S11	A	R	ϵ	ϵ	ϵ	ϵ	ϵ	ϵ		R
S12	A	R								R
S13	K	R								R
S14										
S15										
S16	K	R								R
S17	A	R								R
S18	A	R	ϵ	ϵ	ϵ	ϵ	ϵ	ϵ		R
S19	D	R								R
S20	A	R								R
S21	D	R								R
S22	Emcal									
S23	W	T	T	T	T	T	T	T	T	T
S24	A	R	R, ϵ	R, ϵ	R, ϵ	R, ϵ	R, ϵ	R, ϵ	R	R
S25	M	R	R	R	R	R	R	R	R	R
S26	A	R								R
S27	T2	R	R, ϵ	R, ϵ	R, ϵ	R, ϵ	R, ϵ	R, ϵ	R	R
S28	D	R								R
H1	Cube T1	R								R
V1										
H2	H									T
V2	V		T	T	T	T	T	T	T	T
G1										
G2										
G3	M	R	R	R	R	R	R	R	R	R
G4	W	T	T	T	T	T		T	T	T
G5										
G6										
G7										
G8	W	T								T
G9	M	R	R	R	R	R		R	R	R
G10										
G11										
G12										

TEST 24

TANGENTIAL THRUSTER (PULSE FIRING)

OBJECTIVE: Determine degree of contamination generated by thruster at lower altitudes.

RESULTS: Contamination at 150,000- and 250,000-ft altitudes same as in test 7. More contamination along centerline of thruster.

TEST HARDWARE: Contamination Test Panel 1
Surface Coating Specimens
Mirror and Window Specimens

TEST CONDITIONS: $h = 1.14$ in., $\alpha = 10$ deg, $P_{ox} = 150$ psia,
 $P_F = 125$ psia, Altitude = 150,000 to 250,000 ft

Run No.	Pulsing Mode on / off / No. of (msec)/(msec)/Pulses	Specimen Measurement Sequence	Photographic Coverage
250,000 Feet		None	Motion Pictures ↓
24-1	20/1000/3000		
24-2	50/1000/2400		
24-3	1000/1000/240		
150,000 Feet			
24-4	20/1000/3000		
24-5	50/1000/1997		

TEST 25

TANGENTIAL THRUSTER (PULSE FIRING)

OBJECTIVE: Determine degree of contamination of fuel additives, heating fuel lines with oxidizer at ambient, heating fuel, oxidizer, and combustion chamber simultaneously.

RESULTS: None of above methods had any significant effect on the contamination generated by the the thruster.

TEST HARDWARE: Contamination Test Panel 1
Surface Coating Specimens
Mirror and Window Specimens
Heated Nozzle and Heated Propellants

TEST CONDITIONS: $h = 1.14$ in., $\alpha = 0$ deg, $P_{ox} = 150$ psia,
 $P_F = 125$ psia, Altitude = 400,000 to 600,000 ft

Run No.	Pulsing Mode on / off / No. of (msec)/(msec)/Pulses	Specimen Measurement Sequence	Photographic Coverage
90-Percent MMH, 10-Percent Water		None	Motion Pictures
25-1	20/1000/1000		
25-2	50/1000/1000		
90-Percent MMH, 10-Percent Alcohol			
25-3	20/1000/1000		
25-4	50/1000/1000		
80-Percent MMH, 20-Percent Water			
25-5	20/1000/1000		
25-6	50/1000/1000		
100-Percent MMH			
Heated Fuel to 160°F			
25-7	20/1000/1000		
25-8	50/1000/1000		
Heated Fuel to 140°F			
Heated Oxidizer to 120°F			
40-sec, Steady-State Firing			
Nozzle Temperature = 225°F			
25-9	20/1000/1000		
Heated Fuel to 140°F			
Heated Oxidizer to 120°F			
80-sec, Steady-State Firing			
Nozzle Temperature = 600°F			
25-10	20/1000/1000		

TEST 26

TANGENTIAL THRUSTER (PULSE FIRING)

OBJECTIVE: Rotated thruster 180°F about its axis to determine effect of rotation on amount of contamination deposited on test panel. Fuel additives were again tested.

RESULTS: Reduction of contamination on test panel was significant as a result of thruster rotation.

TEST HARDWARE: Contamination Test Panel 1
Surface Coating Specimens
Rotated Thruster (Thruster was rotated 180°R
flipped over from its original position such
that oxidizer inlet is now closest to the test
panel.)
Heated Nozzle

TEST CONDITIONS: $h = 1.14$ in., $\alpha = 10$ deg, $P_{ox} = 150$ psia,
 $P_F = 125$ psia, Altitude = 400,000 to 600,000 ft

Run No.	Pulsing Mode on / off / No. of (msec)/(msec)/Pulses	Specimen Measurement Sequence	Photographic Coverage
100-Percent MMH		None	Motion Pictures
26-1	20/1000/1000		
26-2	50/1000/500		
80-Percent MMH, 20-Percent Water			
30-sec Steady-State Firing			
26-3	20/1000/1000		
26-4	50/1000/500		
85-Percent MMH, 15-Percent Water			
10-sec Steady-State Firing			
26-5	20/1000/1000		
26-6	50/1000/500		
90-Percent MMH, 10-Percent Water			
30-sec Steady-State Firing			
26-7	20/1000/1000		
26-8	50/1000/500		
80-Percent MMH, 20-Percent Water			
225-sec Steady-State Firing			
Heated Nozzle to 380°F			
26-9	20/1000/1000		
26-10	50/1000/500		

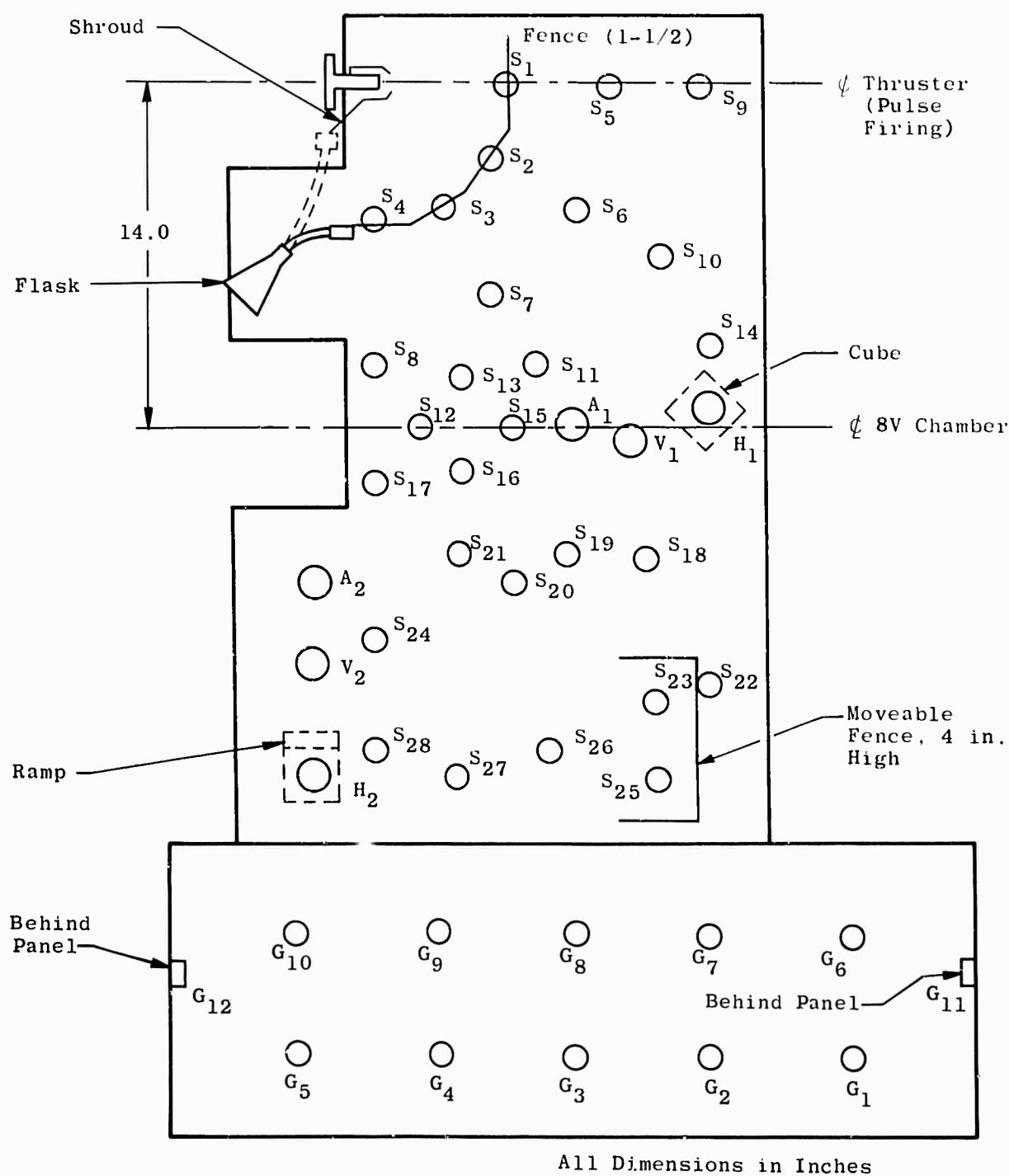


Fig. II-1 Contamination Controls on Thruster and Panel Used during Tangential Thruster Tests

APPENDIX III
TABLES OF OPTICAL MEASUREMENTS

TABLE 1Primary Test 7

Firing No.	Solar Absorptance, α_s	Emittance, ϵ	α_s/ϵ	Average Visible Reflectance, \bar{R}	Specimen Location and Type
0	0.2137	1.004	0.21	0.7138	S7A
4	0.2213	1.043	1.21	0.7099	S7A
7	0.2107	0.9938	0.21	0.7292	S7A
8	0.2183	0.9920	0.22	0.7197	S7A
0	0.2305	0.9753	0.24	0.6922	S8A
4	0.2053	1.063	0.19	0.7313	S8A
7	0.2295	0.9450	0.24	0.6996	S8A
8	0.2140	1.029	0.21	0.7224	S8A
0	0.1743	0.9723	0.18	0.7491	S28A
4	0.1978	0.9847	0.20	0.7325	S28A
7	0.1855	0.9681	0.19	0.7540	S28A
8	0.2034	0.9694	0.21	0.7353	S28A
0	0.2425	0.2466	0.98	0.7562	S15B
4	0.2271	0.2568	0.88	0.7357	S15B
7	0.2785	0.2547	1.09	0.7095	S15B
8		0.2506			S15B
0	0.2454	0.2352	1.04	0.7262	S19B
4	0.1836	0.2384	0.77	0.7863	S19B
7	0.3110	0.2381	1.31	0.6405	S19B
8	0.2500	0.2352	1.06	0.7598	S19B
0	0.2754	0.2492	1.11	0.6960	S25B
4	0.2765	0.2502	1.11	0.6993	S25B
7	0.3002	0.2540	1.18	0.6715	S25B
8	0.4071	0.2477	1.64	0.5549	S25B
0	0.2090			0.7738	G09M
4	0.3303			0.6372	G09M
7					G09M
8	0.2119			0.7473	G09M
0	0.2090			0.7498	G05M
4					G05M

TABLE 1 (Continued)

Primary Test 7

Firing No.	Relative Solar Transmittance, t_s	Average Visible Relative Transmittance, \bar{T}	Specimen Location and Type
0			V2
4	0.7206	0.6918	V2
7	0.8143	0.7808	V2
8	1.074	1.096	V2
12	0.9026	0.8886	V2
0			S27W
4	0.9499	0.9538	S27W
7	1.133	1.177	S27W
8	1.278	1.371	S27W
12	1.163	1.210	S27W
0			G04W
4	1.019	0.9982	G04W
7	1.116	1.091	G04W
8	1.253	1.289	G04W
12	1.273	1.307	G04W

TABLE 3

Primary Test 11

Firing No.	Solar Absorptance, α_s	Emittance, ϵ	α_s/ϵ	Average Visible Reflectance, \bar{R}	Specimen Location and Type
0	0.2064	0.9589	0.22	0.7226	S5A
1	0.2120			0.7161	S5A
2	0.2584			0.6504	S5A
3	0.2833	0.9545	0.30	0.6157	S5A
0	0.1963	0.8069	0.24	0.7329	S7A
1	0.1881			0.7468	S7A
2	0.1919			0.7481	S7A
3	0.2761	0.9739	0.28	0.6834	S7A
4	0.1878	0.9333	0.20	0.7571	S7A
5	0.3571			0.6609	S7A
S. L.	0.1071			0.8558	S7A
0	0.2095			0.7169	S28A
1	0.1832			0.7702	S28A
2	0.2333	0.9830	0.24	0.7036	S28A
3	0.2453	0.9720	0.25	0.6957	S28A
4	0.2258	0.9669	0.23	0.7051	S28A
5	0.2281			0.6966	S28A
S. L.	0.1646			0.7867	S28A
0	0.2660			0.7308	S15B
1	0.3233			0.6615	S15B
2	0.3066			0.6805	S15B
3	0.2880	0.2168	1.34	0.7011	S15B
4	0.2754	0.2133	1.29	0.7241	S15B
5	0.2915	0.2105	1.38	0.6918	S15B
S. L.	0.2027			0.8493	S15B
0	0.8428	0.8448	1.0	0.05563	S10K
1	0.8407			0.06135	S10K
2	0.8453			0.06236	S10K
3	0.8442	0.9190	0.92	0.06666	S10K
4	0.8442	0.9220	0.92	0.05948	S10K
5	0.8435	0.9108	0.93	0.05791	S10K
S. L.	0.5475			0.5965	S10K
0	0.8388			0.06485	S12K
1	0.8360			0.06742	S12K
2	0.8380			0.06540	S12K
3	0.8348	0.9371	0.891	0.06330	S12K
4	0.8425	0.9379	0.898	0.06605	S12K
5	0.8439	0.9465	0.892	0.06179	S12K
S. L.	0.7352			0.2611	S12K

TABLE 2 (Continued)

Primary Test 8

Firing No.	Relative Solar Transmittance, t_s	Average Visible Relative Transmittance, \bar{T}	Specimen Location and Type
0	None	None	V2
4	None	None	V2
5	None	None	V2
6	None	None	V2
7	None	None	V2
0			S27W
4	0.9039	0.8871	S27W
5	1.078	1.105	S27W
6			S27W
7			S27W
0	None	None	G4W
4	None	None	G4W
5	None	None	G4W
6	None	None	G4W
7	None	None	G4W

TABLE 2

Primary Test 8

Firing No.	Solar Absorptance, α_s	Emittance, ϵ	α_s/ϵ	Average Visible Reflectance, \bar{R}	Specimen Location and Type
0	0.1929	0.9792	0.20	0.7408	S5A
4	0.2139			0.7087	S5A
5	0.2432	0.9685	0.25	0.6790	S5A
6	0.2752	0.9533	0.29	0.6318	S5A
7		0.9649			S5A
0	0.1919	0.9988	0.19	0.7441	S7A
4	0.1986	0.9633	0.21	0.7184	S7A
5	0.1863	0.9833	0.19	0.7520	S7A
6	0.1952	0.9727	0.20	0.7396	S7A
7		0.9755			S7A
0	0.1661	0.9775	0.17	0.7710	S28A
4	0.1958	0.9787	0.20	0.7342	S28A
7		0.9718			S28A
0		0.2257			S15B
4	0.2529	0.1662	1.5	0.7527	S15B
5	0.2619			0.7354	S15B
6	0.2538			0.7445	S15B
7		0.2480			S15B
0	0.2512	0.2594	0.97	0.7553	S19B
4	0.2453	0.2497	0.98	0.7563	S19B
5	0.2475	0.2516	0.98	0.7581	S19B
0	0.8374	0.9475	0.88	0.05547	S12K
4	0.8373	0.9305	0.90	0.05517	S12K
7		0.9135			S12K
0	0.1513	0.8442			S25M
4	0.1510	0.8391			S25M
5	0.1543	0.8430			S25M
0	0.2269			0.7848	G9M
4	0.1661			0.8285	G9M
0					G3M
4	0.1580			0.8363	G3M
5					G3M

TABLE 3

Primary Test 11

Firing No.	Solar Absorptance, α_s	Emittance, ϵ	α_s/ϵ	Average Visible Reflectance, \bar{R}	Specimen Location and Type
0	0.1567			0.8417	S25M
1	0.1488			0.8588	S25M
2	0.1538			0.8464	S25M
3	0.1564			0.8335	S25M
4	0.1883			0.7985	S25M
5	0.1813			0.7908	S25M
S.L.	0.1236			0.8913	S25M
0	0.1911			0.7815	G03M
1	0.1598			0.8356	G03M
2	0.1607			0.8460	G03M
3	0.1664			0.8380	G03M
4	0.2127			0.8181	G03M
5	0.1775			0.8000	G03M
S.L.	0.1117			0.9359	G03M
0	0.1781			0.8066	G05M
1	0.3467			0.5854	G05M
2	0.1840			0.8355	G05M
3	0.1519			0.8542	G05M
4	0.2134			0.7968	G05M
5	0.1601			0.8566	G05M
S.L.	0.1103			0.9123	G05M
0	0.1626			0.8339	G09M
1	0.1951			0.8041	G09M
2	0.1626			0.8390	G09M
3	0.1586			0.8351	G09M
4	0.1517			0.8488	G09M
5	0.1502			0.8442	G09M
S.L.	0.0977			0.9500	G09M

TABLE 2 (Continued)

Primary Test 11

Firing No.	Relative Solar Transmittance, t_s	Average Visible Relative Transmittance, \bar{T}	Specimen Location and Type
0			V2
1	0.9419	0.9385	V2
2	1.099	1.149	V2
3	1.018	1.051	V2
4			V2
5			V2
S. L.	1.108	1.110	V2
0			S23W
1	0.9639	0.9476	S23W
2	1.142	1.184	S23W
3	1.097	1.140	S23W
4	1.116	1.147	S23W
5	1.123	1.146	S23W
S. L.	0.8942	0.8752	S23W
0			S27W
1	0.9285	0.9059	S27W
2	1.180	1.240	S27W
3	1.200	1.277	S27W
4	1.167	1.221	S27W
5	1.170	1.233	S27W
S. L.	1.074	1.038	S27W

TABLE 5Primary Test 12

Firing No.	Solar Absorptance, α_s	Emittance, ϵ	α_s/ϵ	Average Visible Reflectance, \bar{R}	Specimen Location and Type
0	0.1287	0.9793	0.15	0.8690	S7A
1	0.1428			0.8050	S7A
0	0.1076	0.9621			S12A
1				0.8348	S12A
0	0.1137				S28A
1				0.8460	S28A
0	0.2468			0.7894	S15B
1	0.3326			0.6346	S15B
0	0.1798				S25M
1				0.7972	S25M
0	0.1073			0.9179	G9M
1	0.1394			0.8718	G9M
0	0.1339			0.8891	G5M
1	0.1811			0.8040	G5M
0	0.1257			0.8838	G3M
1	0.1210			0.8996	G3M

TABLE 6

Primary Test 16

Firing No.	Solar Absorptance, α_s	Emittance, ϵ	α_s/ϵ	Average Visible Reflectance, \bar{R}	Specimen Location and Type
0	0.1721	0.9582	0.18	0.7705	S2A
4	0.2133	0.9612	0.22	0.7075	S2A
7	0.1836	0.9606	0.19	0.7414	S2A
8	0.1974	0.9694	0.20	0.7244	S2A
Pre 9	0.1926	0.9619	0.20	0.7166	S2A
9	0.2607	0.9468	0.28	0.6569	S2A
S.L.	0.2839			0.6319	S2A
0	0.2235	0.9729	0.23	0.7052	S6A
4	0.1600	0.9730	0.16	0.7762	S6A
7		0.9624			S6A
8	0.1682	0.9645	0.17	0.7643	S6A
Pre 9	0.1826	0.9563	0.19	0.7371	S6A
9		0.9687			S6A
S.L.	0.2637			0.6545	S6A
0	0.1706	0.9658	0.18	0.7566	S7A
4	0.5492	0.9657	0.57	0.4074	S7A
7	0.1623	0.9698	0.17	0.7759	S7A
8	0.1884	0.9658	0.20	0.7418	S7A
Pre 9	0.2354	0.9567	0.25	0.7122	S7A
9	0.1676	0.9548	0.18	0.7679	S7A
S.L.	0.2587			0.6673	S7A
0	0.1933	0.9622	0.20	0.7314	S10A
4		0.9614			S10A
7	0.2074	0.9702	0.21	0.7075	S10A
8	0.2010	0.9678	0.21	0.7072	S10A
Pre 9	0.2240	0.9461	0.24	0.6939	S10A
9	0.1773	0.9481	0.19	0.7455	S10A
S.L.	0.2483			0.6948	S10A
0	0.1717	0.9758	0.18	0.7534	S24A
4	0.4216	0.9740	0.43	0.4862	S24A
7		0.9746			S24A
8	0.3972	0.9679	0.41	0.4967	S24A
Pre 9	0.2551	0.9633	0.26	0.6385	S24A
9	0.3259	0.9609	0.34	0.5707	S24A
S.L.	0.3713			0.5217	S24A

TABLE 6

Primary Test 16 (Con't)

Firing No.	Solar Absorptance, α_s	Emittance, ϵ	α_s/ϵ	Average Visible Reflectance, \bar{R}	Specimen Location and Type
0	0.2440	0.4149	0.59	0.7037	S27T2
4	0.2206	0.4117	0.54	0.7284	S27T2
7	0.1879	0.4191	0.45	0.7863	S27T2
8	0.2397	0.4148	0.58	0.7369	S27T2
Pre 9	0.1992	0.4137	0.48	0.7713	S27T2
9		0.4106			S27T2
S.L.	0.2189			0.7381	S27T2
0	0.5455			0.3665	S25M
4	0.5643			0.3413	S25M
7	0.05155			0.9145	S25M
8	0.1227			0.8747	S25M
Pre 9	0.1512			0.8244	S25M
9	0.1533			0.8452	S25M
S.L.	0.3158			0.6055	S25M
0	0.2730			0.6878	G03M
4	0.2184			0.7429	G03M
7	0.2094			0.7738	G03M
8					G03M
Pre 9					G03M
9					G03M
S.L.	0.1781			0.8141	G03M
0	0.3165			0.6750	G09M
4	0.1462			0.8431	G09M
7	0.1613			0.8205	G09M
8					G09M
Pre 9					G09M
9	0.3309			0.6724	G09M
S.L.	0.1467			0.8694	G09M

TABLE 6 (Continued)

Primary Test 16

Firing No.	Relative Solar Transmittance, t_s	Average Visible Relative Transmittance, \bar{T}	Specimen Location and Type
0			V2
4	0.8820	0.8752	V2
7	0.9372	0.9376	V2
8	0.9416	0.9324	V2
Pre 9	0.9021	0.9010	V2
9		0.9755	V2
S.L.		1.017	V2
0			S23W
4	1.077	1.079	S23W
7	1.086	1.076	S23W
8	1.112	1.112	S23W
Pre 9	1.072	1.061	S23W
9			S23W
S.L.		1.096	S23W
0			G04W
4	1.000	0.9990	G04W
7	0.9819	0.9803	G04W
8			G04W
Pre 9			G04W
9			G04W
S.L.		1.0102	G04W

UNCLASSIFIED
Security Classification

DOCUMENT CONTROL DATA - R & D		
(Security classification of title, body of abstract and indexing annotation must be entered when the overall report is classified)		
1. ORIGINATING ACTIVITY (Corporate author) Arnold Engineering Development Center ARO, Inc., Operating Contractor Arnold Air Force Station, Tennessee		2a. REPORT SECURITY CLASSIFICATION UNCLASSIFIED
		2b. GROUP N/A
3. REPORT TITLE EFFECTS AND CONTROL OF CONTAMINATION FROM A SCALED MOL ATTITUDE CONTROL THRUSTER IN A TANGENTIAL ORIENTATION		
4. DESCRIPTIVE NOTES (Type of report and inclusive dates) May through December 21, 1968 - Final Report		
5. AUTHOR(S) (First name, middle initial, last name) David W. Hill, Jr. and Dale K. Smith, ARO, Inc.		
6. REPORT DATE October 1969	7a. TOTAL NO. OF PAGES 108	7b. NO. OF REFS 11
8a. CONTRACT OR GRANT NO. F40600-69-C-0001	9a. ORIGINATOR'S REPORT NUMBER(S) AEDC-TR-69-146	
b. Program Element 35121F		
c. Program Area 632A	9b. OTHER REPORT NO(S) (Any other numbers that may be assigned this report)	
d.	N/A	
10. DISTRIBUTION STATEMENT This document may be further distributed by any holder only with specific prior approval of MOL Project Office (SAFSL-5B), AF Unit Post Office, Los Angeles, California 90045.		
11. SUPPLEMENTARY NOTES Available in DDC	12. SPONSORING MILITARY ACTIVITY MOL Project Office (SAFSL-12C) AF Unit Post Office Los Angeles, California 90045	
13. ABSTRACT A test was conducted to determine the effects of contamination produced by a 1-lb-scaled Manned Orbital Laboratory thruster. The test required pulsing the 1-lb attitude control thruster in its tangential position and determining the effects of contaminants from the thruster impinging on optical and thermal control surface test specimens located on a flat plate exposed to the thruster exhaust plume. The thruster was pulsed with durations of 20, 50, 100, and 1000 msec with 1000 msec off time at altitudes above 400,000 ft. In situ reflectance, emittance, and transmittance measurements were made on optical and thermal control surface test specimens under vacuum conditions and at atmospheric pressure. Pretest and posttest laboratory measurements were also made. Significant contamination was produced for the pulse-mode operation, and the amount of contamination produced decreased as the thruster pulse duration increased. The heated shroud and changed thruster orientation relative to the plate were the most effective controls in reducing contamination on the plate; however, they did not eliminate the contaminants produced by the thruster in the plume. This document may be further distributed by any holder only with specific prior approval of MOL Project Office (SAFSL-5B), AF Unit Post Office, Los Angeles, California 90045.		

DD FORM 1 NOV 65 1473

UNCLASSIFIED
Security Classification

UNCLASSIFIED
Security Classification

14. KEY WORDS	LINK A		LINK B		LINK C	
	ROLE	WT	ROLE	WT	ROLE	WT
Manned Orbital Laboratory thrusters contamination control steady state pulse spacing modulation reflectance emittance transmittance						

AFSC
Arnold AFS Tenn

UNCLASSIFIED
Security Classification